PERFORMANCE ASSESSMENT OF WARM MIX ASPHALT (WMA) PAVEMENTS

Shad Sargand, J. Ludwig Figueroa, William Edwards, and Abdalla S. Al-Rawashdeh

Report FHWA/OH-2009/08

for the
Ohio Department of Transportation
Office of Research and Development

and the
United States Department of Transportation
Federal Highway Administration

State Job Number 134312

September 2009

Ohio Research Institute for Transportation and the Environment

1. Report No. FHWA/OH-2009/08	2. Government Accession No.	3. Recipient's Catalog No.
4. Title and Subtitle Performance Assessment of Warm Mix Asphalt (WMA) Pavements		**5. Report Date** September 2009
		6. Performing Organization Code
7. Author(s) Shad Sargand, J. Ludgwig Figueroa, William Edwards, and Abdalla S. Al-Rawashdeh		**8. Performing Organization Report No.**
9. Performing Organization Name and Address Ohio Research Institute for Transportation and the Environment (ORITE) 141 Stocker Center, Ohio University Athens OH 45701-2979		**10. Work Unit No. (TRAIS)**
		11. Contract or Grant No. State Job No. 134312
12. Sponsoring Agency Name and Address Ohio Department of Transportation Office of Research and Development 1980 West Broad St. Columbus OH 43223		**13. Type of Report and Period Covered** Technical Report
		14. Sponsoring Agency Code

15. Supplementary Notes

Prepared in cooperation with the Ohio Department of Transportation (ODOT) and the U.S. Department of Transportation, Federal Highway Administration

16. Abstract

Warm Mix Asphalt (WMA) is a new technology that was introduced in Europe in 1995. WMA offers several advantages over conventional asphalt concrete mixtures, including: reduced energy consumption, reduced emissions, improved or more uniform binder coating of aggregate which should reduce mix surface aging, and extended construction season in temperate climates.

Three WMA techniques, Aspha-min, Sasobit, and Evotherm, were used to reduce the viscosity of the asphalt binder at certain temperatures and to dry and fully coat the aggregates at a lower production temperature than conventional hot mix asphalt. The reduction in mixing and compaction temperatures of asphalt mixtures leads to a reduction in both fuel consumption and emissions.

This research project had two major components, the outdoor field study on SR541 in Guernsey County and the indoor study in the Accelerated Pavement Load Facility (APLF). Each study included the application of four types of asphalt surface layer, including standard hot mix asphalt as a control and three warm mixes: Evotherm, Aspha-min, and Sasobit. The outdoor study began with testing of the preexisting pavement and subgrade, the results of which indicated that while the pavement and subgrade were not uniform, there were no significant problems or variations that would be expected to lead to differences in performance of the planned test sections. During construction, the outdoor study included collection of emissions samples at the plant and on the construction site as well as thermal readings from the site. Afterwards, the outdoor study included the periodic collection and laboratory analysis of core samples and visual inspections of the road. Roughness (IRI) measurements were made shortly after construction and after a year of service.

The indoor study involved the construction of four lanes of perpetual pavement, each topped with one of the test mixes. The lanes were further divided into northern and southern halves, with the northern halves having a full 16 in (40 cm) perpetual pavement, and with the southern halves with thicknesses decreasing in one in (2.5 cm) increments by reducing the intermediate layer. The dense graded aggregate base was increased to compensate for the change in pavement thickness. The southern half of each lane was instrumented to measure temperature, subgrade pressure, deflection relative to top of subgrade and to a point 5 ft (1.5 m) down, and longitudinal and transverse strains at the base of the fatigue resistance layer (FRL). The APLF had the temperature set to 40°F (4.4°C), 70°F (21.1°C), and 104°F (40°C), in that order. At each temperature, rolling wheel loads of 6000 lb (26.7 kN), 9000 lb (40 kN), and 12,000 lb (53.4 kN) were applied at lateral shifts of 3 in (76 mm), 1 in (25 mm), -4 in (-102 mm), and -9 in (-229 mm) and the response measured. Then each plane was subjected to 10,000 passes of the rolling wheel load of 9000 lb (40 kN) at about 5 mph (8 km/h). Profiles were measured after 100, 300, 1000, 3000, and 10,000 passes with a profilometer to assess consolidation of each surface. After the 10,000 passes of the rolling wheel load were completed, a second set of measurements was made under rolling wheel loads of 6000 lb (26.7 kN), 9000 lb (40 kN), and 12,000 lb (53.4 kN) at the same lateral shifts as before. Additionally, the response of the pavement instrumentation was recorded during drops of a Falling Weight Deflectometer (FWD).

17. Key Words	18. Distribution Statement
Warm Mix Asphalt (WMA), Evotherm, Aspha-min, Sasobit, Asphalt Concrete Perpetual Pavement, falling weight deflectometer (FWD), Dowel bars, Accelerated Pavement Testing,	No Restrictions. This document is available to the public through the National Technical Information Service, Springfield, Virginia 22161

19. Security Classif. (this report)	20. Security Classif. (this page)	21. No. of Pages	22. Price
Unclassified	Unclassified	134	

SI* (MODERN METRIC) CONVERSION FACTORS

APPROXIMATE CONVERSIONS TO SI UNITS

Symbol	When You Know	Multiply By	To Find	Symbol
LENGTH				
in	inches	25.4	millimeters	mm
ft	feet	0.305	meters	m
yd	yards	0.914	meters	m
mi	miles	1.61	kilometers	km
AREA				
in^2	square inches	645.2	square millimeters	mm^2
ft^2	square feet	0.093	square meters	m^2
yd^2	square yards	0.836	square meters	m^2
ac	acres	0.405	hectares	ha
mi^2	square miles	2.59	square kilometers	km^2
VOLUME				
fl oz	fluid ounces	29.57	milliliters	mL
gal	gallons	3.785	liters	L
ft^3	cubic feet	0.028	cubic meters	m^3
yd^3	cubic yards	0.765	cubic meters	m^3
NOTE: Volumes greater than 1000 L shall be shown in m^3.				
MASS				
oz	ounces	28.35	grams	g
lb	pounds	0.454	kilograms	kg
T	short tons (2000 lb)	0.907	megagrams (or "metric ton")	Mg (or "t")
TEMPERATURE (exact)				
°F	Fahrenheit temperature	5(°F-32)/9 or (°F-32)/1.8	Celsius temperature	°C
ILLUMINATION				
fc	foot-candles	10.76	lux	lx
fl	foot-Lamberts	3.426	candela/m^2	cd/m^2
FORCE and PRESSURE or STRESS				
lbf	poundforce	4.45	newtons	N
lbf/in^2 or psi	poundforce per square inch	6.89	kilopascals	kPa

APPROXIMATE CONVERSIONS FROM SI UNITS

Symbol	When You Know	Multiply By	To Find	Symbol
LENGTH				
mm	millimeters	0.039	inches	in
m	meters	3.28	feet	ft
m	meters	1.09	yards	yd
km	kilometers	0.621	miles	mi
AREA				
mm^2	square millimeters	0.0016	square inches	in^2
m^2	square meters	10.764	square feet	ft^2
m^2	square meters	1.195	square yards	yd^2
ha	hectares	2.47	acres	ac
km^2	square kilometers	0.386	square miles	mi^2
VOLUME				
mL	milliliters	0.034	fluid ounces	fl oz
L	liters	0.264	gallons	gal
m^3	cubic meters	35.71	cubic feet	ft^3
m^3	cubic meters	1.307	cubic yards	yd^3
MASS				
g	grams	0.035	ounces	oz
kg	kilograms	2.202	pounds	lb
Mg (or "t")	megagrams (or "metric ton")	1.103	short tons (2000 lb)	T
TEMPERATURE (exact)				
°C	Celsius temperature	1.8°C + 32	Fahrenheit temperature	°F
ILLUMINATION				
lx	lux	0.0929	foot-candles	fc
cd/m^2	candela/m^2	0.2919	foot-Lamberts	fl
FORCE and PRESSURE or STRESS				
N	newtons	0.225	poundforce	lbf
kPa	kilopascals	0.145	poundforce per square inch	lbf/in^2 or psi

* SI is the symbol for the International Symbol of Units. Appropriate rounding should be made to comply with Section 4 of ASTM E380.

(Revised September 1993)

Performance Assessment of Warm Mix Asphalt (WMA) Pavements

Prepared in cooperation with the
Ohio Department of Transportation
and the
U.S. Department of Transportation, Federal Highway Administration

Prepared by

Shad M. Sargand

J. Ludwig Figueroa

William Edwards

Abdalla S. Al-Rawashdeh

Ohio Research Institute for Transportation and the Environment
Russ College of Engineering and Technology
Ohio University
Athens, Ohio 45701-2979

Final Report
September 2009

ACKNOWLEDGEMENTS

The authors would like to acknowledge the assistance and support of the pooled fund study members. The authors would like to acknowledge the contributions of the technical liaisons and project panel members to this project, particularly Roger Green, Dave Powers, and the ODOT Office of Research and Development. We thank Dan Radanovich of ODOT for taking the IRI data. The authors thank the subcontractors for their help on various aspects of the project. The authors also acknowledge the contributions of Associate Professor Sang-Soo Kim, ORITE Research Engineer Issam Khoury, graduate students Andrew Wargo and Carlos Vega-Posada, and undergraduate student Dan Rhine for their assistance.

TABLE OF CONTENTS

LIST OF APPENDICES

LIST OF TABLES

LIST OF FIGURES

LIST OF COLOR PLATES

Color Plates are in Appendix E

1 INTRODUCTION

1.1 Background

Warm Mix Asphalt (WMA) is a new technology which was introduced in 1995 in Europe. WMA is gaining attention all over the world because it offers several advantages over conventional asphalt concrete mixes. The benefits include (1) Reduced energy consumption in the asphalt mixture production process; (2) Reduced emissions, fumes, and undesirable odors; (3) More uniform binder coating on aggregate which should reduce mix surface aging; and (4) Extended construction season in temperate climates.

WMA requires the use of additives to reduce the temperature of production and compaction of asphalt mixtures. It offers an alternative to hot mix asphalt (HMA), which is produced at a temperature between 280°F (138°C) and 320°F (160°C). Warm mix asphalt is compacted at a temperature range of 250°F (121°C) to 275°F (135°C). Three techniques have been used to improve the workability of asphalt mixes at a lower temperature. These include [http://www.warmmixasphalt.com/WmaTechnologies.aspx]:

- Aspha-min, the addition of sodium aluminum silicate or zeolite to the asphalt mix [http://www.aspha-min.de/en/html/overview.html].
- Sasobit, the addition of a paraffin-wax compound extracted from coal gasification [http://www.sasolwax.com/Sasobit_Technology.html].
- Evotherm, the addition of an emulsion to improve the coating and workability of WMA mixes [http://www.meadwestvaco.com/Products/MWV002106].

A fourth technique, WAM Foam, was excluded from the study after consultation with ODOT and Flexible Pavements of Ohio. WMA techniques were used to reduce the viscosity of asphalt binder at certain temperatures and to dry and fully coat the aggregates at a lower production temperature than conventional hot mix asphalt. The reduction in mixing and compaction temperatures of asphalt mixtures can lead to a 30 percent reduction in both fuel energy consumption and emissions, depending on the WMA technology used [APAO, 2003].

1.2 Objectives

The following are the primary objectives of this research:

- To conduct a detailed laboratory study to evaluate the engineering and physical properties of WMA mixtures prepared according to the three techniques mentioned above and a conventional HMA mixture.
- To build and test pavement sections containing each of the selected mixtures (3 WMA types and one conventional) as a wearing (sacrificial) course compacted on conventional HMA layers designed following perpetual pavement guidelines. All sections will be subjected to repeated loads in the (APLF) at Ohio University under high, medium and low temperatures. It is planned to support each of the 4 types of wearing course on two different thicknesses of the planned perpetual pavements, for a total of 8 test sections. It will be necessary to develop a comprehensive instrumentation plan to monitor environmental conditions and response of the pavement structures when subjected to dynamic loading with properly installed instrumentation.

- To examine the influence of pavement thickness on the tensile strain developed at the bottom of the perpetual pavement layer.
- To monitor and test pavement sections containing the three techniques mentioned above to be built on GUE-541. This section was selected by engineers from the Ohio Department of Transportation, as a demonstration and evaluation project.
- To compare the performance of WMA mixtures and pavements with that of conventional HMA in the controlled setting of the APLF and in the field section.
- To document the performance of perpetual pavements containing 3 types of WMA and one conventional wearing course and to monitor pavement response in the form of deflections, strains and pressures in and under perpetual pavements. These data will be of extreme importance in future validations of perpetual pavements' analysis and design procedures
- To assess the advantages of WMA over conventional HMA in regards to reduced energy utilization and fume emanation during processing and placement.

This research includes an assessment of the performance of WMA mixes and conventional HMA test sections at APLF and in the real built road. This research will be used as a reference for the departments of transportation and the pavement community in general. The research will also evaluate the engineering properties of WMA mixes and conventional mixes. All the results obtained from these perpetual pavement sections can be used as a basis for recommendations for future installations of WMA or HMA in the production process of asphalt mixtures and the compaction of roadways. The new pavement technology is expected to reduce the energy consumption in mixing and laying asphalt. It is also expected to be environmentally friendlier and longer lasting.

An independent investigation of the field installation of the three WMA mixes and a conventional HMA mix on SR 541 in Guernsey and Coshocton Counties was performed by the National Center for Asphalt Technology (NCAT) at Auburn University. Laboratory testing was performed to determine various physical properties of the mixes and emissions were monitored as the mixes were placed in the field. A draft version of this report entitled *Ohio Field Trial of Warm Mix Asphalt Technologies: Construction Summary* (September 2009) and authored by Graham C. Hurley, Brian D. Prowell and Andrea N. Kvasnak [2009] was made available to ORITE as this report was being published.

2 LITERATURE REVIEW

2.1 Warm Mix Asphalt (WMA) Technology

2.1.1 Introduction

Hot mix asphalt (HMA) is produced at temperatures ranging from 280°F to 320°F (138°C to 160°C). The high temperature is used to dry the aggregate and decrease the viscosity of the asphalt binder, allowing it to fully coat the aggregate. It also produces the desired workability, and provides time to compact the HMA while it begins to cool. Some techniques have been used since the 1970s to decrease the production and compaction temperature of HMA, such as reducing the moisture of the aggregate, binder foaming, and using emulsified asphalts. The benefits of lowering the production and compaction temperatures include reduced energy consumption, reduced asphalt emissions, and improved performance of the pavement [Button, Estakhri and Wimsatt, 2007, p. 1].

2.1.2 History of WMA Technologies

In 1956, Iowa State University Professor Ladis Csanyi used foamed bitumen as a soil binder. This process consisted of injecting steam into hot bitumen to reduce the mixing temperature. In 1968, Mobil Oil Australia used cold water instead of steam to foam hot bitumen. This increased the practicality of the foaming process [Muthen, 1998].

In the early 1970s, Chevron developed new methods to prepare paving mixtures stabilized by emulsified asphalt. In 1977, Chevron published their "Bitumuls Mix Manual" [Chevron, 1977].

In 1994, Maccarone evaluated the performance of cold mix asphalt by using two different materials, based foamed bitumen and very high binder content emulsions. The results showed a reduction in energy consumption and lower gaseous emissions [Maccarone, 1994].

In 1999, Jenkins came up with a new technique that involves a half-warm foamed bitumen treatment. Jenkins investigated the concept and benefits of preheating aggregate to temperature above ambient level and below 212°F (100°C) before adding foamed bitumen. The results showed a good particle coating, mix cohesion, tensile strength, and compaction [Jenkins, de Groot, van de Ven and Molenaar, 1999].

Warm mix asphalt (WMA) in its present form was first developed in Europe. WMA was reported on by Harrison and Christodulaki at the First International Conference of Asphalt Pavements (FICAP) in Sydney, Australia in 2000 [Harrison and Christodulaki, 2000]. In the same year a paper was prepared by Koenders and his team, who evaluated the performance of WMA by testing a mix in the laboratory and at field locations in Norway, the UK, and the Netherlands. Koenders et al emphasized the production and application of dense graded wearing courses [Koenders, Stoker, Bowen, de Groot, Larsen, Hardy and Wilms, 2000].

In 2002, Koenders introduced the use of Warm Asphalt Mixes with Foam (WAM-Foam) to produce asphalt mixtures at lower operation temperatures [Koenders, Stoker, Robertus, Larsen and Johansen, 2002].

In 2004, Barthel used zeolite as an additive material to the asphalt mixture to increase the workability of the mix at lower temperatures [Barthel, Marchand and Von Devivere, 2005].

In 2005, the National Center for Asphalt Technology (NCAT) published two reports about the use of Sasobit and Aspha-min as additives to the asphalt mixture to produce warm mix asphalt. In 2006, another report was published by NCAT on the use of Evotherm in warm mix asphalt.

In 2007, three of the four prevalent warm mix asphalt techniques were used in the present study, which included a field site in Guernsey County, Ohio and test sections of WMA surface layers on perpetual pavements in a controlled test facility. [Sargand, 2007, p. 24].

2.2 Assessing the Potential for Warm Mix Asphalt

"Warm mix asphalt (WMA) is the broad term typically referring to technologies that seek to lower emissions and reduce energy consumption by lowering the temperature at which asphalt mixtures are produced and placed." [Kristjansdottir, Muench, Michael and Burke, 2007, p. 91]. Asphalt is created by reducing the viscosity of asphalt binder and that of the asphalt mix as well. Lower binder viscosity facilitates coating the aggregate with binder. In hot mix asphalt (HMA) plants, heat is used to dry the aggregate and to reduce binder viscosity. But in warm mix asphalt, the heat is reduced so the viscosity is reduced by adding water, chemicals, or wax as lubricants in the mixing process. Another way to reduce the viscosity of binder is by foaming the asphalt [Kristjansdottir, Muench, Michael and Burke, 2007, p. 91-92].

Lowering asphalt production emissions in plants and lowering the compaction emissions in the field are two of the most important benefits of using the warm mix asphalt. Mixing and compacting WMA at lower temperatures reduces energy consumption by saving fuel, which also saves money. The mixing additives reduce the viscosity of binder and increase the workability of the asphalt mix. Lowering the viscosity of the mix leads to more and better compaction of the asphalt mixture. [Kristjansdottir, Muench, Michael and Burke, 2007, p. 92-94].

The main concerns with using WMA are the long-term performance, which is unknown given such a new technology, and the special equipment, materials, and training required to mix and compact the WMA. The oldest WMA pavement facility is less than ten years of age, so there are no data on the long-term performance of WMA [Kristjansdottir, Muench, Michael and Burke, 2007, p. 95].

2.3 Evaluation of Warm Mix Asphalt

2.3.1 Evaluation of Evotherm for use in Warm Mix Asphalt

Evotherm is a chemical material added to the asphalt mix to increase the workability of asphalt at lower temperatures compared to that of hot mix asphalt. Evotherm is stored in a tank at 176°F (80°C) which is connected to the binder line by one or two heated valves to keep the Evotherm warm in the asphalt plant. Evotherm makes up 30 percent mass of the binder. It decreases the viscosity of the binder at lower mixing temperatures, which leads to fully coated

aggregates at the same temperature. This process reduces the production temperature by 30 percent, as well the fuel energy consumption [Hurley and Prowell, 2006, p. 1].

For the Hurley and Prowell study, two different groups of mixes were prepared, each group containing sixteen mix design combinations. Granite aggregates were used in the first group and limestone in the second. PG 64-22 and PG 76-22 binder grades were used as the control groups, the first number of the binder grade to the left is the highest temperature during the summer in the construction site and the second number which is in minus is the lowest temperature during winter in the construction site; thus PG 64-22 has a temperature range from 64°C (147°F) to -22°C (-7.6°F). The corresponding test mixtures included the binder grades as well as Evotherm. Each mix was compacted at four temperatures: 300°F (149°C), 265°F (129°C), 230°F (110°C), and 190°F (88°C) [Hurley and Prowell, 2006, p. 3].

Resilient modulus and the indirect tensile strength of each sample were measured by using indirect tensile strength test provided by AASHTO and ASTM standards (T 322-03) [Hurley and Prowell, 2006, p. 4-5].

2.3.2 Evaluation of Aspha-Min Zeolite for use in Warm Mix Asphalt

Aspha-min contains a sodium aluminum silicate, also known as zeolite. The crystal structure of zeolite has voids and empty spaces. It contains 20-21 percent water. The binder and Aspha-min are added to the mix at the same time. Aspha-min is 0.3% by mass of the mix. During the mixing processes, the water is released from the crystal structure of Aspha-min, which increases the volume of the binder. This process decreases the viscosity of the binder and increases the workability of the mix. As a result, the aggregate is coated at a temperature of 54°F (12°C), which is a major reduction from hot mix asphalt production temperature [Hurley and Prowell, 2005a, p. 1].

Two different groups of mixes were prepared. Sixteen mix design combinations were used again in each group. Granite aggregates were used in the first group and limestone in the second one. PG 64-22 and PG 58-28 binder grades were used as the control group. The corresponding test groups included the binder grades as well as Aspha-min. Each mix was compacted at four temperatures: 300°F (149°C), 265°F (129°C), 230°F (110°C), and 190°F (88°C) [Hurley and Prowell, 2005a, p. 2-3].

Resilient modulus and the indirect tensile strength of each sample were measured by using indirect tensile strength test provided by AASHTO and ASTM standard (T 322-03) [Hurley and Prowell, 2006, p. 5].

There was no effect on the resilient modulus of an asphalt mix by adding the zeolite. In standard HMA, rutting increases when one lowers the production and compaction temperature because the binder aging is reduced. Zeolite lowered the production and compaction temperature but did not affect the rutting potential of resulting asphalt mix [Hurley and Prowell, 2005a, p. 27-28].

2.3.3 Evaluation of Sasobit for use in Warm Mix Asphalt

Sasobit is a Sasol Wax and it is produced from coal gasification, commercially known as FT hard wax because it is produced by the Fischer-Tropsch process. The small crystalline structure of FT wax helps asphalt mixes resist thermal cracking at low temperatures because of the reduction in stiffness of the asphalt mix. Sasobit added directly to an asphalt mix at a rate of

0.8% to 3% by binder mass lowers the viscosity of the asphalt binder and increases the workability during the production and compaction of asphalt mix. The production temperature is decreased by 32°F (18C°) to 97°F (54C°) [Hurley and Prowell, 2005b, p. 1-2].

Two different groups of mixes were prepared, with eighteen mix design combinations in each group. Granite aggregates were used in the first group and limestone in the second one. PG 64-22 and PG 58-28 binder grades were used as the control groups. The corresponding test mixtures included the binder grades as well as Sasobit. Three different percentages of Sasobit were used to develop new binder grades. In the first one, 2.5% Sasobit was added to PG 58-28 to produce a PG 64-22. In the second, 4% Sasobit was added to PG 58-28 to produce PG 70-22. In the third, 4% Sasobit was added to PG 64-22 to produce PG 76-22. Each mix was compacted at four temperatures: 300°F (149°C), 265°F (129°C), 230°F (110°C), and 190°F (88°C) [Hurley and Prowell, 2005b, p. 4-5].

Resilient modulus and strength of each sample were measured by using indirect tensile strength test provided by AASHTO and ASTM standards. All samples were tested at 77°F (25°C) [Hurley and Prowell, 2006, p. 7].

There was no effect observed on the resilient modulus of an asphalt mix by adding the Sasobit. In general, the addition of Sasobit decreased the rutting of the asphalt mixes despite the lowered temperature. The tensile strength of asphalt containing Sasobit was lower than the control hot mix asphalt [Hurley and Prowell, 2005b, p. 25].

"Workability in the field can be defined as a property that describes the ease with which a HMA can be placed, worked by hand, and compacted". [Gudimettla, Allen Cooley and Ray Brown, 2003, p. iii]. "A device was successfully designed to measure the laboratory workability of HMA mixes. The device immerses a paddle into a sample of HMA. The torque required to keep the paddle rotating at a constant speed within the sample is then measured. Workability was defined as the inverse of the torque required to rotate the paddle within the sample of HMA." [Gudimettla, Allen Cooley and Ray Brown, 2003, p. iii].

2.4 Warm Mix Asphalt and Cold Weather paving

The objective of Kristjansdottir's research was to assess the performance of warm mix asphalt for the cold weather environment in Iceland by comparing the advantages and disadvantages of warm mix asphalt with hot mix asphalt (HMA) [Kristjansdottir, 2006, p. 1].

Different techniques of preparing warm mix asphalt were used and investigated to lower the production and paving temperatures of hot mix asphalt (HMA) without any change of the specification and quality of the asphalt mixture and the pavement. The first technique was Warm Asphalt Mix with Foam (WAM-Foam), which uses soft and hard foamed binders introduced at different stages during plant production. The second technique was Aspha-min, which is the addition of zeolite to the mixing process to foam the binder. The third technique was Sasobit, which is the addition of paraffin wax to the asphalt mix to reduce the viscosity. Other methods, such as Asphaltan B, low molecular weight wax, and Evotherm were also used. These methods involve mixing chemical additives with the binder to reduce its viscosity [Kristjansdottir, 2006, p. 7-8].

In the cold climate of Iceland the pavements must be well compacted. Increased compaction improves the stability of the pavements by squeezing the aggregate particles closer and thereby reducing the permeability of the pavements. Softer grades of binders were used in the asphalt mixtures to improve the compaction process at lower temperature but these mixes are unstable during the summer [Kristjansdottir, 2006, p. 44-45]. "Total compaction time between placement and cessation temperature for different grades is roughly the same." [Kristjansdottir, 2006, p. 45]. "The mix design process does not need to be altered for cold weather conditions but particular care must be taken to ensure that mixtures are not overly susceptible to moisture damage." [Kristjansdottir, 2006, p. 45].

At the end of the study, Kristjansdottir concluded that the most important advantages of using WMA are: reduced energy consumption, reduced emissions at asphalt plant and the paving site, and reduced viscosity of asphalt mixture. The report concluded that warm mix asphalt is suitable for paving in cold climates, with the most appropriate method being the Sasobit mix [Kristjansdottir, 2006, p. 84-86].

3 PAVEMENT DESCRIPTIONS

This study included data collected at two locations: a test site consisting of an overlay on Ohio State Route 541 in Guernsey County, and a test pavement constructed in the Accelerated Pavement Load Facility in Lancaster.

3.1 Field Site Description

A portion of Ohio State Route 541 connecting Kimbolton and Plainfield, west of Interstate 77 in Guernsey and Coshocton Counties, was selected for this research. The road was originally constructed in the early 1960's using 1.25 inches (31.8 mm) asphalt surface, 1.75 inches (44.5 mm) asphalt intermediate layer, 5 inches (127 mm) of granular base, and 4 inches (102 mm) of granular material. An overlay of 1.5 inches (38 mm) of asphalt was applied to the west end in 1985 and the east end in 1987. Another overlay of 1.5 inches (38 mm) asphalt was added to the entire segment in 1994.

For this research, another overlay was constructed in September 2006 by Shelly and Sands. The test pavement includes four experimental sections. Each section consists of a 0.75 inch (1.90 cm) layer of conventional HMA with 1.25 inch (3.18 cm) top layer containing one of three types of WMA or HMA as a control. The Evotherm section was paved on September 7, 2006, and is 2.7 miles (4.34 km) long. The Aspha-min section is 2.7 miles (4.34 km) long and was paved on September 15, 2006. The Sasobit section was paved on September 16, 2006 and is 3.07 miles (4.94 km) long. The control section was paved in the beginning of September 2006 and its length is 3.03 miles (4.88 km). In each case, the top layer also featured a different aggregate that made that layer distinct from the lower layer in core samples taken after construction. Details of the mix designs are given in Appendix A. The sections were not instrumented. Dynamic Cone Penetrometer (DCP) and Falling Weight Deflectometer (FWD) tests were conducted along this route prior to applying the experimental overlay. Figure 1 shows the map location of SR 541.

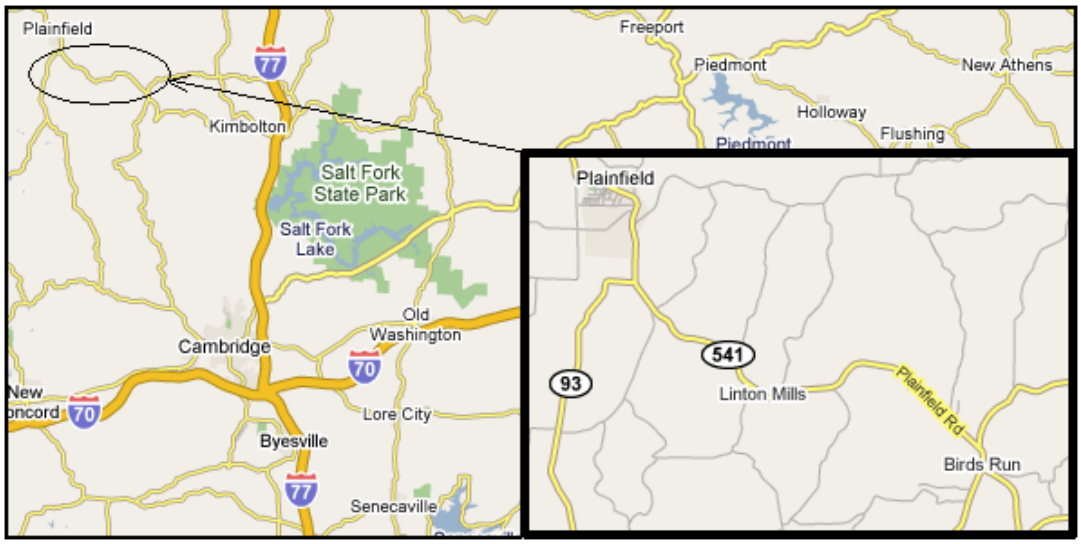

Figure 1. Map Location SR 541 [Google Map]. See Color Plate 1 in Appendix E for color version.

3.2 Test Perpetual Pavement Description

The Accelerated Pavement Loading Facility (APLF) in Lancaster Ohio is an indoor facility where dual or wide-based single wheel loads of up to 30,000 lbs. (133 kN) can be applied to full-scale sections of rigid and flexible pavement constructed in a 45 feet (13.7 m) long by 38 feet (11.6 m) wide by 8 feet (2.4 m) deep concrete test pit. During testing, air temperature can be controlled between +10°F (-12.2°C) and +130°F (54.4°C), and water can be added to the subgrade. Instrumentation installed in the pavement sections during construction measures dynamic responses under the rolling wheels and environmental conditions in the pavement structures. Surface profiles are measured on flexible pavement to monitor rutting performance.

The test pavement constructed for this project at the APLF included a total of 8 pavement sections containing three types of Warm Mix Asphalt and one conventional wearing course placed on two thicknesses of perpetual pavement cross sections along each lane, as shown in Figure 2 and Figure 3. The 38 foot (11.6 m) width of the APLF was divided into four 8 foot (2.4 m) wide lanes, one for each surface treatment. Each lane was divided into a north and south half of 22.5 ft (6.9 m) length. The northern pavement sections each had the same profile with perpetual pavement thickness 16 inches (406.4 mm), with the only difference between each being the type of warm or hot asphalt mix used in the 1.25 in (31.8 mm) surface layer. The perpetual pavement was constructed in the same manner as that constructed on the US Route 30 test road in Wayne County, also known as the WAY-30 test pavement [Sargand, Figueroa, and Romanello, 2008].

The four southern sections had progressively thinner perpetual pavement depths of 16 inches (406.4 mm), 15 inches (381 mm), 14 inches (356 mm), and 13 inches (330 mm). The different section thicknesses in the southern part of the APLF were designed to provide data useful to future verifications of perpetual pavement analysis and design procedures. The different surface mixes are expected to have negligible impact on the perpetual pavement behavior.

The 16 in (406.4 mm) perpetual pavements were built up from the bottom in the following layers, as shown in Figure 2: 12 in (30 cm) coarse aggregate topped by ~5 ft (~1.5 m) of type A6-A7 subgrade soil, a dense graded aggregate base (DGAB, ODOT Item 304) of depth 6 in (15 cm), a 4 in (10 cm) Fatigue Resistant Layer, a 7.75 in (19.7 cm) intermediate AC (ODOT Item 448) layer, a 3 in (7.6 cm) AC leveling layer of ODOT Item 446 Type II, and a 1.75 in (3.2 cm) surface layer of ODOT Item 446 Type I HMA or one of the WMA mixes. For the southern half of each WMA lane, the intermediate layer (ODOT Item 448) was reduced by 1 in (2.54 cm), 2 in (5.08 cm), or 3 in (7.62 cm) and the DGAB increased a corresponding amount to keep the surface of each pavement structure at the same elevation.

The conventional asphalt mixes were delivered to the APLF from the Shelley and Sands Asphalt Plant located in Logan, Ohio, while the WMA mixes were brought in from the plant site established near the GUE-541 project, and are the same as used at the field site. All sections were supported on a uniform dense graded aggregate base (DGAB) and subgrade. Subgrade moisture was not varied throughout the project in an effort to limit the number of variables to be monitored and used in the analysis.

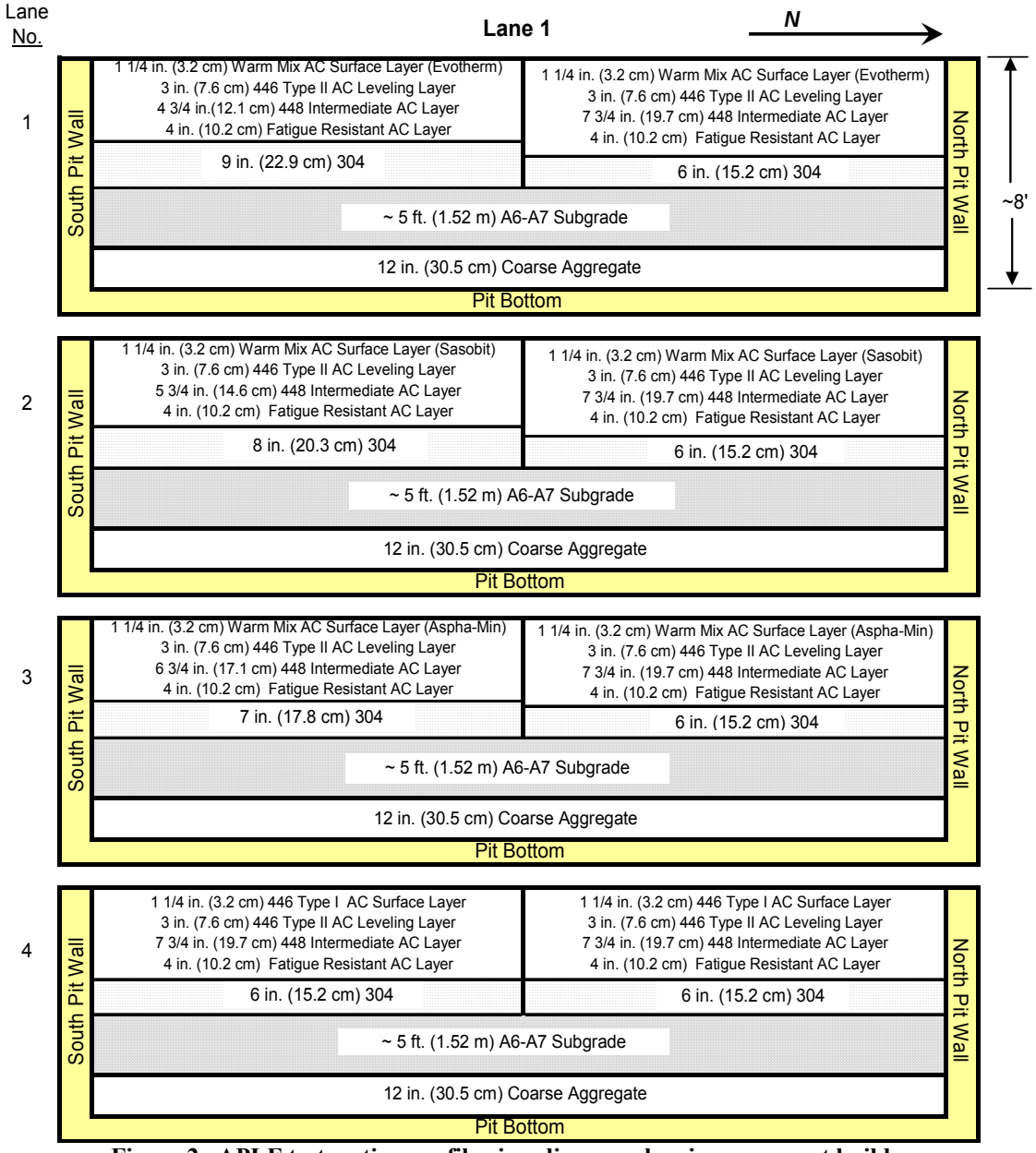

Figure 2. APLF test section profile view diagram showing pavement build-up.

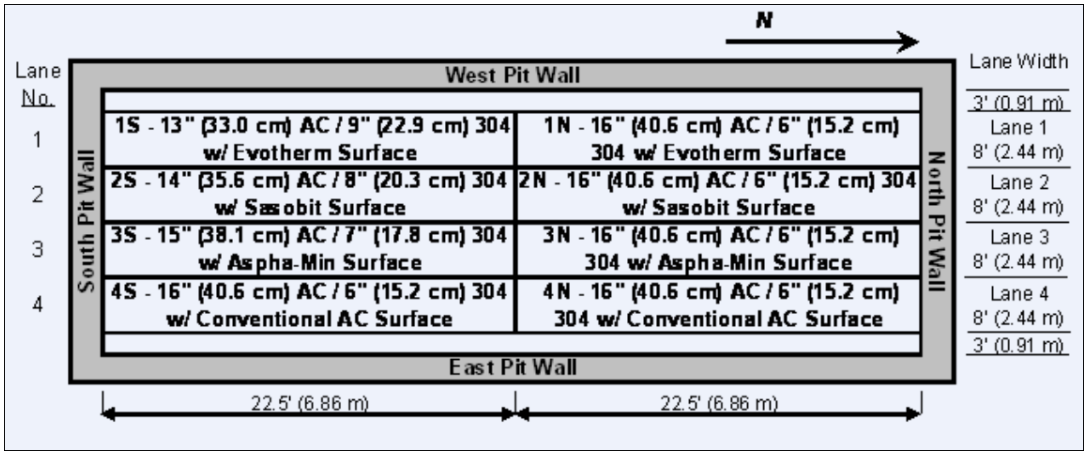

Figure 3. Overhead plan view diagram of APLF test section layout.

The southern sections of the APLF were instrumented to measure dynamic response to load in the form of strains, pressure, and deflections. Figure 4 shows the sensor layout along the centerline of the lane. The instrumentation consisted of four Dynatest PAST II AC strain gauges oriented to measure longitudinal and transverse strain 1 inch (2.54 cm) above the bottom of the fatigue resistant AC layer, two Micro Sensors GHSD 750 LVDTs and one Geokon Earth Pressure Cell, all spaced 18 inches (45.7 cm) apart longitudinally along the lane centerlines to measure the dynamic response of the four perpetual pavements of different thickness. The two LVDTs were installed so that one measured surface deflection referenced to the top of the subgrade and the second deflection to a depth of approximately 5 feet (1.52 m) below the pavement surface. A hole for the deep LVDT was drilled about 3 feet (0.91 m) into the 304 aggregate, lined with PVC pipe, capped to keep it clean, and referenced for future drilling through the pavement to install the LVDT. Thermocouples were also placed one inch (2.5 cm) below the surface, at the center and one inch (2.5 cm) above the bottom of the AC to monitor pavement temperature during the tests.

Installation proceeded as follows: The pressure cell was placed on the finished subgrade before placement of the aggregate for the DGAB layer. Upon completion of the DGAB layer, strain gauges were installed by sieving out large particles from a portion of the hot fatigue resistant mix, placing a 1 inch (2.5 cm) thick pad of the sieved material on the aggregate, laying the gauge on the pad, covering it over with another inch (2.5 cm) of sieved material, hand compacting the asphalt encasing the strain gauge, and then letting the paver complete placement of the fatigue resistant layer. Thermocouples were held in place with loose AC ahead of the paver. After all paving was completed, holes were drilled through the AC and the two LVDTs were installed as shown in Figure 4. An infrared camera was used during the APLF test section construction to document WMA cooling throughout the placement and compaction processes.

Each specific section was tested at low, medium, and high temperatures of 40°F (4.4°C), 70°F (21.1°C), and 104°F (40°C), respectively, applied in that order to the pavement pad. Once the temperature of the asphalt had stabilized and initial sensor measurements taken, 10,000 passes were applied using a 9000 lb (40.0 kN) single axle load moving at a constant speed of 5 mph (8 km/h). A second set of sensor readings under loads was taken after the set of passes was completed. During the 10,000 passes of the load, periodic visual condition surveys were

performed to document the development of distress as the number of loads applied to the pavement increased. Surface profile surveys were also obtained with a profilometer (traveling laser instrument) that monitored rutting development as the loading of pavement sections progressed under the three planned temperature levels. If rutting was equal to 0.5 inches (12.7 mm) developed under the constant 9 kip (40 kN) single axle load, testing was to be discontinued on that strip.

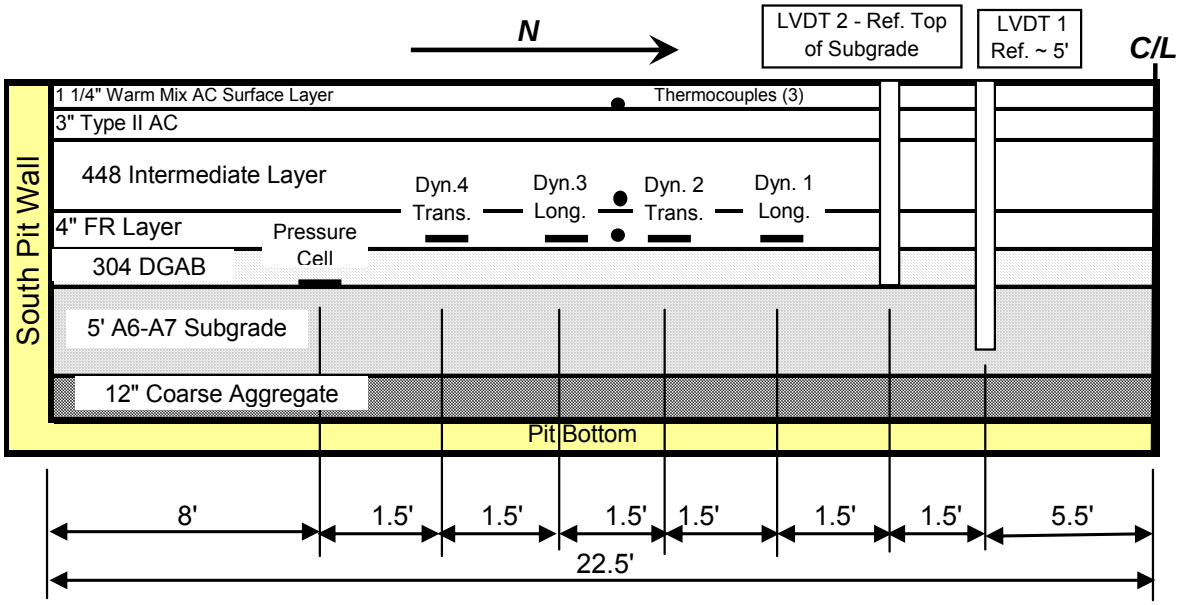

Figure 4. Profile view showing sensor locations along centerline in southern section of each APLF lane (not to scale).

4 PAVEMENT MATERIAL PROPERTIES

4.1 Dynamic Cone Penetrometer Test State Route (SR 541)

The GUE-541 experimental pavement location was subjected to testing with a Dynamic Cone Penetrometer (DCP) following established methods [Wu and Sargand, 2007]. The DCP is shown in Figure 5. The DCP was used to provide important information about the stiffness of the base and subgrade. The depth of limitation of this test is 3.5 feet (1.07m). The depth of penetration per blow, or the Penetration Index (PI), generated from this test can be translated into other the strength parameters such as the California Bearing Ratio (CBR) and the resilient modulus (M_R) [Wu and Sargand, 2007]. Figure 6 shows typical results in the form of the penetration depth as a function of the number of blows. Figure 7 shows the penetration index (PI) in mm/blow as a function of depth; a lower PI indicates a stiffer material resisting the impact of the DCP point. Finally Figure 8 shows the resilient modulus (M_R) as a function of depth.

Figure 5. DCP test device: at left is the DCP rod and driving weight assembly, and on the right is the DCP in use. [Wu and Sargand, 2007]. See Color Plate 2 in Appendix E.

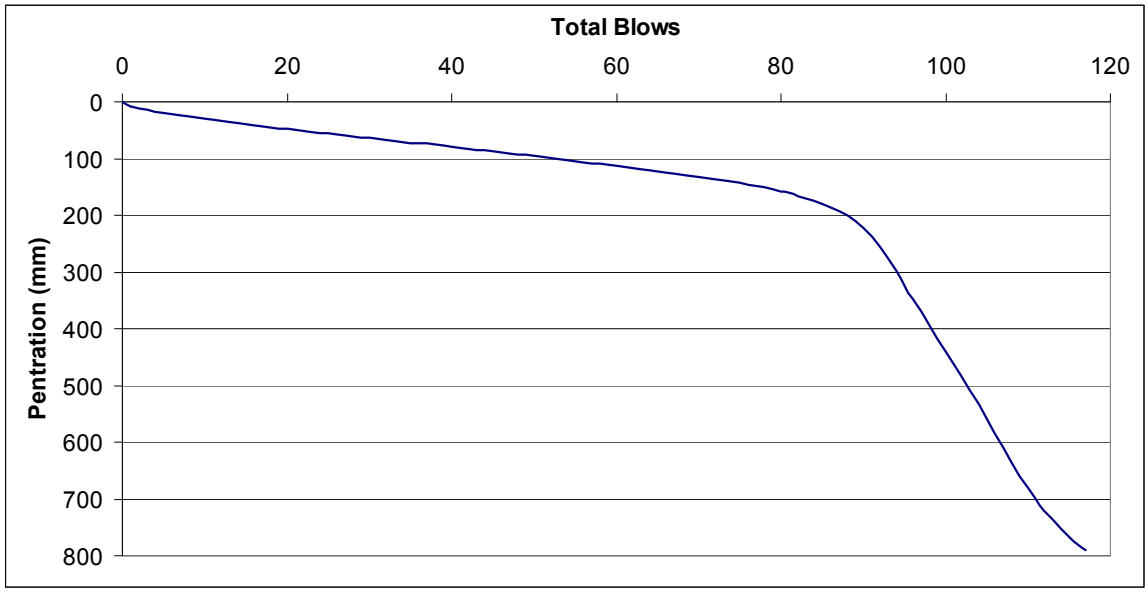

Figure 6. DCP – Total Blows Versus Depth: HMA Control Section, GUE-541 (25.4 mm = 1 in).

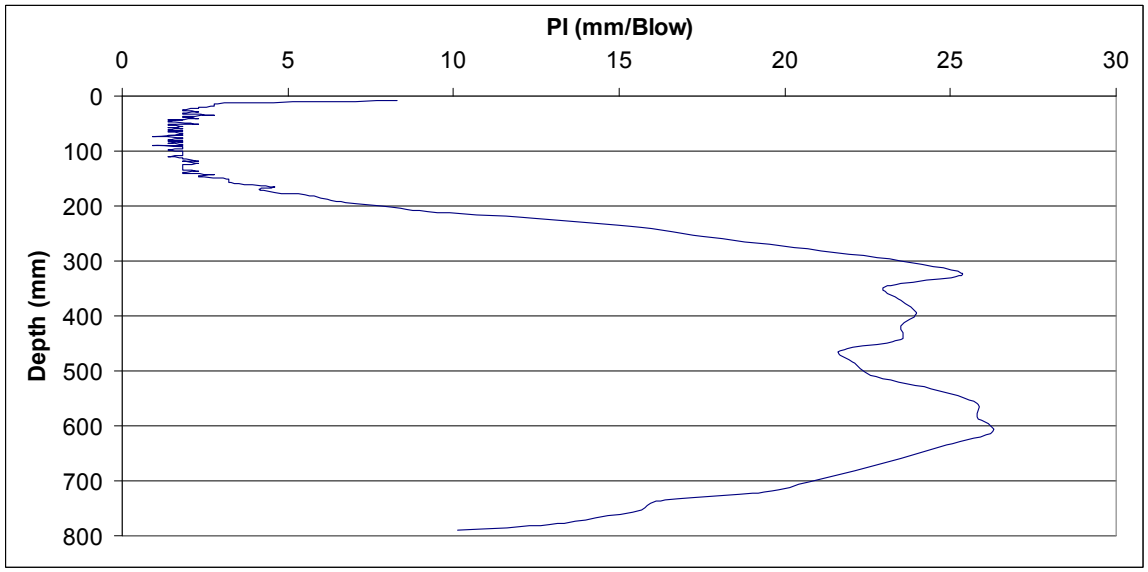

Figure 7. DCP – Penetration Index versus Depth: HMA Control Section, GUE-541 (25.4 mm = 1 in).

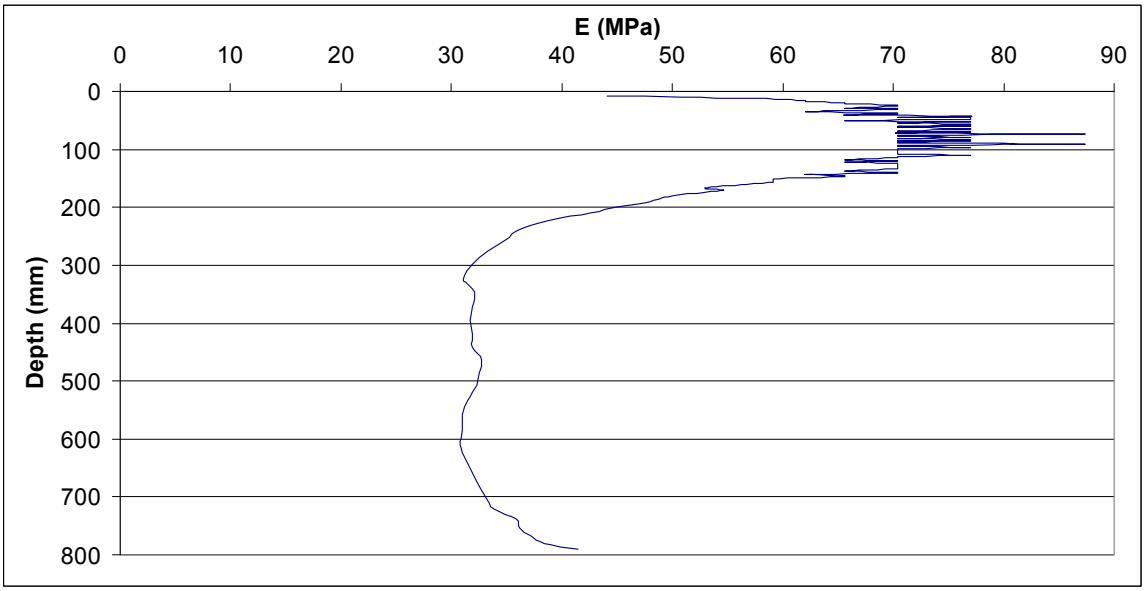

Figure 8. DCP – Resilient Modulus Versus Depth: HMA Control Section, GUE-541 (25.4 mm = 1 in, 1 MPa = 0.145 ksi).

CBR values were estimated from the PI using the relationship determined by the United States Army Corps of Engineers [Webster, Grau, and Williams, 1992, p. 9]

$$CBR = 292/PI^{1.12} \quad \text{.....(3.1)}$$

M_R values were estimated from the CBR using the relationship determined by Transport and Road Research Laboratory (TRRL) (UK).

$$E(MPa) = 17.6 * CBR^{0.64} \quad \text{.....(3.2)}$$

By analyzing the resulting graphs, potential weak zones in the base and subgrade can be determined. The weaker areas are those with high penetration index values shown in Figure 7 at depths of 12 inches (30 cm) to 28 inches (70cm), which correlate with the lower M_R values of 4.6 ksi (32 MPa) to 5.8 ksi (40 MPa) given in Figure 8. From Table 1, the average M_R for the base is 9.3 ksi (64 MPa) and the average M_R for the subgrade is 5.2 ksi (36 MPa) for all sections.

Table 1. DCP PI values and derived CBR and MR values for SR541 base and subgrade.

S.R 541		Sample Section						
		Control		Section 1	Section 2	Section 3		
		MEG1	MEG3	MEG5	MEG6	MEG8	MEG9	MEG10
Avg PI Base	(mm/blow)	2.14	1.94	2.95	2.52	2.74	3.55	3.83
	(in/blow)	0.08	0.08	0.12	0.10	0.11	0.14	0.15
Avg PI Subgrade	(mm/blow)	22.40	11.37	24.02	17.69	29.33	25.23	18.35
	(in/blow)	0.88	0.45	0.95	0.70	1.15	0.99	0.72
Avg CBR Base		8.57	9.09	7.24	7.85	7.55	6.47	6.33
Avg CBR Subgrade		2.61	3.97	2.55	2.95	2.47	3.38	2.87
Avg M_R Base	(MPa)	69.29	72.10	62.27	65.81	64.10	59.46	56.49
	(ksi)	10.05	10.46	9.03	9.55	9.30	8.62	8.19
Avg M_R Subgrade	(MPa)	34.21	41.76	32.89	35.31	32.66	38.68	34.62
	(ksi)	4.96	6.06	4.77	5.12	4.74	5.61	5.02

4.2 Asphalt Material Properties Testing

4.2.1 Laboratory Prepared Samples

Nine samples were prepared for each mix used in the field study. Each sample was 150 mm (6 in) in diameter and 38 mm (1.5 in) to 50 mm (2 in) high. After the air voids were measured, the samples were prepared for the indirect tensile creep and tensile strength tests at three different temperatures: 0°C (32°F), -10°C (14°F), and -20°C (-4°F). The results were used to determine the creep compliance curve, unconfined tensile strength, and Poisson's ratio. These material properties can be used to calculate the low temperature and cracking potential of asphalt concrete as well as to assess the quality of the pavement materials.

The material properties were measured with an Indirect Tensile Test (IDT) device like that shown in Figure 9 [Rutgers, 2005]. This device is used to determine tensile strength (*St*), the creep compliance, the time-dependent strain (*D(t)*) divided by the applied stress, and the Poisson's ratio of the asphalt mix [Witczak, Kaloush, Pellinen, El-Basyouny and Von Quintus, 2002].

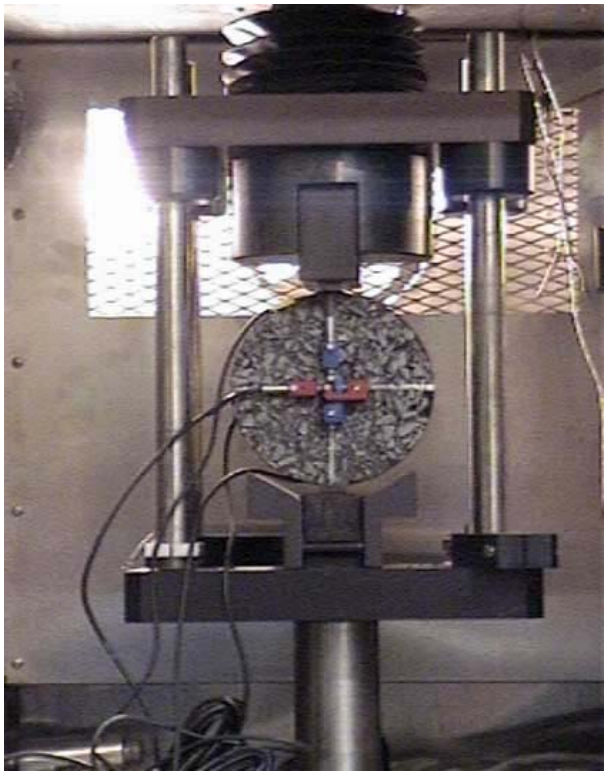

Figure 9. Indirect Tensile test (IDT) [Rutgers, 2005].

Table 2. Poisson's ratio for Warm Mix Asphalt (WMA) at different temperatures.

Temperature °C (°F)	Poisson's ratio (Diameter 150 mm (6 inches))			
	Evotherm	Sasobit	Aspha-min	Control
0 (32)	0.5*	0.311	0.487	0.263
-10 (14)	0.407	0.242	0.369	0.299
-20 (-4)	0.122	0.5*	0.364	0.076
* maximum value of 0.5 measured				

The Poisson's ratio for a mixture varies at different temperatures; different mixtures at the same temperature may also have differing Poisson's ratio values. The results tabulated in Table 2 were calculated using the equations in the standard method of test for determining the creep compliance and strength of hot mix asphalt (HMA) using the IDT test, which were found in the IDT device instructions handout, a handout provided by AASHTO, and in ASTM standard T 322-03. Here are the equations to calculate the creep compliance and Poisson's Ratio [Buttlar, and Roque, 1994]:

$$Bavg = \frac{\sum_{n=1}^{3} Bn}{3} \quad \text{..... (3.3)}$$

$$Davg = \frac{\sum_{n=1}^{3} Dn}{3} \quad \text{..... (3.4)}$$

$$Pavg = \frac{\sum_{n=1}^{3} Pn}{3} \quad \text{..... (3.5)}$$

Bavg, Davg, Pavg = thickness, diameter, and creep load, respectively, each averaged over three replicate specimens; and
Bn, Dn, Pn = thickness, diameter, and creep load of specimen *n* (*n* =1 to 3).

$$\Delta Xn,i,t = \Delta Xi,t \times \frac{Bn}{Bavg} \times \frac{Dn}{Davg} \times \frac{Pavg}{Pn} \quad \text{..... (3.6)}$$

$$\Delta Yn,i,t = \Delta Yi,t \times \frac{Bn}{Bavg} \times \frac{Dn}{Davg} \times \frac{Pavg}{Pn} \quad \text{..... (3.7)}$$

$\Delta Xn,i,t$ = normalized horizontal deformation for face *i* (*i*=1 to 6) at time *t* (*t*= 0 to $t_{final,}$ where t_{final} is the total creep time);

$\Delta Yn,i,t$ = normalized vertical deformation for face *i* at time *t*;

$\Delta X,i,t$ = measured horizontal deformation for face *i* at time *t*; and

$\Delta Y,i,t$ = measured vertical deformation for face *i* at time *t*;

$$\Delta Xa,i = \Delta Xn,i,t_{mid} \quad \text{..... (3.8)}$$

$$\Delta Ya,i = \Delta Yn,i,t_{mid} \quad \text{..... (3.9)}$$

$\Delta Xa,i$, $\Delta Ya,i$ = average horizontal and vertical deformations for face *i*;

$\Delta Xn,i,t_{mid}$ = normalized horizontal deformation for face *i* at the midpoint of the time interval during which the test was run; and

$\Delta Yn,i,t_{mid}$ = normalized vertical deformation for face *i* at the midpoint of the time interval during which the test was run;
The next step is to take trimmed means of the ΔX and ΔY values. This done by removing the highest and lowest values from the data set and averaging over the rest. In formal notation:

$$\Delta Xt = \frac{\sum_{j=2}^{5} \Delta Xr, j}{4} \quad \text{(3.10)}$$

$$\Delta Yt = \frac{\sum_{j=2}^{5} \Delta Yr, j}{4} \quad \text{(3.11)}$$

$\Delta Xr,j$ = $\Delta Xa,i$ values sorted in ascending order;

$\Delta Yr,j$ = $\Delta Ya,i$ values sorted in ascending order;

ΔXt = trimmed mean of horizontal deformations; and

ΔYt = trimmed mean of vertical deformations;

$$\frac{X}{Y} = \frac{\Delta Xt}{\Delta Yt} \quad \text{(3.12)}$$

$$\Delta Xtm,t = \frac{\sum_{j=2}^{5} \Delta Xr, j,t}{4} \quad \text{(3.13)}$$

$\Delta Xr,j,t$ = $\Delta Xi,t$ arrays sorted, where the i = 6 arrays are sorted according to the sorting order already established for $\Delta Xr,j$; and

$\Delta Xtm,t$ = Trimmed mean of the $\Delta Xi,t$ arrays.

Creep compliance $D(t)$ in kPa is computed as a function of time using:

$$D(t) = \frac{\Delta Xtm,t \times Davg \times Bavg}{Pavg \times GL} \times Ccmpl \quad \text{(3.14)}$$

where GL = gauge length in meters (0.038 m (1.5 in) for 150-mm diameter specimens); and

$$Ccmpl = 0.6354 \times \left(\frac{X}{Y}\right)^{-1} - 0.332 \quad \text{(3.15)}$$

Poissons's ratio is computed from the laboratory results as follows:

$$\nu = -0.1 + 1.48\left(\frac{X}{Y}\right)^2 - 0.778\left(\frac{Bavg}{Davg}\right)^2\left(\frac{X}{Y}\right)^2 \quad \text{(3.16)}$$

This equation is valid in the range $0.05 \le \nu \le 0.5$

To calculate the indirect tensile strength *St*, the following equations are used:

Bn, Dn, = thickness and diameter, respectively, of specimen *n* ($n \in \{1,2,3\}$).

$$St,n = \frac{2 \times Pf,n}{\pi \times Bn \times Dn} \quad \text{..... (3.17)}$$

Pf,n = first failure load for specimen, n; and

St,n = tensile strength of specimen, n;

$$St = \frac{\sum_{n=1}^{3} St,n}{3} \quad \text{..... (3.18)}$$

St = average tensile strength of the mixture.

Table 3 shows the tensile strength for Warm Mix Asphalt sections and the control section at three different temperatures as determined from the IDT test data.

Table 3. Indirect tensile strength for Warm Mix Asphalt (WMA) at different temperatures.

Temperature (°F)	Tensile Strength (psi)			
	Evotherm	Sasobit	Aspha-min	Control
32	527.5	564.7	469.9	552.8
14	685.6	703.7	714	750.6
-4	854.6	815.1	742.5	865

Temperature (°C)	Tensile Strength (MPa)			
	Evotherm	Sasobit	Aspha-min	Control
0	3.64	3.89	3.24	3.81
-10	4.73	4.85	4.92	5.18
-20	5.89	5.62	5.12	5.96

The tensile strength increases with decreasing temperature. The Evotherm and control samples have nearly the same tensile strength at 0°C and -20°C (32°F, and -4°F).

Figure 10 compares the indirect tensile strength of WMA mixes with the HMA control at different temperatures. The Evotherm is generally closest to the control in terms of indirect tensile strength, though none of the mixes differs from the control by more than 15%. Evotherm and Sasobit are consistently within 10% of the control value, thus there is no significant difference in indirect tensile strength in the mixes.

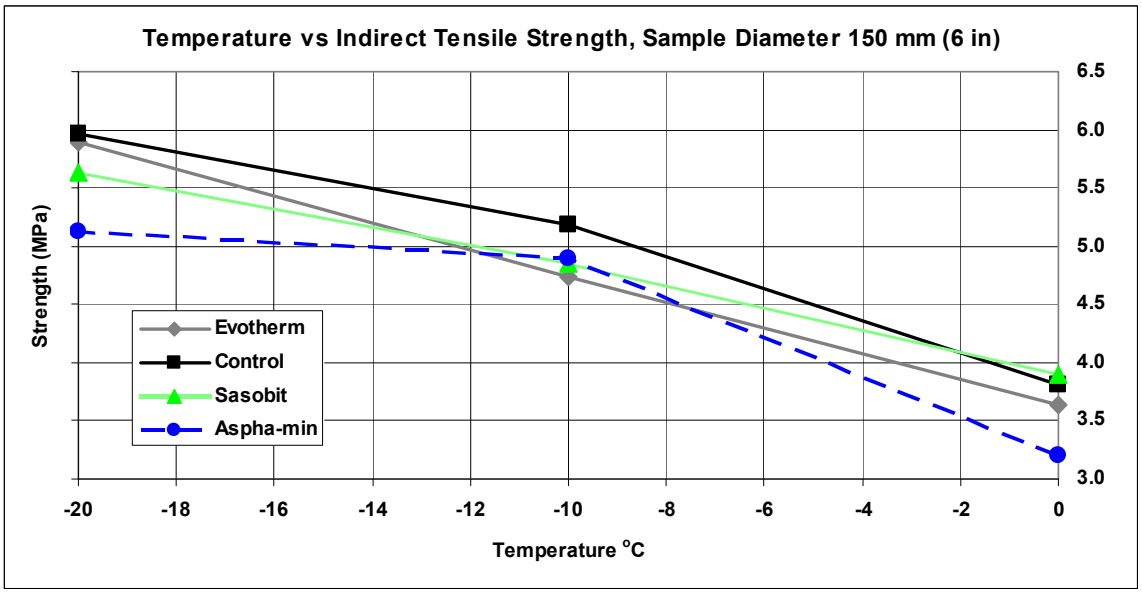

Figure 10. Indirect Tensile Strength versus Temperature for Control (HMA) and WMA mixes (1 MPa = 145 psi).

The creep compliance is defined as the time-dependent strain divided by the applied stress. Figure 11 shows the creep compliance of Evotherm, Sasobit, Aspha-min, and the control at 0°C (32°F). According to Figure 11, the creep compliance curve for Evotherm mix is the one closest to the creep compliance curve for control mix, but Aspha-min has the best creep-compliance properties. It is the softest mix at this temperature and will best resist low temperature thermal cracking.

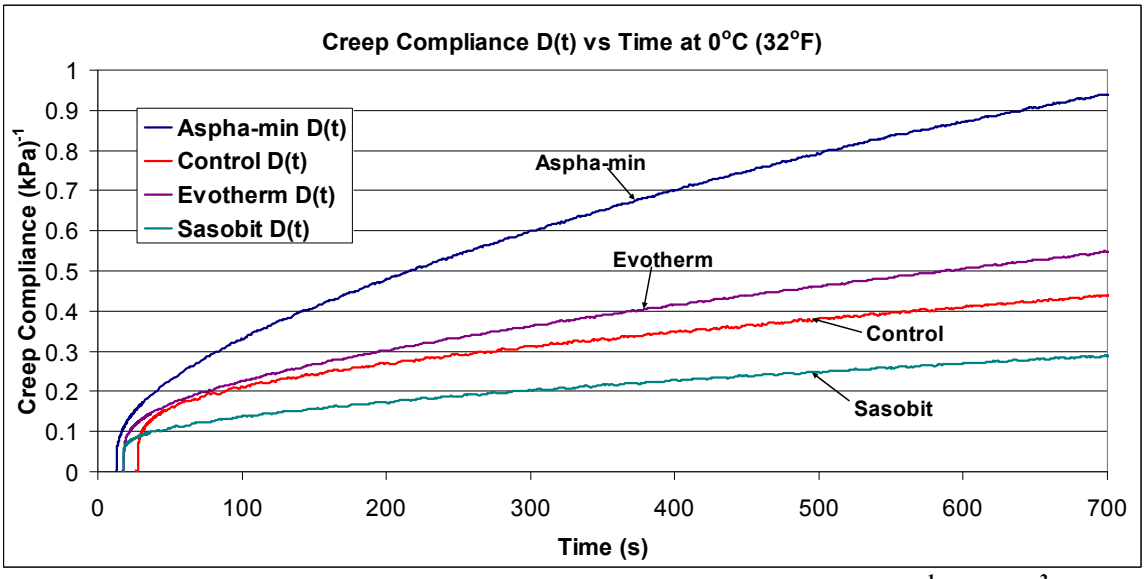

Figure 11. Creep Compliance D(t) versus Time for all mixes at 0°C (32°F) (1 kPa^{-1} = 6.89 in^2/lb).

Figure 12 illustrates the creep compliance of Evotherm, Sasobit, Aspha-min, and the HMA control at -10°C (14°F). At this temperature, the creep compliance curve for Sasobit mix is the closest to that of the control mix, but the Evotherm and Aspha-min are clearly softer than the control at this temperature and better resist low temperature thermal cracking.

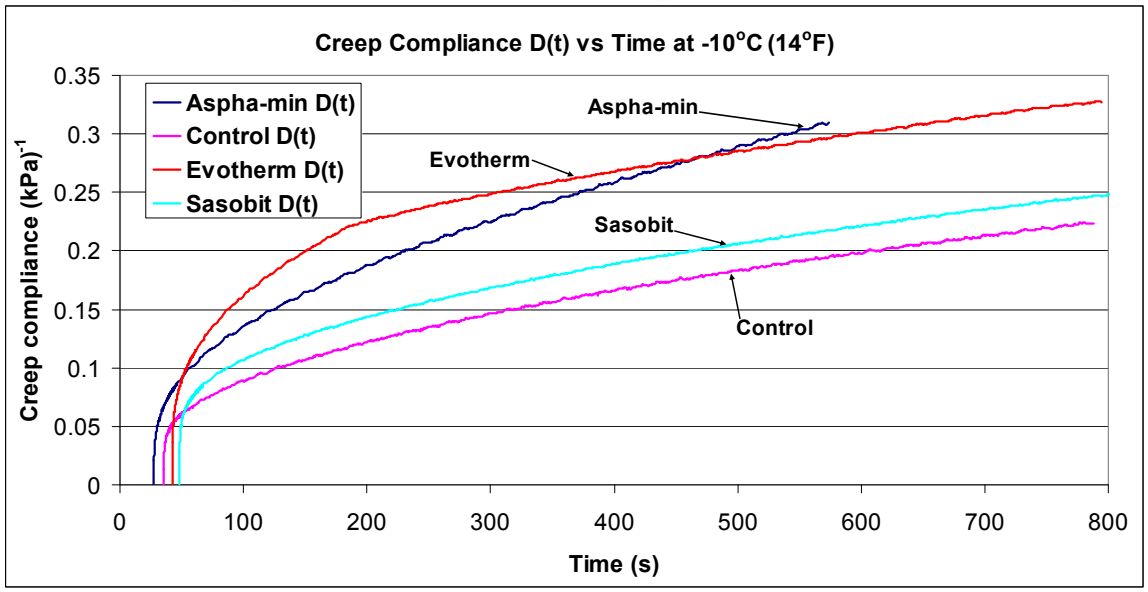

Figure 12. Creep Compliance D(t) versus Time for all mixes at -10°C (14°F) (1 kPa^{-1} = 6.89 in^2/lb).

Figure 13 shows the creep compliance of Evotherm, Sasobit, Aspha-min, and HMA control at -20°C (-4°F). Figure 13 indicates that the creep compliance curve for Evotherm mix is the closest to the creep compliance curve for the control mix. The best mix at this temperature is Aspha-min because it's the softest mix. Creep compliance as a function of time increases with increasing temperature. Again, the data substantiates that the creep compliance curves for Evotherm and Control at 0°C (32°F) and -20°C (-4°F) are very close to each other.

Considering behavior at all three temperatures, Aspha-min appears to offer the best resistance to low-temperature cracking, while Sasobit offers the worst. Both Evotherm and Aspha-min appear to generally perform better than conventional HMA in terms of avoiding thermal cracking. An examination of the slopes in the steady-state (later time) portions of Figure 11 through Figure 13 shows that Aspha-min clearly has a higher slope, which indicates faster relaxation of this mix. The other WMA mixes have steady-state slopes that are similar to that of the control mix.

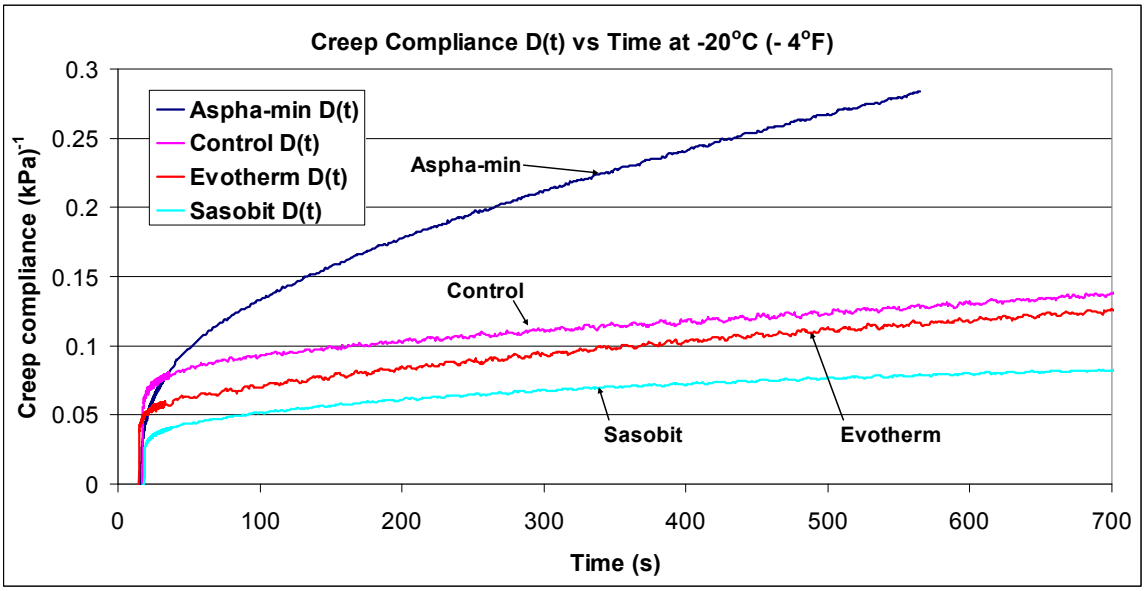

Figure 13. Creep Compliance D(t) versus Time for all mixes at -20°C (-4°F) (1 kPa^{-1} = 6.89 in^2/lb).

4.2.2 Core Samples from APLF and State Route (SR 541)

Core samples were collected from State Route 541 three months after construction, one year after construction, and again twenty months after construction. These cores were collected in two places, the center line and the wheel path. There were four different kinds of cores corresponding to the different surface mixes: Evotherm, Sasobit, Aspha-min, and control HMA. The first couple of inches from the top of the core were considered as new pavement. In addition, at the SR541 test site an extra strip of asphalt was constructed at the outpost at the time of the road construction. Cores were taken from this strip immediately after construction and sent to National Center for Asphalt Technology (NCAT) for an independent analysis. Cores were also taken at the APLF at the time of construction. Air void was measured for the APLF core samples and the SR541 samples collected three months and twenty months after the overlay.

The results of the data have been tabulated and graphed to compare the warm mix asphalt with the conventional mix, thus clarifying which one is the best to use as a perpetual pavement material mix in place of the conventional mix. The samples at the time of construction were collected from the APLF facility in Lancaster.

Table 4. Air Void Ratio (%) for Warm Mix Asphalt (WMA) at different points in time.

Time after construction (months)	% Air Void			
	Evotherm	Sasobit	Aspha-min	Control
	Wheel Path	Wheel Path	Wheel Path	Wheel Path
0 (APLF)	5.4	4.2	4.9	7.7
3	4.9	6.5	6.8	7.7
20	4.3	5.3	5.9	5.7

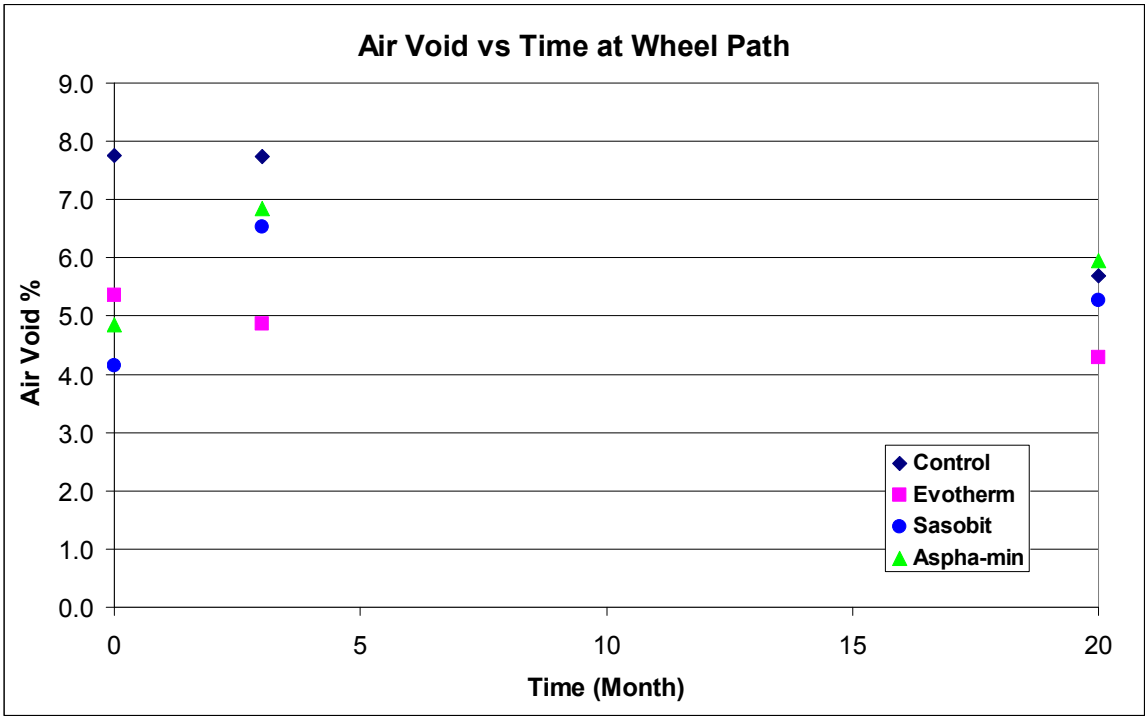

Figure 14. Air Void Ratio for Control and WMA mixes as a function of time after construction in months. Values at 0 month are for APLF, others from GUE-541.

Figure 14 and Table 4 show that the air void decreases after twenty months of exposure to traffic. The lower values recorded at the time of construction may be due to the samples being collected at the APLF rather than from SR 541. The APLF mix is the same as the SR541 mix in each case (the material came from the same batch at the same plant, which was transported to both locations), but the compaction of the pavements may have been somewhat different.

The following tables show the indirect tensile strength for samples collected from APLF right after construction and from SR 541, three, twelve, and twenty months after opening the road to traffic. The equations to calculate the indirect tensile strength are as follows [Buttlar, and Roque, 1994]:

$$St,n = \frac{2 \times Pf,n}{\pi \times Bn \times Dn} \quad \text{..... (3.21)}$$

Bn, Dn = thickness, and diameter of specimen *n* (*n* =1 to 3).
Pf,n = first failure load for specimen, n; and
St,n = tensile strength of specimen, n;

$$St = \frac{\sum_{n=1}^{3} St,n}{3} \quad \text{..... (3.22)}$$

St = average indirect tensile strength of mixture.

The samples were taken from the center line and wheel path. The indirect tensile strength for the control section did not vary significantly between the two locations, and for this reason

only the wheel path data were used for all sections. The indirect tensile strength of each core was measured at room temperature in the laboratory. The test results are displayed in Table 5 and plotted in Figure 15. The indirect tensile strength remains within the same range, 100-160 psi (690-1100 kPa) over time, with the slight dips at 12 months explainable by the fact that the cores were taken in the summer, when the heat made the coring process more likely to disturb the cores. The main conclusion is that no significant difference in indirect tensile strength is seen between the different mixes.

Table 5. Indirect Tensile Strength at 25°C (85°F) for all mixes in wheel path at different periods of time.

Time after construction (months)	Indirect Tensile Strength in wheel path (psi)			
	Evotherm	Sasobit	Aspha-min	Control
0 (APLF)	96.5	157.4	147.5	116.5
3	121.9	120.8	128.2	112.3
12	105.5	84.3	95.2	114.9
20	117.8	145.9	136.2	122.9

Time after construction (months)	Indirect Tensile Strength in wheel path (MPa)			
	Evotherm	Sasobit	Aspha-min	Control
0 (APLF)	0.67	1.09	1.02	0.80
3	0.84	0.83	0.88	0.77
12	0.73	0.58	0.66	0.79
20	0.81	1.01	0.94	0.85

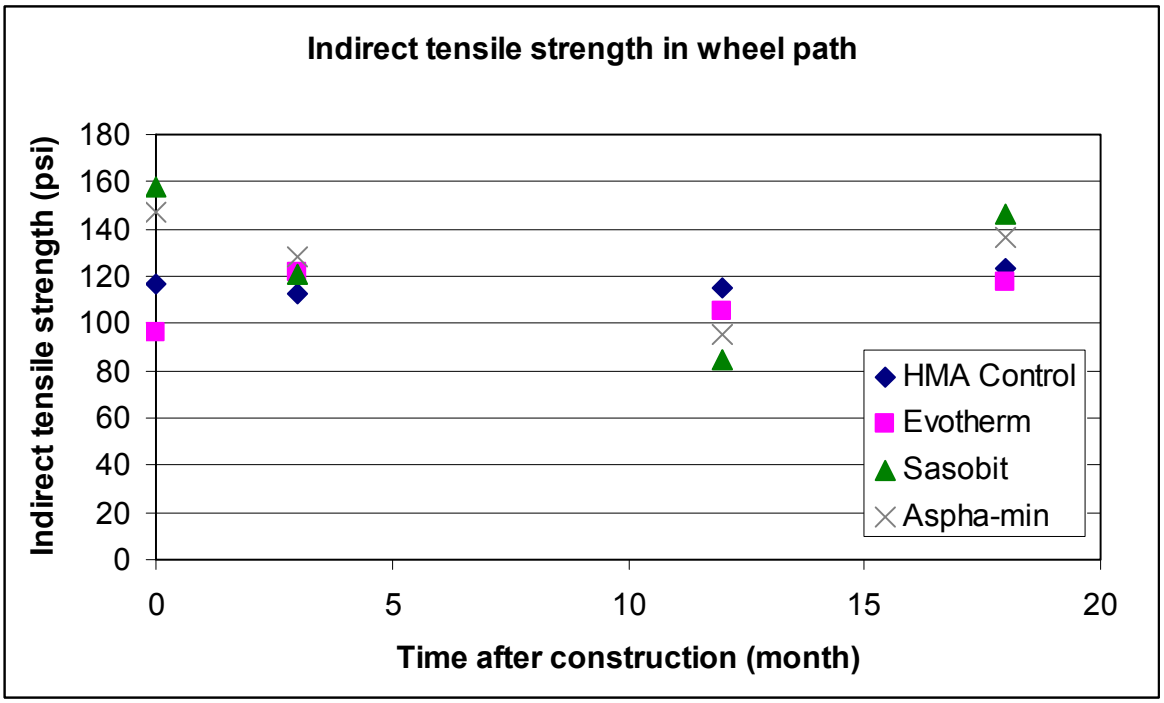

Figure 15. Indirect Tensile Strength in Wheel Path for Control and WMA mixes.

4.3 Additional Warm Mix Asphalt Properties

Samples of the three WMA mixes and the HMA control mix were sent to the National Center for Asphalt Technology (NCAT) at Auburn University for analysis. Their report will be submitted separately to ODOT.

Properties to be included in the testing were listed in the proposal:

"Specimens will be tested to determine their engineering properties including resilient modulus at a minimum of three temperatures and three frequencies, fatigue and rutting characteristics, long term durability an aging, low temperature cracking resistance, as well as moisture resistance and to assess their physical properties. The effects of lowered production temperatures on asphalt binder aging will also be investigated. For this, in addition to mixture property measurements, one or more sets of asphalt binders will be prepared with modified RTFO/PAV aging conditions reflecting the reduced production temperature. Tests will be performed on each binder according to AASHTO MP1. WMA and conventional asphalt mixes will also be tested using the LWT (Load Wheel Testing) device available at ORITE, to determine the rutting potential of all mixes.

"The laboratory study will also include testing of granular base materials and subgrade soils placed in the APLF to determine their resilient modulus along with the K_1, K_2 and K_3 coefficients following NCHRP 1-37A Guidelines."

5 ROUGHNESS MEASUREMENTS ON GUE-541

Roughness measurements were made on the entire overlay on GUE-541 by ODOT on December 20, 2006, shortly after construction, and two years later, on December 11, 2008. On both occasions the road was dry. Measurements were taken on both westbound and eastbound lanes, applying a 528 ft (160.9 m) segment length with a 250 mm (9.8 in) filter and no point reset. The ProVAL reports reported left and right IRI elevation data for each segment in units of in/mi (1 in/mi = 15.78 mm/km or 0.00001578 m/m). The average of the left and right IRI, or MRI values were computed for each segment. Each segment was also identified by type of WMA surface treatment applied. For each WMA section the boundary segments were discarded as not completely of one type of WMA; the remaining values were averaged to obtain an overall mean for that treatment. The standard deviation and standard deviation of the mean computed; the latter by dividing by the square root of the number of data points averaged.

Graphs of the left and right and average elevations from 2006 are presented in Figure 16 for eastbound lanes and Figure 17 for westbound lanes, and those from 2008 in Figure 18 for eastbound lanes and Figure 19 for westbound lanes. In addition to the actual data, the endpoints of each section are indicated and within each section the mean and single standard deviation range boundaries marked with horizontal lines. One can see the average IRI values are about the same for each section, thus the smoothness of ride, as measured by IRI, is about the same for each WMA section as for the HMA. The means, standard deviations, standard deviations of the mean, and differences of each mean from the HMA mean value are given in Table 6 for 2006 and Table 7 for 2008. In all but one case, for each WMA section, for both measurements, the absolute value of the difference between the mean of each WMA treatment and the HMA control section is less than the sum of the standard deviations of the mean of that WMA section and the HMA section, indicating that the mean IRI of each WMA section is statistically indistinguishable from the HMA mean. The exception is the Sasobit section measurement from 2006, which has a slightly lower value than the HMA.

Table 8 shows the differences between the 2008 and 2006 means for each section. In the WAY30 project report [Sargand, Figueroa, and Romanello, 2008], the IRI criterion for failure used in the ME-PDG simulation was 0.002710 (2710 mm/km or 172 in/mi). The values measured on GUE-541 range from 50.73% to 57.66% of this value, indicating that the IRI of these test sections are all well below this value. In addition, the difference between the 2008 and 2006 IRI values does show a trend towards increased IRI over the two years. This trend, if linearly extrapolated, indicates that failure will not occur for at least 16 years, as shown in Table 8. However, two data points, each with a fairly large uncertainty as represented by standard deviation, are too few to make solid judgment of pavement surface longevity. Some additional measurements at 5 or 10 years may yield a better answer.

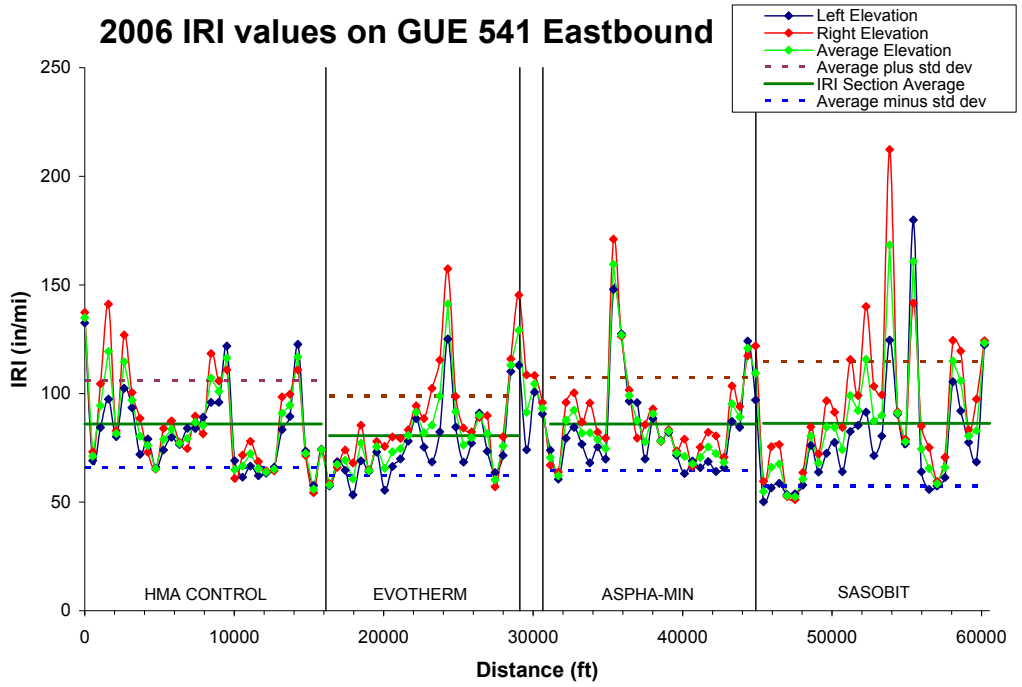

Figure 16. IRI values measured in December 2006 on GUE-541 Eastbound, with averages and single standard deviation ranges marked in each section. (1 in/mi = 15.78 mm/km = 0.00001578 in dimensionless units). See Color Plate 3 in Appendix E.

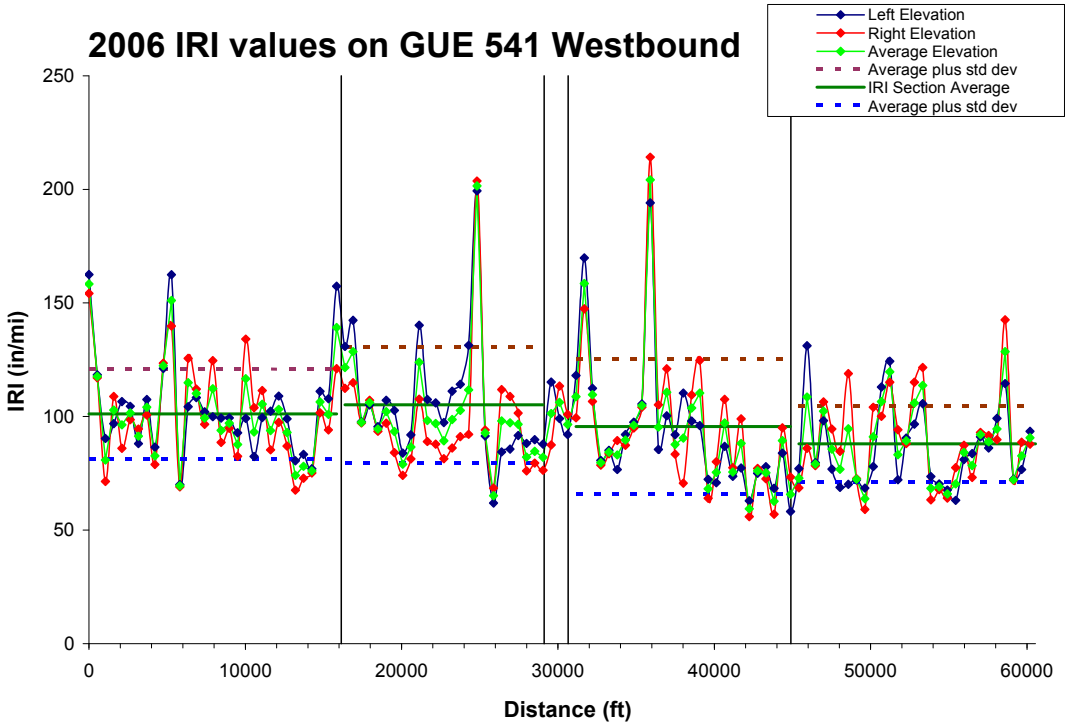

Figure 17. IRI values measured in December 2006 on GUE-541 Westbound, with averages and single standard deviation ranges marked in each section. (1 in/mi = 15.78 mm/km = 0.00001578 in dimensionless units). See Color Plate 4 in Appendix E.

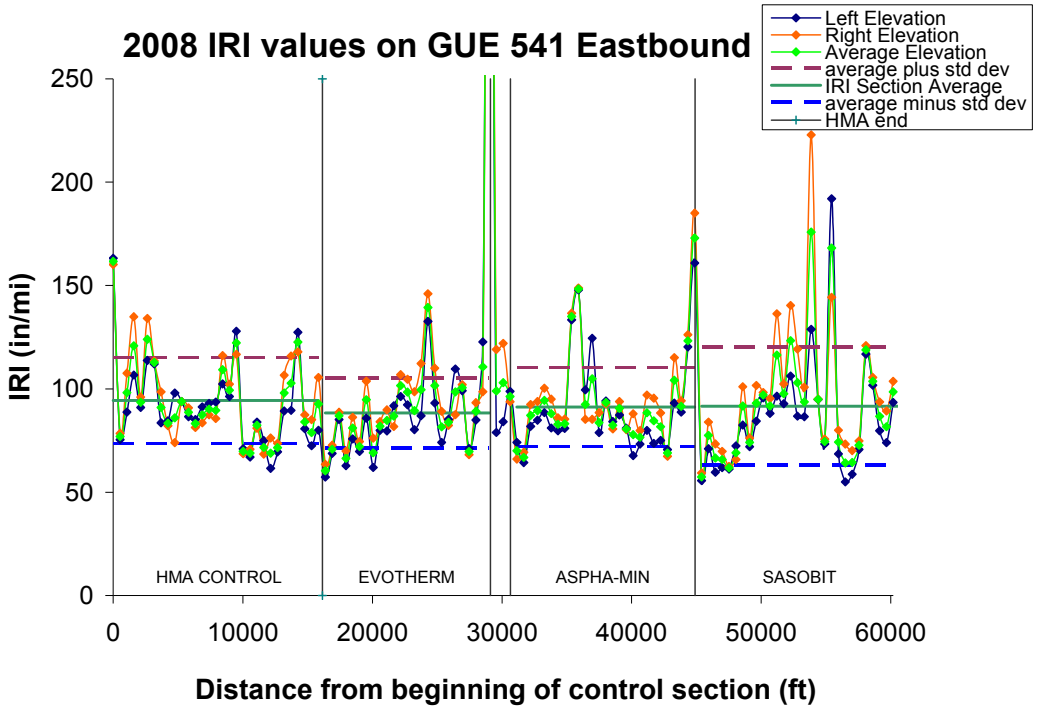

Figure 18. IRI values measured in December 2008 on GUE-541 Eastbound, with averages and single standard deviation ranges marked in each section. (1 in/mi = 15.78 mm/km = 0.00001578 in dimensionless units). See Color Plate 5 in Appendix E.

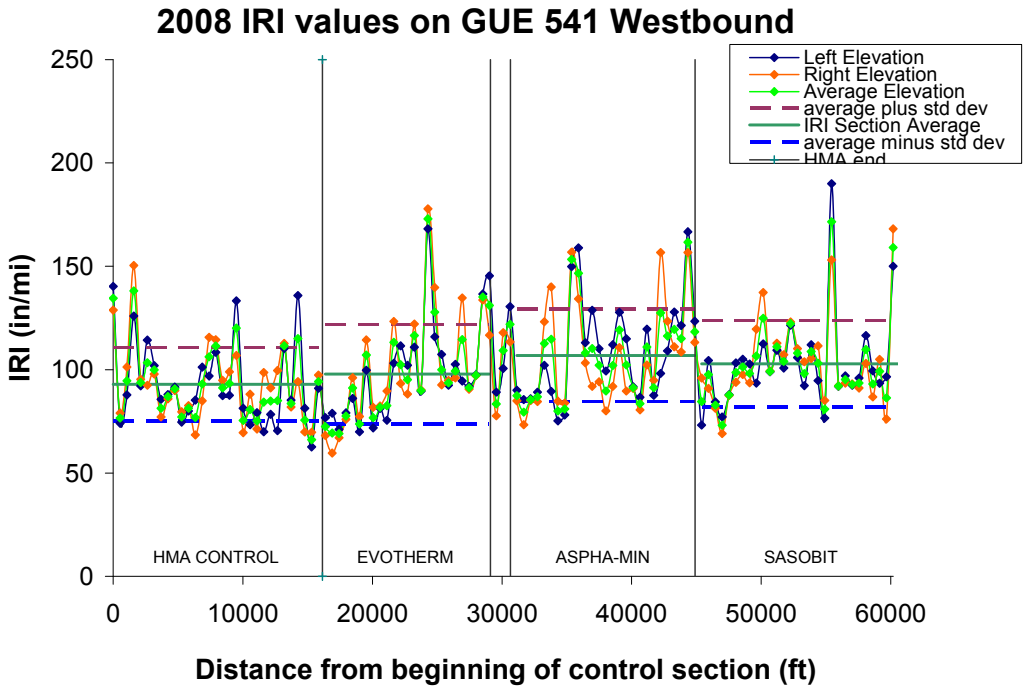

Figure 19. IRI values measured in December 2008 on GUE-541 Westbound, with averages and single standard deviation ranges marked in each section. (1 in/mi = 15.78 mm/km = 0.00001578 in dimensionless units). See Color Plate 6 in Appendix E.

Table 6. Average IRI values (μ) for each section of GUE-541 as measured in December 2006. Also included are standard deviation (σ), standard deviation of the mean (σ_m), and difference from HMA mean (Δ). Data are averaged over eastbound and westbound directions of each section.

	Surface	HMA	Evotherm	Aspha-min	Sasobit
	N	60	50	52	58
(in/mi)	μ	93.57	91.89	90.77	87.10
	σ	21.16	24.60	26.12	23.32
	σ_m	2.732	3.479	3.622	3.063
	Δ	-	-1.678	-2.797	-6.463
(mm/km)	μ	1477	1450	1433	1375
	σ	334	388	412	368
	σ_m	43	55	57	48
	Δ	-	-26	-44	-102
(%)	σ	22.62%	26.77%	28.77%	26.78%
	σ_m	2.920%	3.786%	3.990%	3.516%
	Δ	-	-1.79%	-2.99%	-6.91%

Table 7. Average IRI values (μ) for each section of GUE-541 as measured in December 2008. Also included are standard deviation (σ), standard deviation of the mean (σ_m), and difference from HMA mean (Δ). Data are averaged over eastbound and westbound directions of each section.

	Surface	HMA	Evotherm	Aspha-min	Sasobit
	N	60	48	52	58
(in/mi)	μ	93.66	93.11	99.01	97.27
	σ	19.21	21.20	22.05	25.34
	σ_m	2.480	3.060	3.058	3.327
	Δ	-	-0.544	5.348	3.610
(mm/km)	μ	1478	1470	1563	1535
	σ	303	335	348	400
	σ_m	39	48	48	53
	Δ	-	-9	84	57
(%)	σ	20.51%	22.77%	22.27%	26.05%
	σ_m	2.648%	3.286%	3.089%	3.420%
	Δ	-	-0.58%	5.71%	3.85%

Table 8. Differences in mean IRI values between 2008 and 2006 measurements for each test section on GUE-541, value of IRI failure criterion used in Sargand, Figueroa, and Romanello [2008], mean IRI as a fraction of failure criterion, and years to failure based on linear extrapolation of measurements.

	Surface	HMA	Evotherm	Aspha-min	Sasobit
Δ_μ	(in/mi)	0.09	1.23	8.24	10.17
	(mm/km)	1.47	19.37	130.03	160.45
	(%)	0.10%	1.32%	8.32%	10.45%
Failure IRI	(in/mi)	171.7	171.7	171.7	171.7
	(mm/km)	2710	2710	2710	2710
μ/Failure	2006	54.49%	53.51%	52.86%	50.73%
	2008	54.55%	54.23%	57.66%	56.65%
Time to failure	(yr)	1674	130.0	19.65	16.64

Time to failure based on linear extrapolation of change in IRI

5.1 Pavement condition observations

Visual inspections by ORITE personnel while taking core samples or making other measurements such as the IRI measurements discussed above did not indicate any problems developing any of the pavement sections. ODOT's regular inspection of that pavement in 2007, conducted about 14 months after the resurfacing, gave the pavement a score of 99, with no structural deductions, a significant improvement over the previous surface. ODOT's pavement condition ratings for SR541 from 2005, 2006, and 2007 are shown in Table 9; the 2005 and 2006 evaluations were conducted before applying the WMA pavement. The only damage listed in 2007 was low levels of occasional raveling. ODOT defines raveling in its Pavement Condition Rating Manual [ODOT, 1998] as "Disintegration of the pavement from the surface downward due to the loss of aggregate particles". Low level raveling consists of the loss of fine aggregate at the surface, with little loss of coarse aggregate, and occasional raveling means less than 20 percent of the surface is affected. Occasional low-level raveling such as this is to be expected from new asphalt pavements in the first year of service.

Table 9. ODOT Pavement Condition Ratings of GUE541 project pavements in 2007 and of the preexisting pavement in 2005 and 2006.

												raveling	bleeding	patching	surface disintegration or debonding	crack seal deficiency	rutting	settlement	corrugations	wheel track cracking	block cracking	longitudinal joint cracking	edge cracking	random cracking	thermal cracking	pot holes
County	Route	BLOG	ELOG	Length	PCR	Total Deduct	Structural Deduct	Month	Day	Year	Project No.	Code 1	Code 2	Code 3	Code 4	Code 5	Code 6	Code 7	Code 8	Code 9	Code 10	Code 11	Code 12	Code 13	Code 14	Code 15
COS	541R	31.87	34.90	3.03	99	1.5	0	9	10	07	30106	LO														
GUE	541R	0.00	8.48	8.48	99	1.5	0	10	26	07	30106	LO														
COS	541R	31.87	34.90	3.03	65	34.9	17.6	5	23	06	68294	LE		LO	LO	F	MF	LO		MO	MF	MO	MF		MO	
GUE	541R	0.00	7.28	7.28	70	29.6	16.2	7	5	06	68294	LE		LO		O	MO			MO	MO	MO	MF		MO	
GUE	541R	7.28	8.48	1.20	67	33.3	14.7	7	5	06	68294	LE		MO		F	MO	LO		LE	MF	LO	MO		MF	
COS	541R	31.87	34.90	3.03	67	33.5	16.2	9	26	05	68294	LE		LO	LO	F	MO			MO	MF	MO	MF		MO	
GUE	541R	0.00	7.28	7.28	70	30.5	16.2	9	15	05	68294	LE		MO		O	MO			MO	MO	MO	MF		MO	
GUE	541R	7.28	8.48	1.20	67	33.3	14.7	9	15	05	68294	LE		MO		F	MO			LE	MF	LO	MO		MF	

6 COMPARISON OF TEMPERATURES AND EMISSIONS

6.1 Comparison of temperatures during installation

An infrared camera was used to record temperatures of the surface courses of different mixes during construction at the GUE-541 field site and at the APLF. Figure 20 shows sample images taken with the infrared camera of each type of mix used in the project. For Aspha-min, only images from SR541 are available, while for the conventional mix, only images from the APLF installation are available; for the other two mixes there are images from both project installations. In each image, the number in the upper right is the temperature read at the location where the cross hairs (large +) at the center of the image is focused, and the bar on the right is a false color scale showing the range of temperature readings. All temperatures in these images are in Fahrenheit. Generally speaking, for the images from the APLF, the bottom of the picture is off the edge of the asphalt, and the temperatures are very low, just above 102-113°F (39-45°C). The high ends of the scales on all pictures represent the temperatures of the asphalt, however, and the low temperatures on the SR541 images are also likely to be asphalt temperatures.

Table 10 compares the average maximum temperatures observed in the infrared images for each mix at each location. For example, there were 5 images from the Aspha-min construction at SR541. From each picture the number at the top of the scale on the right was taken as the maximum value, and the five values were averaged to obtain the average, denoted μ on the table. A standard deviation, σ was also computed. The number of available images (N in the table) ranged from 3 for the HMA and Sasobit mixes at the APLF to 9 for the Sasobit mixes on SR541. The temperature difference, ΔT, was computed by subtracting each mix's average from that of the HMA; by definition that for the HMA is 0. The ratio of the temperature difference to the standard deviation, $\Delta T/\sigma$, is greater than 3 in all cases, and sometimes much higher, indicating that the warm mix asphalt mixes are clearly being applied at a cooler temperature than the HMA. Table 11 replicates the same analysis as for Table 10, but this time using the selected "cross-hair" temperatures in the upper right of each image. The other difference is that two of the Sasobit SR541 images were not included because in those images the cross-hairs were aimed at the paving machine rather than at the pavement. Again, the values show that all the warm mixes are clearly cooler than the HMA control. Note also that the WMA maximum temperatures recorded at the APLF are about 13°F (7C°) lower than those at SR541; this difference can be attributed to the longer travel time from the Mar-Zane asphalt plant in Zanesville.

These results were also confirmed by the subcontractor emissions report [EES Group, 2006], who report that the working temperatures for the HMA mixes were 50 to 70°F (28 to 39 C°) cooler than the HMA.

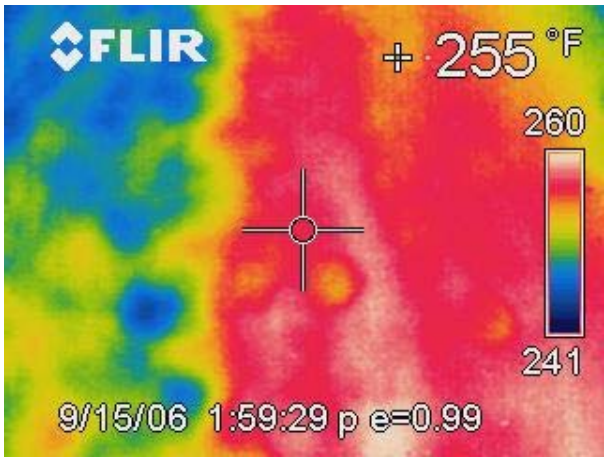

a) Aspha-min on SR541

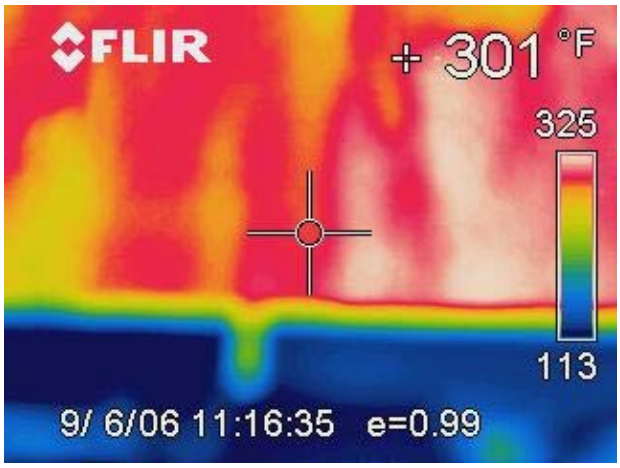

b) HMA Control mix in APLF

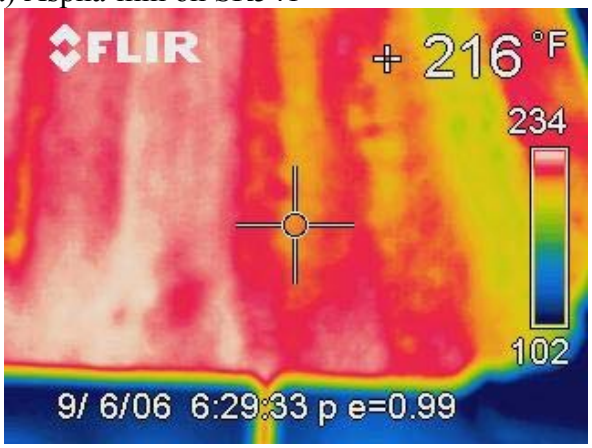

c) Evotherm mix in APLF

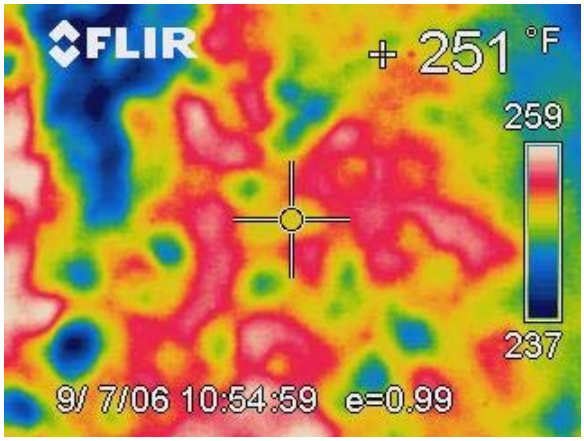

d) Evotherm mix on SR541

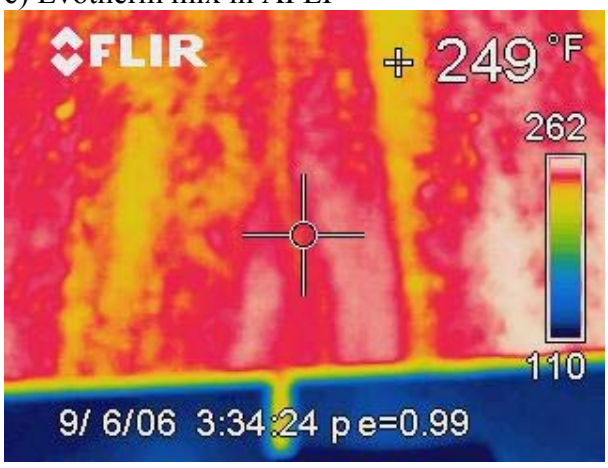

e) Sasobit mix in APLF

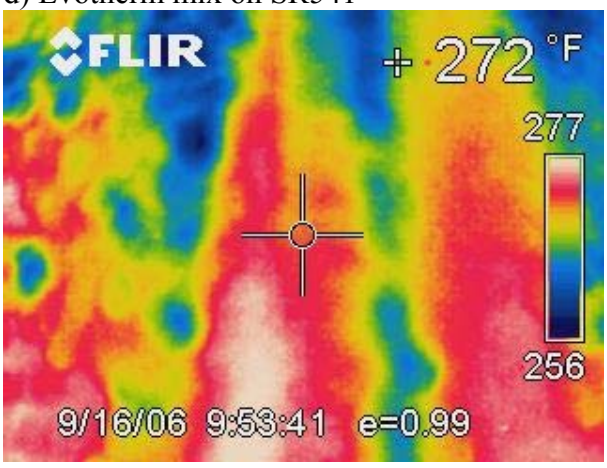

f) Sasobit mix on SR541

Figure 20. Infrared camera pictures of HMA and WMA mixes at time of construction. The number in the upper right corner is the temperature registered at the location of the large cross-hairs in the image, and the scale at the right edge shows the colors associated with temperatures over the entire image. All temperatures are in Fahrenheit. The lowest temperatures in the APLF images are off the pavement area. See Color Plate 7 in Appendix E.

Table 10. Maximum temperatures as registered on infrared camera images taken at APLF and SR541 sites.

Maximum temperature		μ		σ		ΔT				ΔT_{avg}	
Mix	Site	(°F)	(°C)	(°F)	(C°)	(°F)	(C°)	ΔT/σ	N	(°F)	(C°)
Aspha-min	SR541	259.6	126.4	1.1	0.6	59.1	32.8	51.8	5	44.1	24.5
Control HMA	APLF	318.7	159.3	7.8	4.3	0	0	0	3	0	0
Evotherm	APLF	235.8	113.2	7.7	4.3	82.9	46.1	10.8	4	75.5	41.9
	SR541	250.6	121.5	7.0	3.9	68.0	37.8	9.7	8		
Sasobit	APLF	261.7	127.6	0.6	0.3	57.0	31.7	98.7	3	51.4	28.5
	SR541	272.9	133.8	13.8	7.7	45.8	25.4	3.3	9		

Note on symbols: μ is the average, σ is the standard deviation, ΔT is the difference between the average of the given mix and that of the conventional HMA at the APLF, N is the number of images over which the average was taken, and ΔT_{avg} is the average over both APLF and SR541, where applicable.

Table 11. Selected temperatures as registered at cross-hairs at center of infrared camera images taken at APLF and SR541 sites.

Selected temperature		μ		σ		ΔT				ΔT_{avg}	
Mix	Site	(°F)	(°C)	(°F)	(C°)	(°F)	(C°)	ΔT/σ	N	(°F)	(C°)
Aspha-min	SR541	253.2	122.9	2.4	1.3	44.1	24.5	18.5	5	44.1	24.5
Control HMA	APLF	297.3	147.4	11.0	6.1	0	0	0	3	0	0
Evotherm	APLF	218.0	103.3	10.0	5.5	79.3	44.1	8.0	4	65.8	36.5
	SR541	245.1	118.4	6.4	3.5	52.2	29.0	8.2	8		
Sasobit	APLF	244.3	118.0	10.8	6.0	53.0	29.4	4.9	3	38.0	21.1
	SR541	274.4	134.7	6.7	3.7	22.9	12.7	3.4	7		

Note on symbols: μ is the average, σ is the standard deviation, ΔT is the difference between the average of the given mix and that of the conventional HMA at the APLF, N is the number of images over which the average was taken, and ΔT_{avg} is the average over both APLF and SR541, where applicable.

6.2 Emissions at the project site

EES Group was subcontracted to monitor the emissions of the WMA paving operations in SR541. Their report will be submitted separately as a companion to this report [EES Group, 2006]. The major points are summarized here. To monitor the emissions, six low-volume air-sampling pumps were attached to the paver, as shown in Figure 21, and two additional pumps were mounted on tripods to collect samples upwind to monitor background air conditions, shown in Figure 22. The samplers collected 480 – 500 l (127 – 132 gal) of air over four hours. The air samples were then processed using 2.0μm filters, placed on ice, and sent to an accredited laboratory where samples were analyzed using National Institute of Safety & Health (NIOSH) Method 5042 for total particulates and benzene soluble matter. EES Group also recorded ambient weather conditions during sampling.

Figure 21. Photograph of the paving operation on SR541 showing monitoring equipment attached to paver, indicated with arrows. See Color Plate 8 in Appendix E.

Figure 22. Photograph of paving operation on SR541, showing ambient air sampling equipment on tripods in foreground. The ambient air samplers are upwind of the paving. See Color Plate 9 in Appendix E.

Salient conclusions from the environmental study report are given below; the body or summary of the report is brief and is included in Appendix B. The pollutant level values are compared to the NIOSH Respiratory Exposure Limit (REL) of 5 mg/m^3 (0.059 grain/yd^3) for Total Particulate Matter (TPM) and the American Council of Gov. Industry Hygienists Threshold Limit Value (ACGIH TLV) of 0.5 mg/m^3 (0.0059 grain/yd^3) for Benzene Soluble Matter (BSM).

- The Evotherm WMA mix exhibited a 77% reduction in Total Particulate Matter (TPM) and a 72% reduction in Benzene Soluble Matter BSM, compared with conventional HMA.
- The Aspha-min WMA mix exhibited a 67% reduction in TPM and an 81% reduction in BSM, compared with conventional HMA.
- The Sasobit WMA mix exhibited a 74% reduction in TPM and an 81% reduction in BSM, compared with conventional HMA.
- Average emissions for all three WMA mixes were below the NIOSH REL of 5 mg/m^3 for TPM and also below the ACGIH TLV of 0.5 mg/m^3 for BSM.
- The average conventional HMA emissions exceeded the ACGIH TLV of 0.5 mg/m^3 for BSM and were below the NIOSH REL of 5 mg/m^3 for TPM.
- Samples were obtained at fixed locations and may not represent the actual emissions experienced by workers around the paver.

6.3 Emissions at the plant

A stack emissions test was also conducted by Chief Environmental Group of Zanesville. The summary portion of the report is attached as Appendix B. They measured the production of the following pollutants at the plant: sulfur dioxide (SO_2), nitric oxides (NO_x), carbon monoxide (CO), and volatile organic compounds (VOC). The emissions test results are summarized in Table 12. Negative percent change values indicate a reduction in emissions compared to conventional HMA production, while positive values represent increases of emittants. Aspha-min and Sasobit both show substantial reductions in various pollutants, ranging from 83.3% for SO_2 to 21.2% for NO_x. On the other hand, Evotherm shows a negligible 1.92% decrease in NO_x, and substantial increases of the other emittants. In particular, over two and a half times as much volatile organic compounds are released in the Evotherm process compared to conventional HMA.

Table 12. Stack emissions as measured by Chief Environmental at the Shelly and Sands asphalt plant. A negative sign indicates a decrease relative to HMA emissions.

Emittant	SO_2			NO_x			CO			VOC		
Mix	(lb/hr)	(kg/hr)	(% change)	(lb/hr)	(kg/hr)	(% change)	(lb/hr)	(kg/hr)	(% change)	(lb/hr)	(kg/hr)	(% change)
Control HMA	0.24	0.109	0	5.2	2.36	0	63.1	28.62	0	7.8	3.54	0
Evotherm	0.37	0.168	54.2%	5.1	2.31	-1.92%	50.3	22.82	-20.3%	20.2	9.16	159.0%
Aspha-min	0.04	0.018	-83.3%	3.6	1.63	-30.8%	24.0	10.89	-62.0%	2.9	1.32	-62.8%
Sasobit	0.04	0.018	-83.3%	4.1	1.86	-21.2%	23.2	10.52	-63.2%	3.8	1.72	-51.3%

Notes: SO_2 is sulfur dioxide, NO_x are nitrogen oxides, CO is carbon monoxide, and VOC are volatile organic compounds

7 ACCELERATED PAVEMENT LOAD FACILITY (APLF) STUDY

7.1 Strains under Fatigue Resistance Layer (FRL) in Perpetual Pavements

Four strain gauges, two longitudinal and two transverse, were installed in each southern perpetual pavement section in the APLF, under the center line of the Fatigue Resistance Layer (FRL). Recall that the sections differed in thickness, with the Type 2 thickness varying from 7.75 in (19.7 cm) down to 4.75 in (12.1 cm) and the DGAB underneath changed to compensate for the change in Type 2 depth. The overall thicknesses of the sections were 13 in (33.0 cm), 14 in (35.6 cm), 15 in (38.1 cm), and 16 in (40.6 cm); each also had a different mix on the surface layer, though the effect of the surface layer on the responses measured in the sensors in the FRL and base layers was expected to be negligible. Rolling wheel loads (RWL) of 6000 lb (26.7 kN), 9000 lb (40 kN), and 12000 lb (53.4 kN) were applied by the speed-controlled tire at 5 mph (8 km/h) before and after the set of 10,000 runs (load wheel passes) with a 9000 lb (40 kN) load applied at each temperature. RWLs were applied in both directions. During each measurement session, each load was applied four times across the section along four different parallel tracks laterally shifted by the following amounts from the sensor line: 1 inch (25.4 mm), 3 inches (76.2 mm), -4 inches (-102 mm), and -9 inches (-229 mm), where positive is east (left) of the sensor line. Table 13, Table 14, and Table 15 show the longitudinal and transverse strain in microstrains (με) in the FRL after 0 runs (before the first run) with an ambient temperature of 40°F (4.4°C), 70°F (21.1°C), and 104°F (40°C), respectively.

Table 13. Longitudinal and Transverse Strain in Fatigue Resistance Layer (FRL) in APLF under Rolling Wheel Load after 0 runs and 40°F (4.4°C).

				Strain (με) at bottom of FRL after 0 runs at 40°F (4.4°C)							
AC thickness				13" (33.0 cm)		14" (35.6 cm)		15" (38.1 cm)		16" (40.6 cm)	
Item 448 layer thickness				4.75" (12.1 cm)		5.75" (14.6 cm)		6.75"(17.1 cm)		7.75" (19.7 cm)	
Wheel load		Lateral shift		Evotherm surface		Sasobit surface		Aspha-min surface		HMA surface	
(lb)	(kN)	(in)	(mm)	Long	Tran	Long	Tran	Long	Tran	Long	Tran
6000	26.7	3	76.2	11.4	14.85	11.35	13.75	11.05	13.95	12.05	12.85
		1	25.4	11.2	14.55	11.2	14.15	11.85	13.6	17.1	18.15
		-4	-102	11.3	13.8	10.7	12.9	11.85	12.3	24.6	25.35
		-9	-229	8.9	11.85	8.35	12.7	7.65	10.35	11.55	12.75
9000	40	3	76.2	17	21.7	17.15	20.85	16.4	20.15	17.5	18.65
		1	25.4	17.6	21.95	17.35	21	18.15	20.75	24.3	25.1
		-4	-102	17.75	20.6	17.15	20.5	18.05	20.3	10.8	11.8
		-9	-229	13.2	17.6	11.7	18.35	12.7	17.55	16.9	17.8
12000	53.4	3	76.2	24.6	30.15	23.7	27.8	22.45	27.05	22.35	23.8
		1	25.4	24.5	29.5	24.05	28	23.65	27	7.75	10.3
		-4	-102	24.55	27.25	23.35	27.5	23.75	26.75	11.75	15.4
		-9	-229	18.25	23.65	15.85	24.8	16.5	23.45	11.8	15.3

Table 14. Longitudinal and Transverse Strain in Fatigue Resistance Layer (FRL) in APLF under Rolling Wheel Load after 0 runs and 70°F (21.1°C).

				Strain (με) at bottom of FRL after 0 runs at 70°F (21.1°C)							
AC thickness				13" (33.0 cm)		14" (35.6 cm)		15" (38.1 cm)		16" (40.6 cm)	
Item 448 layer thickness				4.75" (12.1 cm)		5.75" (14.6 cm)		6.75"(17.1 cm)		7.75" (19.7 cm)	
Wheel load		Lateral shift		Evotherm surface		Sasobit surface		Aspha-min surface		HMA surface	
(lb)	(kN)	(in)	(mm)	Long	Tran	Long	Tran	Long	Tran	Long	Tran
6000	26.7	3	76.2	23.2	34	23	32.4	26.2	32.75	20.65	21.4
		1	25.4	22.3	32.9	21.55	31.75	27.6	33.7	20.35	21.9
		-4	-102	23	30.25	22.9	30.25	33.3	33.15	17.3	20.2
		-9	-229	16.5	24.85	13.4	27.9	20.55	28.8	8.75	16.85
9000	40	3	76.2	33.75	49	37.4	52.05	38.65	48	33	33.3
		1	25.4	35.45	49.6	34.6	48.2	42.9	50	31.85	32.75
		-4	-102	35.75	44.85	34.65	46.45	48.2	48.5	28	30.7
		-9	-229	24.25	37.05	18.15	40.05	29.7	43.8	14.25	25.6
12000	53.4	3	76.2	49.9	67.95	54.45	71.95	58.85	69.7	47.3	46.6
		1	25.4	49.85	66.45	54.1	72.8	63.8	70.85	46.8	46.3
		-4	-102	51.3	62.15	54.45	69.05	66.4	68.8	41.05	43.15
		-9	-229	35.75	52.2	28.6	59.2	41.6	60.7	21.25	37

Table 15. Longitudinal and Transverse Strain in Fatigue Resistance Layer (FRL) in APLF under Rolling Wheel Load after 0 runs and 104°F (40°C).

				Strain (με) at bottom of FRL after 0 runs at 104°F (40°C)							
AC thickness				13" (33.0 cm)		14" (35.6 cm)		15" (38.1 cm)		16" (40.6 cm)	
Item 448 layer thickness				4.75" (12.1 cm)		5.75" (14.6 cm)		6.75"(17.1 cm)		7.75" (19.7 cm)	
Wheel load		Lateral shift		Evotherm surface		Sasobit surface		Aspha-min surface		HMA surface	
(lb)	(kN)	(in)	(mm)	Long	Tran	Long	Tran	Long	Tran	Long	Tran
6000	26.7	3	76.2	15	74.35	3.9	55.55	8.5	56.9	27.15	46.2
		1	25.4	14.6	76.7	3.6	55.25	15.6	64.1	28.3	46
		-4	-102	34.6	70.85	9.25	52.1	38.2	67.3	29.05	42.15
		-9	-229	25.45	54.55	2.05	44.1	22.9	55.65	9.1	34.95
9000	40	3	76.2	22.7	118.65	6.65	92.45	17.45	97.05	47.5	75.9
		1	25.4	24.65	122.7	7	98.4	27.9	107.55	49.1	73.25
		-4	-102	57.85	113.8	14.6	92.7	63.65	108.1	51.5	70.25
		-9	-229	42.8	88.5	3.45	77.95	35.95	92.45	14.4	58.95
12000	53.4	3	76.2	37.15	178.4	12.75	144.4	33.85	155.3	74.1	109.3
		1	25.4	41.45	185.8	13.75	151	48.25	167.65	78.4	111.6
		-4	-102	85.7	172.1	24.35	145.65	98	168.95	78.2	105.9
		-9	-229	65.75	136.65	7.35	124	57.1	141.95	26.3	86.7

The data in Table 13, Table 14, and Table 15 indicate that the transverse strains observed in the FRL under the thinner pavements are considerably higher than in the FRL under the ful;l-

depth 16 in (40.6 cm) pavement. This trend holds at all temperatures and under all loads, and is most pronounced under the highest load at the highest temperature. That said, the magnitude of the longitudinal strains stays below the critical design parameter of 70 με at all times, with a few exceptions under 12 kip (53.4 kN) at the high temperature. Because the APLF conditions represent a uniform high temperature of 104°F (40°C) without a gradient, these results represent extreme conditions not likely to appear in the field. In addition, the full-depth section with the thickest intermediate layer performed about as well as the other sections. This suggests that it may be possible to maintain perpetual pavement conditions in a thinner pavement structure compensated for by a thicker and stiffer base.

Figure 23 shows the longitudinal strain in microstrains in the fatigue resistance layer. The longitudinal strain for the conventional mix increases with increasing load and ambient temperature.

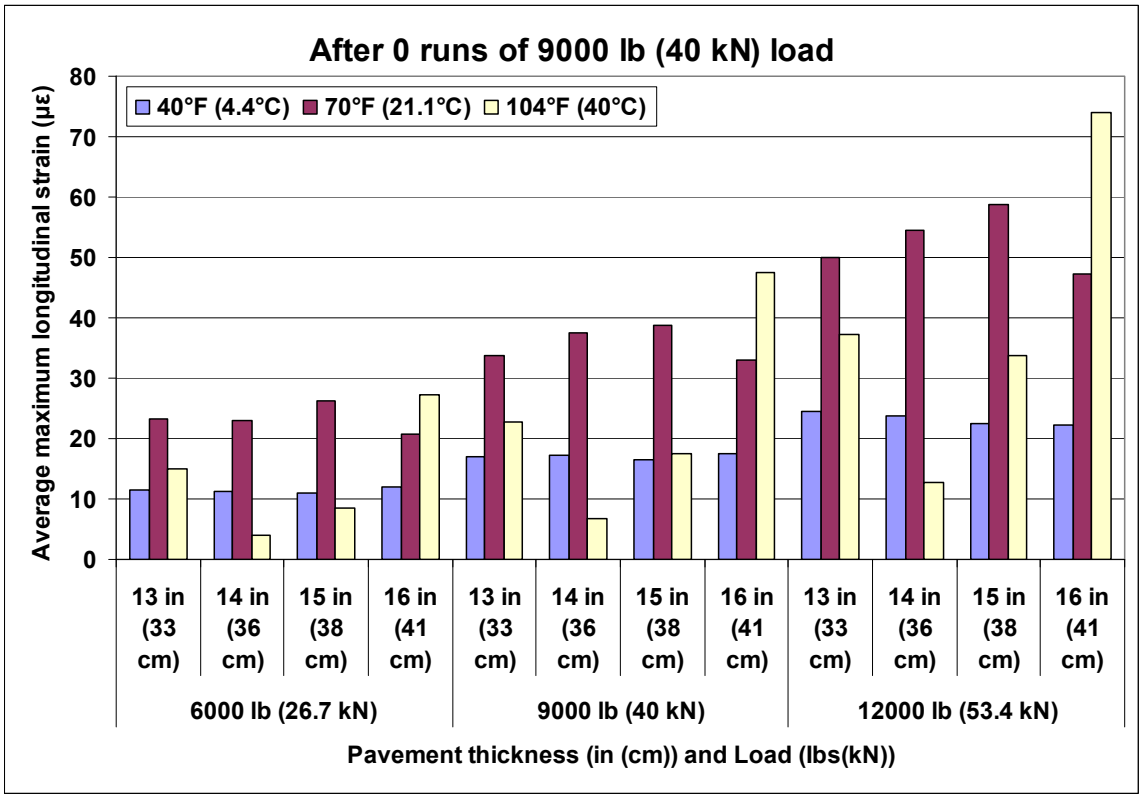

Figure 23. Longitudinal Strain in Fatigue Resistance Layer (FRL) in APLF after 0 runs.

Figure 24 illustrates the transverse strain under the fatigue resistance layer. The strain increases as the load of the rolling wheel and the ambient temperature of the facility are increased. There is also a relationship to the resilient modulus of asphalt layer. The stiffness of the asphalt layer decreases when the temperature increases, resulting in an increase in the strain under the fatigue resistance layer. The strain differs from one section to another at the same load and ambient temperature. Comparatively, the thinnest (13 in (33 cm)) section had a higher strain under fatigue resistance layer than the other sections tested.

The strain under the fatigue resistance layer increases as the thickness of the intermediate asphalt layer is decreased. High strain at the bottom of the fatigue resistance layer with a repeated load will cause fatigue cracking for the asphalt pavement. Fatigue cracking can be prevented by increasing the asphalt thickness.

For the thinner sections, the strain under the fatigue resistance layer was almost the same for the same load and at an ambient temperature of 40°F (4.4°C) and 70°F (21.1°C). The strain is lower for the full-depth section for the same load at an ambient temperature of 40°F (4.4°C) and 70°F (21.1°C). The performance of the asphalt layer of the thinnest section is very close to that of the control sections at lower temperatures.

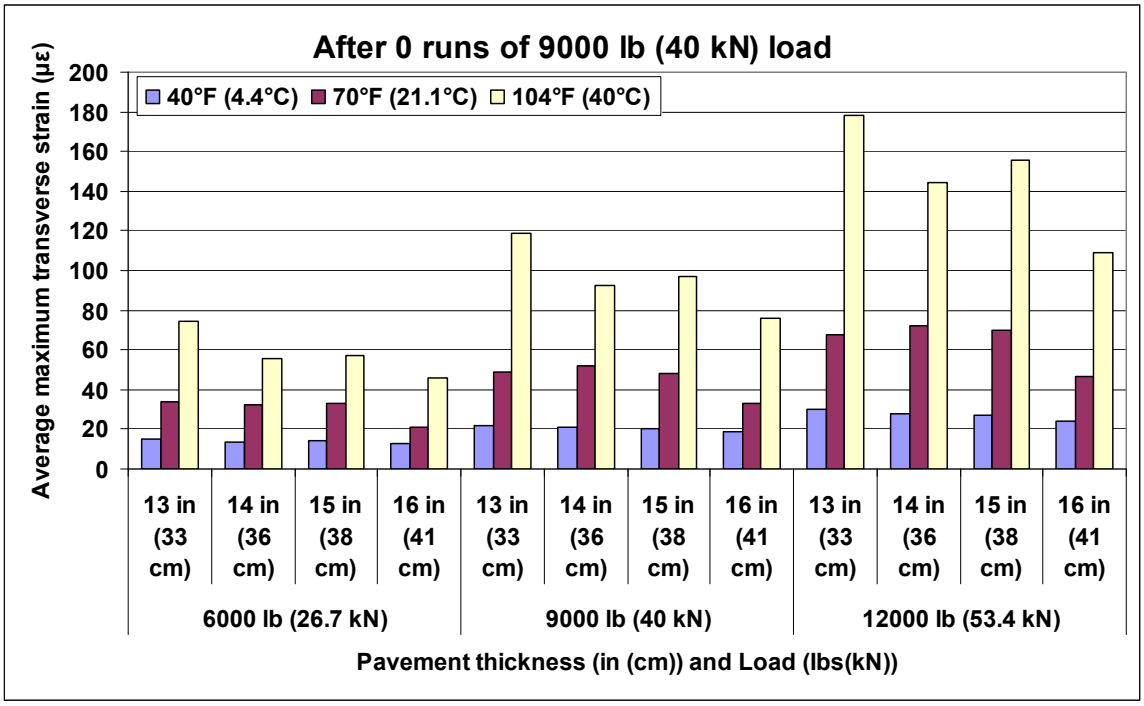

Figure 24. Transverse Strain in Fatigue Resistance Layer (FRL) in APLF after 0 runs.

Figure 25 shows the longitudinal and transverse strains under the fatigue resistance layer (FRL) of the 13 inch (33 cm) perpetual pavement section at 40°F (4.4°C). The following are the observations collected from a wheel that ran from north to south. As the wheel approached the first longitudinal strain gauge (DYN-016 in Figure 25) a compression strain developed on that gauge, indicated by the negative value at approximately time = 4.7 seconds. When the wheel was directly over the gauge at time = 5 seconds, a tensile strain developed on the same gauge. Then, a compression strain developed as the wheel left the gauge, signified by the negative strain at time = 5.8 seconds. For the transverse strain gauge (DYN-015 in Figure 25), only a tensile strain is observed, peaking at about time = 5.3 seconds. The other two traces, DYN-014 and DYN-013 in Figure 25, are for the second longitudinal and second transverse strain gauge, and mimic the curves of the other gauges. This process was repeated every time the axle load passes over the pavement. The repeated compression and tension strain in the longitudinal direction caused a permanent deformation in the asphalt layer, which manifests as rutting and fatigue cracking after sufficient repetitions.

The data collected from the graph in Figure 25 was entered into Table 13 through Table 18 as follows: the two peak values of the longitudinal strains were determined (time = 5 seconds for DYN-016 and time = 5.3 seconds for DYN-014 in the figure) and these two values averaged for entry into the appropriate place in the appropriate table as a longitudinal strain. Similarly, the two peaks for the other two sensors (DYN-015 and DYN-013) were averaged to obtain the transverse strain values for the tables.

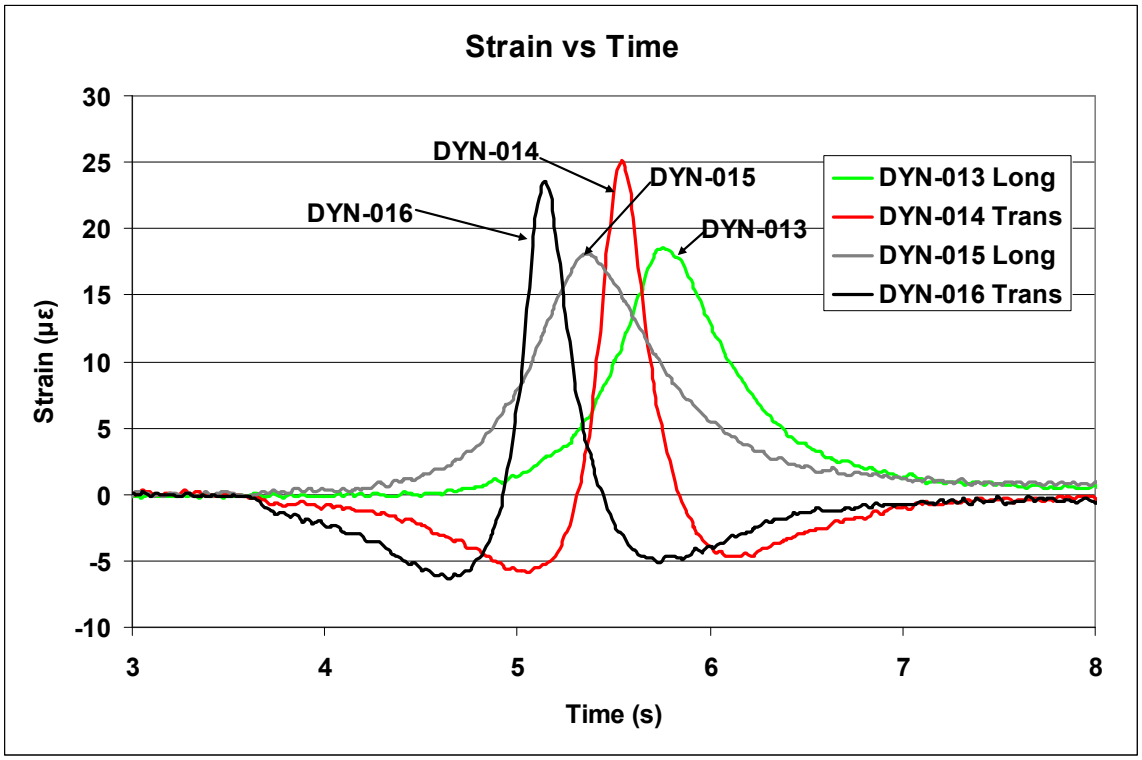

Figure 25. Example data for Longitudinal and Transverse Strain as function of time during loaded rolling wheel pass in Fatigue Resistance Layer (FRL) in APLF. See Color Plate 10 in Appendix E.

Table 16, Table 17, and Table 18 show the longitudinal and transverse strain in microstrains (με) in the Fatigue Resistance Layer (FRL) after 10,000 runs or passes of the 9000 lbs (40 kN) load wheel. The ambient temperature was 40°F (4.4°C), 70°F (21.1°C), and 104°F (40°C), respectively. The Rolling wheel loads (RWLs) of 6000 lbs (26.7 kN), 9000 lbs (40 kN), and 12000 lbs (53.4 kN) were applied. Longitudinal and transverse strains under the fatigue resistance layer are higher after 10,000 runs than before at an ambient temperature of 104°F (40°C) as shown in the following tables and figures.

The same trend observed before each set of runs in Table 13, Table 14, and Table 15 is also observed in Table 16, Table 17, and Table 18, namely that the thinner perpetual pavements experience greater transverse strains than does the full-depth control section pavement. There is also the same pattern in the longitudinal strains, with one run somewhat above the 70με criterion in each thinner section and the rest below it, and with three runs on the full-depth control section slightly above the criterion. The differences in the strains before and after 10,000 runs at the high temperature are low, which indicates that each section withstood the repeated runs well.

Table 16. Longitudinal and Transverse Strain in Fatigue Resistance Layer (FRL) in APLF after 10,000 runs and 40°F (4.4°C).

				Strain (με) at bottom of FRL after 10,000 runs at 40°F (4.4°C)							
AC thickness				13" (33.0 cm)		14" (35.6 cm)		15" (38.1 cm)		16" (40.6 cm)	
Item 448 layer thickness				4.75" (12.1 cm)		5.75" (14.6 cm)		6.75"(17.1 cm)		7.75" (19.7 cm)	
Wheel load		Lateral shift		Evotherm surface		Sasobit surface		Aspha-min surface		HMA surface	
(lb)	(kN)	(in)	(mm)	Long	Tran	Long	Tran	Long	Tran	Long	Tran
6000	26.7	3	76.2	11.85	15.8	10.25	13	10.95	13.9	11.95	13
		1	25.4	12.6	15.8	10.1	12.85	11.85	13.55	11.85	13.05
		-4	-102	12.1	14.45	10.65	13.25	11.55	11.7	10.9	11.65
		-9	-229	9.45	12.65	7.6	12.1	7.3	10.65	7.8	10.7
9000	40	3	76.2	17.55	22.45	17.1	21.15	15.8	19.5	17.55	18.8
		1	25.4	18.2	22.55	17	21.25	16.95	20.35	17.8	19.2
		-4	-102	17.7	20.75	16.65	20.25	17.65	19.5	16.2	17.75
		-9	-229	13.5	17.8	11.75	18.15	12	17.25	11.65	15.3
12000	53.4	3	76.2	24.1	30.25	22.9	27.9	21.15	25.6	23.6	24.8
		1	25.4	24.4	30.3	23.95	28.75	22.4	26.4	23.45	24.6
		-4	-102	24.3	28.1	22.85	27.65	22.55	25.3	22.1	23.5
		-9	-229	18.35	24.35	16.25	24.1	15.6	22.45	15.75	20.65

Table 17. Longitudinal and Transverse Strain in Fatigue Resistance Layer (FRL) in APLF after 10,000 runs and 70°F (21.1°C).

				Strain (με) at bottom of FRL after 10,000 runs at 70°F (21.1°C)							
AC thickness				13" (33.0 cm)		14" (35.6 cm)		15" (38.1 cm)		16" (40.6 cm)	
Item 448 layer thickness				4.75" (12.1 cm)		5.75" (14.6 cm)		6.75"(17.1 cm)		7.75" (19.7 cm)	
Wheel load		Lateral shift		Evotherm surface		Sasobit surface		Aspha-min surface		HMA surface	
(lb)	(kN)	(in)	(mm)	Long	Tran	Long	Tran	Long	Tran	Long	Tran
6000	26.7	3	76.2	25.6	39	24.65	36.75	20	27.55	21.95	23.35
		1	25.4	25.45	38.1	24.7	37	22.2	28.35	21.5	23.35
		-4	-102	26.95	34.35	25.6	36.15	25.7	27.75	18.55	21.05
		-9	-229	18.5	28.1	14.25	31.4	17.5	23.4	10.2	17.55
9000	40	3	76.2	37.15	54.9	40.35	58.25	29.55	38.1	33.3	33.6
		1	25.4	39.45	56.1	39.5	57.8	33.55	40.35	32.6	33.7
		-4	-102	39.65	49.6	37.65	53	36.85	38.8	28.35	30.35
		-9	-229	28.5	42.2	21.7	45.55	23.55	33.15	14.7	26.15
12000	53.4	3	76.2	51.8	74.1	57.7	79.9	41.8	51.9	46.05	45.75
		1	25.4	52.1	72.05	56.4	77.95	46.25	53.4	44.95	45.5
		-4	-102	54.6	66.7	55.3	74.6	47.5	51.65	38.8	41.8
		-9	-229	38.35	56.4	30.55	64.05	30.9	45.25	21.45	35.6

Table 18. Longitudinal and Transverse Strain in Fatigue Resistance Layer (FRL) in APLF after 10,000 runs and 104°F (40°C).

				Strain (με) at bottom of FRL after 10,000 runs at 104°F (40.0°C)							
AC thickness				13" (33.0 cm)		14" (35.6 cm)		15" (38.1 cm)		16" (40.6 cm)	
Item 448 layer thickness				4.75" (12.1 cm)		5.75" (14.6 cm)		6.75"(17.1 cm)		7.75" (19.7 cm)	
Wheel load		Lateral shift		Evotherm surface		Sasobit surface		Aspha-min surface		HMA surface	
(lb)	(kN)	(in)	(mm)	Long	Tran	Long	Tran	Long	Tran	Long	Tran
6000	26.7	3	76.2	24.3	125.05	20.7	119.25	21	111.3	41.5	86.55
		1	25.4	26.25	116.2	20.6	109.65	34	117.85	44.95	80.8
		-4	-102	47.65	100.35	38.4	99.25	60.9	109.55	46.75	69.25
		-9	-229	32.35	76.1	9.5	75	34.25	87.3	18	53.45
9000	40	3	76.2	30.6	174.8	33.7	165.7	30.25	159.1	56.85	116.2
		1	25.4	34.25	169.3	32.9	162.45	40.6	165.05	61.55	115.8
		-4	-102	67.3	144.95	49.7	144.85	78	150.15	64.45	101.55
		-9	-229	51.1	118	20.15	118.35	42.95	124.45	27.8	84.2
12000	53.4	3	76.2	38.7	223.6	43.4	209.25	40	200.3	74.8	153.5
		1	25.4	43.35	220.75	42.45	208.1	49.7	205.35	80.6	150.35
		-4	-102	88.3	193.5	61.25	188.65	93.8	190.1	85.65	135
		-9	-229	69.7	162.6	26.6	162.7	55.85	161.3	32.6	116.05

Figure 26 and Figure 27 respectively show the longitudinal and transverse strain in the FRL after 10,000 runs.

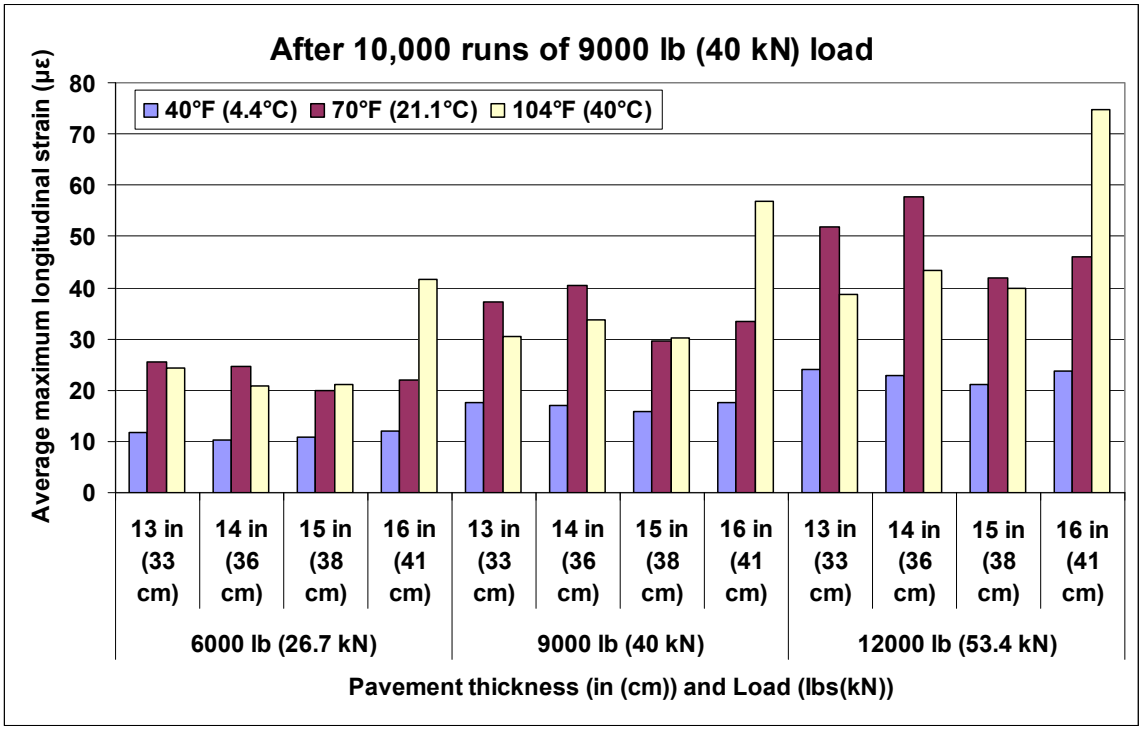

Figure 26. Longitudinal Strain in Fatigue Resistance Layer (FRL) in APLF after 10,000 runs.

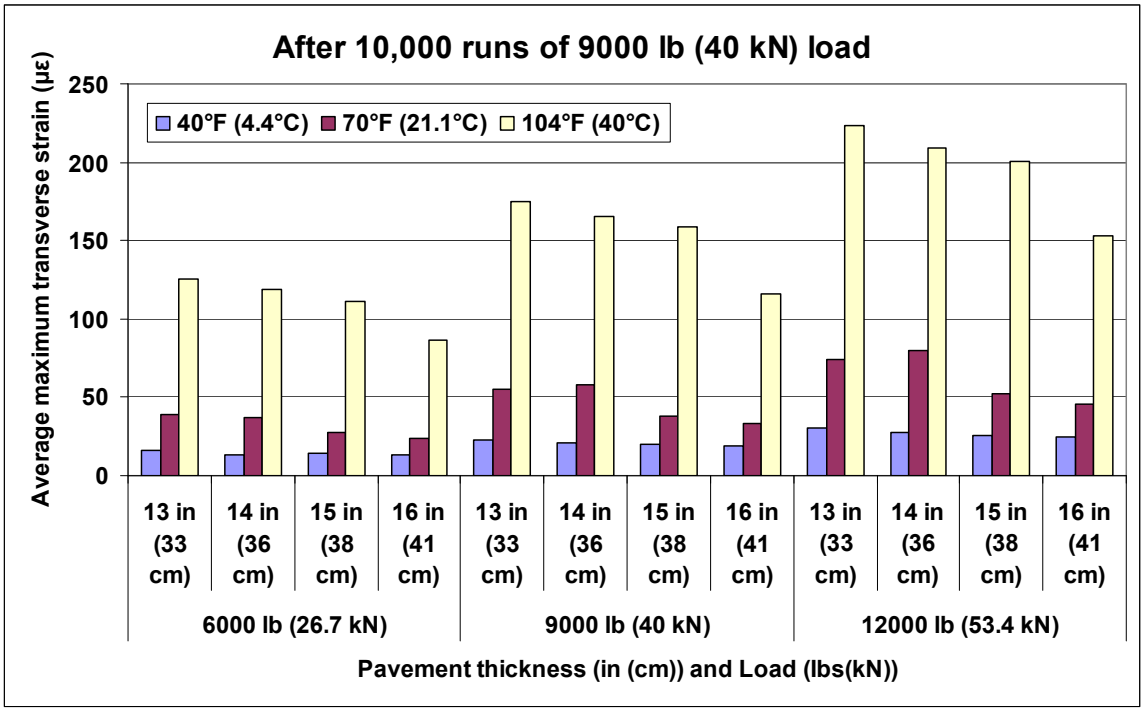

Figure 27. Transverse Strain in Fatigue Resistance Layer (FRL) in APLF after 10,000 runs.

7.2 Pressure under Base Layer

Table 19 through Table 21 show the pressure under the wheel path under the base layer (ODOT item 304) at ambient temperatures of 40°F (4.4°C), 70°F (21.1°C), and 104°F (40°C) after 0 runs, and Table 22 through Table 24 show the pressures at each ambient temperature after 10,000 runs. As with the strain measurements, the RWLs applied during measurement were 6000 lbs (26.7 kN), 9000 lbs (40 kN), and 12000 lbs (53.4 kN) at each temperature. The pressure under the aggregate base increases with increasing the load and the ambient temperature of the facility. The difference in the pressure at each section is very small. The lowest pressure measured was under the full-depth section at different loads and different ambient temperatures. This may be due to the greater thickness of the Item 448 (intermediate AC) layer in this section and the greater stiffness of the conventional HMA mix on the surface. The pressure under the base layer is almost the same after 0 and 10,000 runs for the same applied load and ambient temperature.

Table 19. Pressure under Base Layer in APLF after 0 runs and 40°F (4.4°C).

				Pressure at top of subgrade after 0 runs at 40°F (4.4°C)							
AC thickness				13" (33.0 cm)		14" (35.6 cm)		15" (38.1 cm)		16" (40.6 cm)	
FRL thickness				4.75" (12.1 cm)		5.75" (14.6 cm)		6.75"(17.1 cm)		7.75" (19.7 cm)	
Wheel load		Lateral shift		Evotherm surface		Sasobit surface		Aspha-min surface		HMA surface	
(lb)	(kN)	(in)	(mm)	(psi)	(kPa)	(psi)	(kPa)	(psi)	(kPa)	(psi)	(kPa)
6000	26.7	3	76.2	0.754	5.20	0.365	2.52	0.668	4.61	0.488	3.36
		1	25.4	0.74	5.10	0.367	2.53	0.61	4.21	0.689	4.75
		-4	-102	0.732	5.05	0.333	2.30	0.547	3.77	0.974	6.72
		-9	-229	0.65	4.48	0.368	2.54	0.499	3.44	0.492	3.39
9000	40	3	76.2	1.153	7.95	0.605	4.17	1.067	7.36	0.697	4.81
		1	25.4	1.217	8.39	0.585	4.03	1.101	7.59	0.969	6.68
		-4	-102	1.101	7.59	0.589	4.06	1.001	6.90	0.427	2.94
		-9	-229	0.99	6.83	0.515	3.55	0.867	5.98	0.658	4.54
12000	53.4	3	76.2	1.643	11.33	0.857	5.91	1.445	9.96	0.904	6.23
		1	25.4	1.643	11.33	0.831	5.73	1.444	9.96	0.401	2.76
		-4	-102	1.547	10.67	0.833	5.74	1.389	9.58	0.58	4.00
		-9	-229	1.382	9.53	0.729	5.03	1.231	8.49	0.578	3.99

Table 20. Pressure under Base Layer in APLF after 0 runs and 70°F (21.1°C).

				Pressure at top of subgrade after 0 runs at 70°F (21.1°C)							
AC thickness				13" (33.0 cm)		14" (35.6 cm)		15" (38.1 cm)		16" (40.6 cm)	
FRL thickness				4.75" (12.1 cm)		5.75" (14.6 cm)		6.75"(17.1 cm)		7.75" (19.7 cm)	
Wheel load		Lateral shift		Evotherm surface		Sasobit surface		Aspha-min surface		HMA surface	
(lb)	(kN)	(in)	(mm)	(psi)	(kPa)	(psi)	(kPa)	(psi)	(kPa)	(psi)	(kPa)
6000	26.7	3	76.2	2.737	18.87	2.019	13.92	2.648	18.26	2.002	13.80
		1	25.4	2.686	18.52	2.146	14.80	2.734	18.85	1.937	13.36
		-4	-102	2.544	17.54	2.045	14.10	2.623	18.08	1.806	12.45
		-9	-229	2.204	15.20	1.834	12.64	2.174	14.99	1.471	10.14
9000	40	3	76.2	3.752	25.87	3.088	21.29	3.744	25.81	2.823	19.46
		1	25.4	3.81	26.27	2.886	19.90	3.793	26.15	2.716	18.73
		-4	-102	3.516	24.24	2.642	18.22	3.719	25.64	2.536	17.49
		-9	-229	2.953	20.36	2.311	15.93	3.057	21.08	2.095	14.44
12000	53.4	3	76.2	4.869	33.57	3.972	27.39	4.894	33.74	3.614	24.92
		1	25.4	4.748	32.74	3.96	27.30	4.923	33.94	3.6	24.82
		-4	-102	4.494	30.99	3.583	24.70	4.802	33.11	3.231	22.28
		-9	-229	3.854	26.57	3.126	21.55	4.127	28.45	2.732	18.84

Table 21. Pressure under Base Layer in APLF after 0 runs and 104°F (40.0°C).

				Pressure at top of subgrade after 0 runs at 104°F (40.0°C)							
AC thickness				13" (33.0 cm)		14" (35.6 cm)		15" (38.1 cm)		16" (40.6 cm)	
FRL thickness				4.75" (12.1 cm)		5.75" (14.6 cm)		6.75"(17.1 cm)		7.75" (19.7 cm)	
Wheel load		Lateral shift		Evotherm surface		Sasobit surface		Aspha-min surface		HMA surface	
(lb)	(kN)	(in)	(mm)	(psi)	(kPa)	(psi)	(kPa)	(psi)	(kPa)	(psi)	(kPa)
6000	26.7	3	76.2	5.413	37.32	5.046	34.79	5.152	35.52	3.997	27.56
		1	25.4	5.969	41.15	4.957	34.18	5.571	38.41	4.136	28.52
		-4	-102	5.305	36.58	4.662	32.14	5.456	37.62	3.737	25.77
		-9	-229	4.491	30.96	3.667	25.28	4.481	30.90	2.786	19.21
9000	40	3	76.2	7.999	55.15	7.109	49.01	7.461	51.44	6.01	41.44
		1	25.4	8.078	55.70	7.217	49.76	7.725	53.26	5.78	39.85
		-4	-102	7.433	51.25	6.284	43.33	7.544	52.01	5.007	34.52
		-9	-229	6.074	41.88	4.918	33.91	6.32	43.57	3.872	26.70
12000	53.4	3	76.2	10.242	70.62	9.278	63.97	9.383	64.69	7.534	51.95
		1	25.4	10.222	70.48	9.178	63.28	9.62	66.33	7.218	49.77
		-4	-102	9.435	65.05	8.298	57.21	9.337	64.38	6.526	45.00
		-9	-229	7.827	53.97	6.447	44.45	7.88	54.33	5.094	35.12

Table 22. Pressure under Base Layer in APLF after 10,000 runs and 40°F (4.4°C).

				Pressure at top of subgrade after 10,000 runs at 40°F (4.4°C)							
AC thickness				13" (33.0 cm)		14" (35.6 cm)		15" (38.1 cm)		16" (40.6 cm)	
FRL thickness				4.75" (12.1 cm)		5.75" (14.6 cm)		6.75"(17.1 cm)		7.75" (19.7 cm)	
Wheel load		Lateral shift		Evotherm surface		Sasobit surface		Aspha-min surface		HMA surface	
(lb)	(kN)	(in)	(mm)	(psi)	(kPa)	(psi)	(kPa)	(psi)	(kPa)	(psi)	(kPa)
6000	26.7	3	76.2	1.011	6.97	0.412	2.84	0.748	5.16	0.626	4.32
		1	25.4	0.997	6.87	0.41	2.83	0.718	4.95	0.591	4.07
		-4	-102	2.465	17.00	0.411	2.83	0.671	4.63	0.541	3.73
		-9	-229	2.005	13.82	0.371	2.56	0.612	4.22	0.463	3.19
9000	40	3	76.2	1.498	10.33	0.745	5.14	1.24	8.55	0.863	5.95
		1	25.4	1.507	10.39	0.733	5.05	1.233	8.50	0.847	5.84
		-4	-102	1.427	9.84	0.696	4.80	1.184	8.16	0.791	5.45
		-9	-229	1.266	8.73	0.595	4.10	1.009	6.96	0.68	4.69
12000	53.4	3	76.2	2.074	14.30	1.125	7.76	1.633	11.26	1.193	8.23
		1	25.4	2.102	14.49	1.137	7.84	1.653	11.40	1.198	8.26
		-4	-102	1.922	13.25	1.065	7.34	1.614	11.13	1.107	7.63
		-9	-229	1.742	12.01	0.87	6.00	1.387	9.56	0.95	6.55

Table 23. Pressure under Base Layer in APLF after 10,000 runs and 70°F (21.1°C).

				Pressure at top of subgrade after 10,000 runs at 70°F (21.1°C)							
AC thickness				13" (33.0 cm)		14" (35.6 cm)		15" (38.1 cm)		16" (40.6 cm)	
FRL thickness				4.75" (12.1 cm)		5.75" (14.6 cm)		6.75"(17.1 cm)		7.75" (19.7 cm)	
Wheel load		Lateral shift		Evotherm surface		Sasobit surface		Aspha-min surface		HMA surface	
(lb)	(kN)	(in)	(mm)	(psi)	(kPa)	(psi)	(kPa)	(psi)	(kPa)	(psi)	(kPa)
6000	26.7	3	76.2	2.718	18.74	2.065	14.24	2	13.79	1.739	11.99
		1	25.4	2.631	18.14	2.017	13.91	2.035	14.03	1.668	11.50
		-4	-102	2.465	17.00	1.922	13.25	1.812	12.49	1.507	10.39
		-9	-229	2.005	13.82	1.7	11.72	1.61	11.10	1.278	8.81
9000	40	3	76.2	3.755	25.89	3.033	20.91	2.838	19.57	2.506	17.28
		1	25.4	3.866	26.66	3.021	20.83	3.015	20.79	2.397	16.53
		-4	-102	3.509	24.19	2.644	18.23	2.831	19.52	2.204	15.20
		-9	-229	3.043	20.98	2.351	16.21	2.453	16.91	1.851	12.76
12000	53.4	3	76.2	5.093	35.11	4.171	28.76	3.877	26.73	3.403	23.46
		1	25.4	4.966	34.24	4.061	28.00	3.95	27.23	3.286	22.66
		-4	-102	4.674	32.23	3.775	26.03	3.802	26.21	3.032	20.90
		-9	-229	4.054	27.95	3.264	22.50	3.311	22.83	2.508	17.29

Table 24. Pressure under Base Layer in APLF after 10,000 runs and 104°F (40°C).

				Pressure at top of subgrade after 10,000 runs at 104°F (40.0°C)							
AC thickness				13" (33.0 cm)		14" (35.6 cm)		15" (38.1 cm)		16" (40.6 cm)	
FRL thickness				4.75" (12.1 cm)		5.75" (14.6 cm)		6.75"(17.1 cm)		7.75" (19.7 cm)	
Wheel load		Lateral shift		Evotherm surface		Sasobit surface		Aspha-min surface		HMA surface	
(lb)	(kN)	(in)	(mm)	(psi)	(kPa)	(psi)	(kPa)	(psi)	(kPa)	(psi)	(kPa)
6000	26.7	3	76.2	5.433	37.46	4.526	31.21	4.697	32.38	4.233	29.19
		1	25.4	5.183	35.74	4.188	28.88	4.876	33.62	4.229	29.16
		-4	-102	4.527	31.21	3.904	26.92	4.314	29.74	3.476	23.97
		-9	-229	3.545	24.44	2.866	19.76	3.757	25.90	2.727	18.80
9000	40	3	76.2	7.588	52.32	6.665	45.95	6.637	45.76	6.22	42.89
		1	25.4	7.37	50.81	6.442	44.42	6.874	47.39	5.889	40.60
		-4	-102	6.312	43.52	5.322	36.69	6.35	43.78	5.108	35.22
		-9	-229	5.417	37.35	4.278	29.50	5.391	37.17	4.088	28.19
12000	53.4	3	76.2	9.841	67.85	9.069	62.53	8.871	61.16	8.369	57.70
		1	25.4	9.766	67.33	8.603	59.32	9.07	62.54	8.15	56.19
		-4	-102	8.471	58.41	7.352	50.69	8.451	58.27	6.98	48.13
		-9	-229	7.334	50.57	5.805	40.02	6.997	48.24	5.507	37.97

Figure 28 and Figure 29 show the pressure under the wheel path under the base layer (304) after 0 and 10000 runs at ambient temperatures of 40°F (4.4°C), 70°F (21.1°C), and 104°F (40°C). The highest pressure was measured under the base layer of the thinnest AC section.

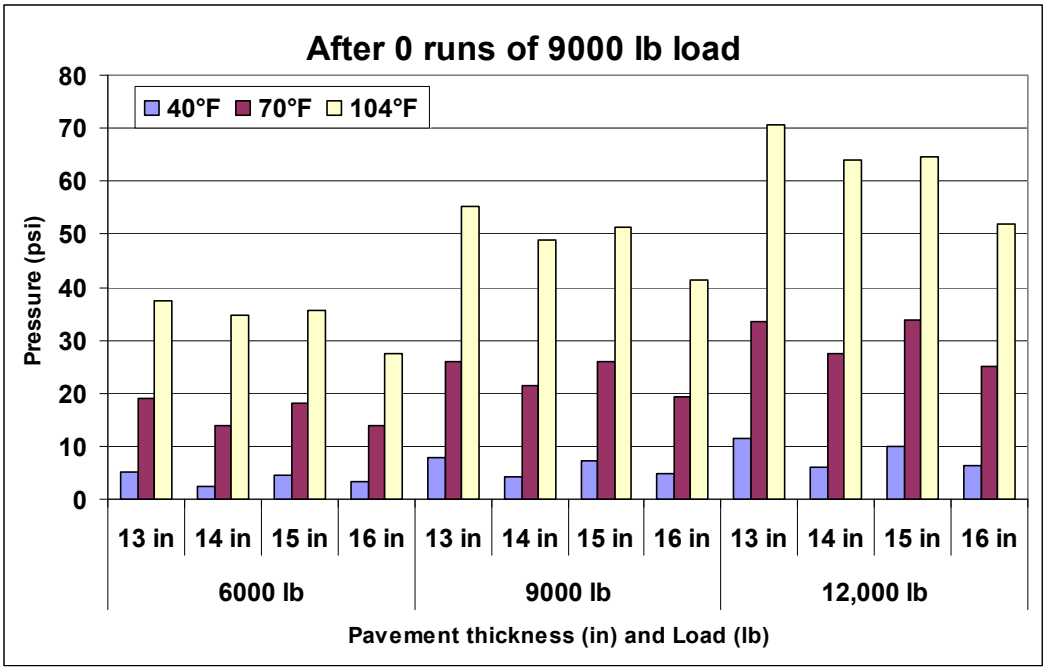

a)

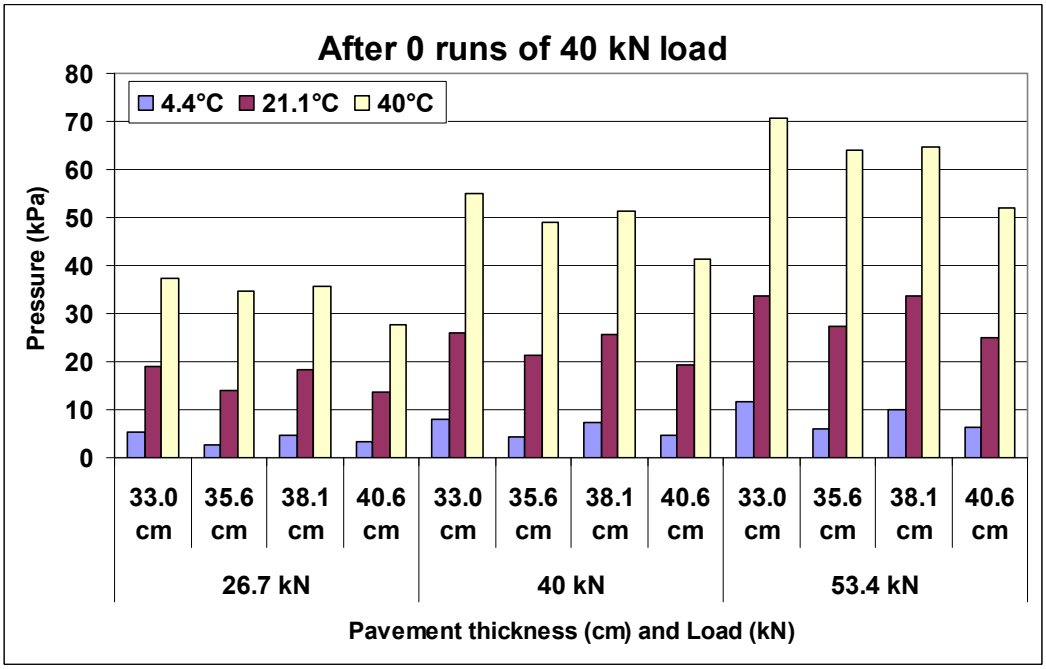

b)

Figure 28. Pressure under base with load on wheel path after 0 runs: a) English units, b) metric units.

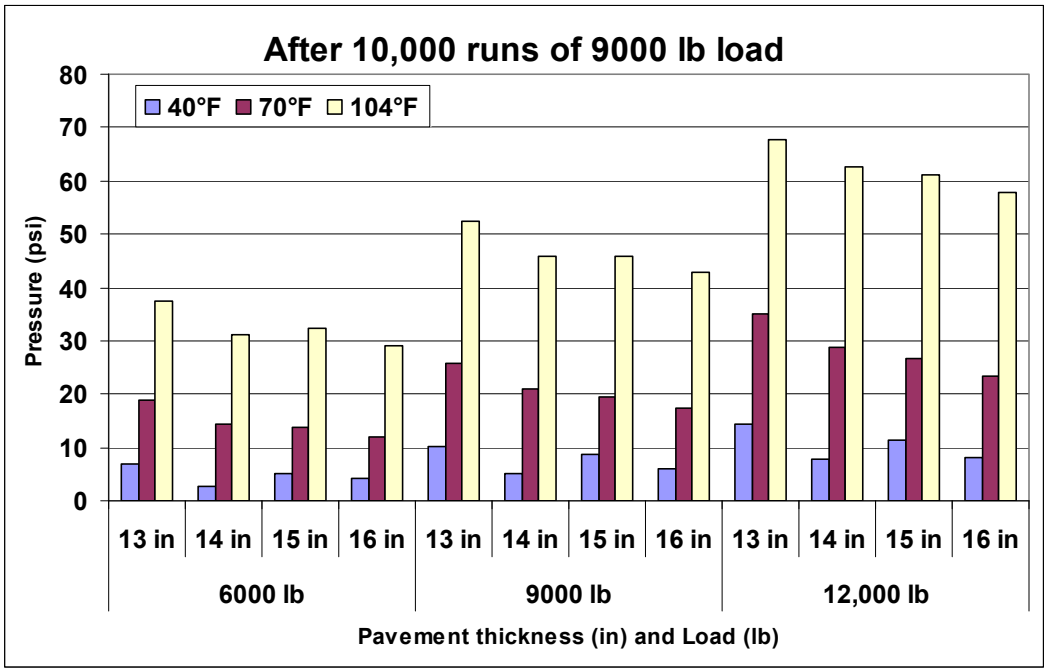

a)

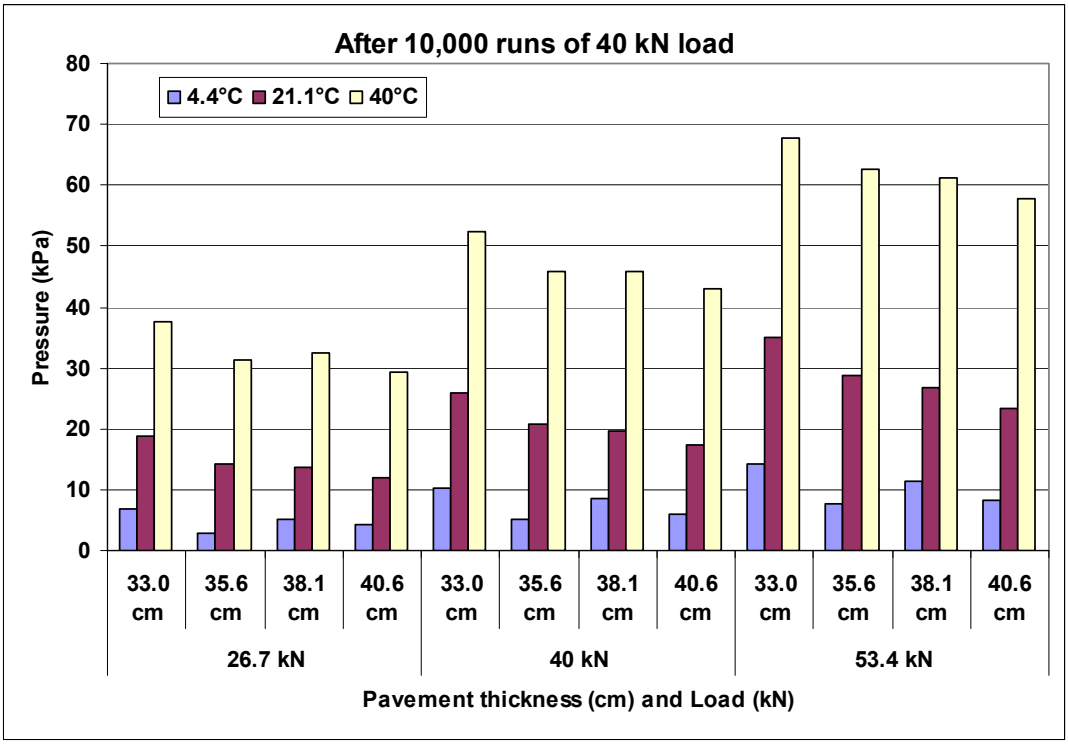

b)

Figure 29. Pressure under base with load on wheel path after 10,000 runs: a) English units, b) metric units.

7.3 Deflection of Subgrade

Table 25 through Table 27 show the deflection of the subgrade layer under 6000 lb (26.7 kN), 9000 lb (40 kN), and 12000 lb (53.4 kN) at the three different ambient temperatures after 0 runs of the load wheel; Table 28 through Table 30 show the deflections under the three applied loads at the three different ambient temperatures after 10,000 runs of the 9000 lb (40 kN) load.. The deflection of the subgrade layer is obtained by taking the deflection reading from the LVDT referenced to a depth of about 5 ft (1.5 m) of each section and subtracting the deflection registered from the LVDT referenced to the top of the subgrade, which corresponds to the deflection in the asphalt and DGAB layers. The deflection of subgrade increases with increasing the load applied and the ambient temperature of the facility at each section. Any change in the ambient temperature will affect the resilient modulus of the asphalt layer and this will alter the deflection of LVDT. The deflection is lower after 10,000 runs than the deflection after 0 runs.

Table 25. Deflection of Subgrade layer in APLF after 0 runs at 40°F (4.4°C).

				Deflection of subgrade after 0 runs at 40°F (4.4°C)							
AC thickness				13" (33.0 cm)		14" (35.6 cm)		15" (38.1 cm)		16" (40.6 cm)	
FRL thickness				4.75" (12.1 cm)		5.75" (14.6 cm)		6.75"(17.1 cm)		7.75" (19.7 cm)	
Wheel load		Lateral shift		Evotherm surface		Sasobit surface		Aspha-min surface		HMA surface	
(lb)	(kN)	(in)	(mm)	(mil)	(μm)	(mil)	(μm)	(mil)	(μm)	(mil)	(μm)
6000	26.7	3	76.2	1.185	30.10	0.894	22.71	0.886	22.50	1.008	25.60
		1	25.4	0.984	24.99	0.618	15.70	0.965	24.51	1.465	37.21
		-4	-102	1.067	27.10	0.724	18.39	1.059	26.90	2.102	53.39
		-9	-229	1.063	27.00	0.87	22.10	0.969	24.61	1.031	26.19
9000	40	3	76.2	1.622	41.20	1.413	35.89	1.374	34.90	1.555	39.50
		1	25.4	1.776	45.11	1.268	32.21	1.524	38.71	2.24	56.90
		-4	-102	1.606	40.79	1.362	34.59	1.465	37.21	1.059	26.90
		-9	-229	1.594	40.49	1.299	32.99	1.417	35.99	1.673	42.49
12000	53.4	3	76.2	2.598	65.99	1.941	49.30	1.949	49.50	2.24	56.90
		1	25.4	2.232	56.69	1.768	44.91	2.012	51.10	0.969	24.61
		-4	-102	2.339	59.41	1.866	47.40	2.098	53.29	1.488	37.80
		-9	-229	2.28	57.91	1.76	44.70	1.937	49.20	1.496	38.00

Table 26. Deflection of Subgrade layer in APLF after 0 runs at 70°F (21.1°C).

				Deflection of subgrade after 0 runs at 70°F (21.1°C)							
AC thickness				13" (33.0 cm)		14" (35.6 cm)		15" (38.1 cm)		16" (40.6 cm)	
FRL thickness				4.75" (12.1 cm)		5.75" (14.6 cm)		6.75"(17.1 cm)		7.75" (19.7 cm)	
Wheel load		Lateral shift		Evotherm surface		Sasobit surface		Aspha-min surface		HMA surface	
(lb)	(kN)	(in)	(mm)	(mil)	(µm)	(mil)	(µm)	(mil)	(µm)	(mil)	(µm)
6000	26.7	3	76.2	1.472	37.39	1.685	42.80	1.76	44.70	1.346	34.19
		1	25.4	1.528	38.81	1.705	43.31	1.961	49.81	1.476	37.49
		-4	-102	1.504	38.20	1.535	38.99	1.823	46.30	1.39	35.31
		-9	-229	1.39	35.31	1.618	41.10	1.48	37.59	1.126	28.60
9000	40	3	76.2	2.346	59.59	5.689	144.50	2.752	69.90	2.126	54.00
		1	25.4	2.516	63.91	2.717	69.01	2.882	73.20	2.169	55.09
		-4	-102	2.098	53.29	2.575	65.41	2.65	67.31	2.118	53.80
		-9	-229	2.043	51.89	2.374	60.30	2.563	65.10	1.72	43.69
12000	53.4	3	76.2	3.358	85.29	4.433	112.60	4.402	111.81	2.906	73.81
		1	25.4	3.307	84.00	4.177	106.10	4.303	109.30	3.323	84.40
		-4	-102	3.016	76.61	4.043	102.69	4.244	107.80	3.232	82.09
		-9	-229	2.965	75.31	3.673	93.29	3.752	95.30	2.48	62.99

Table 27. Deflection of Subgrade layer in APLF after 0 runs at 104°F (40°C).

				Deflection of subgrade after 0 runs at 104°F (40.0°C)							
AC thickness				13" (33.0 cm)		14" (35.6 cm)		15" (38.1 cm)		16" (40.6 cm)	
FRL thickness				4.75" (12.1 cm)		5.75" (14.6 cm)		6.75"(17.1 cm)		7.75" (19.7 cm)	
Wheel load		Lateral shift		Evotherm surface		Sasobit surface		Aspha-min surface		HMA surface	
(lb)	(kN)	(in)	(mm)	(mil)	(µm)	(mil)	(µm)	(mil)	(µm)	(mil)	(µm)
6000	26.7	3	76.2	2.24	56.90	2.76	70.10	2.854	72.49	1.925	48.90
		1	25.4	2.169	55.09	2.524	64.11	2.701	68.61	2.823	71.70
		-4	-102	2.575	65.41	3.185	80.90	2.287	58.09	3.354	85.19
		-9	-229	2.543	64.59	2.327	59.11	1.988	50.50	1.953	49.61
9000	40	3	76.2	3.744	95.10	5.224	132.69	4.583	116.41	3.555	90.30
		1	25.4	3.362	85.39	4.646	118.01	4.453	113.11	5.063	128.60
		-4	-102	3.728	94.69	4.748	120.60	5.315	135.00	5.402	137.21
		-9	-229	1.067	27.10	4.24	107.70	4.331	110.01	3.031	76.99
12000	53.4	3	76.2	3.811	96.80	8.02	203.71	7.535	191.39	5.453	138.51
		1	25.4	4.354	110.59	7.693	195.40	6.319	160.50	6.843	173.81
		-4	-102	2.63	66.80	8.035	204.09	7.76	197.10	7.362	186.99
		-9	-229	-0.772	-19.61	6.693	170.00	6.929	176.00	4.492	114.10

Table 28. Deflection of Subgrade layer in APLF after 10,000 runs at 40°F (4.4°C).

				Deflection of subgrade after 10,000 runs at 40°F (4.4°C)							
AC thickness				13" (33.0 cm)		14" (35.6 cm)		15" (38.1 cm)		16" (40.6 cm)	
FRL thickness				4.75" (12.1 cm)		5.75" (14.6 cm)		6.75"(17.1 cm)		7.75" (19.7 cm)	
Wheel load		Lateral shift		Evotherm surface		Sasobit surface		Aspha-min surface		HMA surface	
(lb)	(kN)	(in)	(mm)	(mil)	(µm)	(mil)	(µm)	(mil)	(µm)	(mil)	(µm)
6000	26.7	3	76.2	0.89	22.61	0.917	23.29	0.898	22.81	1.083	27.51
		1	25.4	1.028	26.11	0.641	16.28	0.961	24.41	1.016	25.81
		-4	-102	0.874	22.20	0.835	21.21	1.091	27.71	1.122	28.50
		-9	-229	0.961	24.41	0.752	19.10	0.972	24.69	0.929	23.60
9000	40	3	76.2	1.496	38.00	1.441	36.60	1.358	34.49	1.575	40.01
		1	25.4	1.539	39.09	1.228	31.19	1.453	36.91	1.575	40.01
		-4	-102	1.417	35.99	1.307	33.20	1.52	38.61	1.626	41.30
		-9	-229	1.429	36.30	1.213	30.81	1.409	35.79	1.461	37.11
12000	53.4	3	76.2	2.287	58.09	1.89	48.01	1.894	48.11	2.063	52.40
		1	25.4	2.248	57.10	1.752	44.50	1.913	48.59	2.217	56.31
		-4	-102	2.217	56.31	1.795	45.59	2.028	51.51	2.157	54.79
		-9	-229	2.138	54.31	1.709	43.41	1.902	48.31	2.043	51.89

Table 29. Deflection of Subgrade layer in APLF after 10,000 runs at 70°F (21.1°C).

				Deflection of subgrade after 10,000 runs at 70°F (21.1°C)							
AC thickness				13" (33.0 cm)		14" (35.6 cm)		15" (38.1 cm)		16" (40.6 cm)	
FRL thickness				4.75" (12.1 cm)		5.75" (14.6 cm)		6.75"(17.1 cm)		7.75" (19.7 cm)	
Wheel load		Lateral shift		Evotherm surface		Sasobit surface		Aspha-min surface		HMA surface	
(lb)	(kN)	(in)	(mm)	(mil)	(µm)	(mil)	(µm)	(mil)	(µm)	(mil)	(µm)
6000	26.7	3	76.2	1.512	38.40	1.87	47.50	1.52	38.61	1.453	36.91
		1	25.4	1.524	38.71	1.768	44.91	1.661	42.19	1.476	37.49
		-4	-102	1.638	41.61	1.831	46.51	1.602	40.69	1.488	37.80
		-9	-229	1.421	36.09	1.724	43.79	1.335	33.91	1.091	27.71
9000	40	3	76.2	2.382	60.50	3.138	79.71	2.551	64.80	2.291	58.19
		1	25.4	2.657	67.49	3.047	77.39	2.319	58.90	2.22	56.39
		-4	-102	2.264	57.51	2.846	72.29	2.291	58.19	2.311	58.70
		-9	-229	2.205	56.01	2.65	67.31	1.996	50.70	1.602	40.69
12000	53.4	3	76.2	3.819	97.00	4.563	115.90	3.28	83.31	3.079	78.21
		1	25.4	3.78	96.01	4.378	111.20	3.122	79.30	3.063	77.80
		-4	-102	3.437	87.30	4.276	108.61	3.287	83.49	3.094	78.59
		-9	-229	3.339	84.81	3.894	98.91	2.874	73.00	2.516	63.91

Table 30. Deflection of Subgrade layer in APLF after 10,000 runs at 104°F (40°C).

				Deflection of subgrade after 10,000 runs at 104°F (40.0°C)							
AC thickness				13" (33.0 cm)		14" (35.6 cm)		15" (38.1 cm)		16" (40.6 cm)	
FRL thickness				4.75" (12.1 cm)		5.75" (14.6 cm)		6.75"(17.1 cm)		7.75" (19.7 cm)	
Wheel load		Lateral shift		Evotherm surface		Sasobit surface		Aspha-min surface		HMA surface	
(lb)	(kN)	(in)	(mm)	(mil)	(μm)	(mil)	(μm)	(mil)	(μm)	(mil)	(μm)
6000	26.7	3	76.2	2.622	66.60	4.083	103.71	4.209	106.91	1.791	45.49
		1	25.4	2.594	65.89	3.61	91.69	3.413	86.69	1.476	37.49
		-4	-102	2.524	64.11	3.906	99.21	3.252	82.60	1.61	40.89
		-9	-229	1.902	48.31	2.811	71.40	3.185	80.90	1.067	27.10
9000	40	3	76.2	4.248	107.90	6.961	176.81	6.555	166.50	2.988	75.90
		1	25.4	4.236	107.59	6.732	170.99	6.874	174.60	3	76.20
		-4	-102	4.654	118.21	6.591	167.41	6.146	156.11	3.504	89.00
		-9	-229	3.181	80.80	5.728	145.49	5.197	132.00	2.323	59.00
12000	53.4	3	76.2	6.65	168.91	9.657	245.29	8.374	212.70	4.602	116.89
		1	25.4	6.555	166.50	9.602	243.89	8.953	227.41	4.547	115.49
		-4	-102	7.106	180.49	9.728	247.09	8.74	222.00	4.783	121.49
		-9	-229	5.394	137.01	7.795	197.99	6.717	170.61	3.516	89.31

Figure 30 and Figure 31 show the deflections of subgrade layer under each section after 0 and 10000 runs under 6000 lb (26.7 kN), 9000 lb (40 kN), and 12000 lb (53.4 kN) loads at the three different ambient temperatures. The deflections of subgrade layer under the thinner AC sections were very similar to those under the full-depth AC. The change in deflections for the thinner sections and control section was very small with respect to the changes in load and temperature. This suggests that any effect that might have come from the reduction in Item 448 layer thicknesses was mitigated by the compensatory increase in the DGAB thickness. The thickness of subgrade layer was uniform under all sections. Because of these differences in the thicknesses of the Item 448 layer and DGAB in the instrumented sections resulted in differences in the depths of the strain gauges between the sections, strain responses under rolling wheel loads cannot be directly compared across lanes.

Wheel load responses measured on pavement sections in the APLF also would not be expected to agree with dynamic responses measured on the same pavement sections in the field because of dramatically different temperature distributions at the two sites. Field sections are exposed to daily temperature cycles where surface warming and cooling can generate significant gradients within the pavement layer over a 24 hour cycle. APLF sections are maintained at a constant air temperature, thereby reducing any gradients in the pavement to a few degrees. This difference in gradients will have a major impact on measured responses.

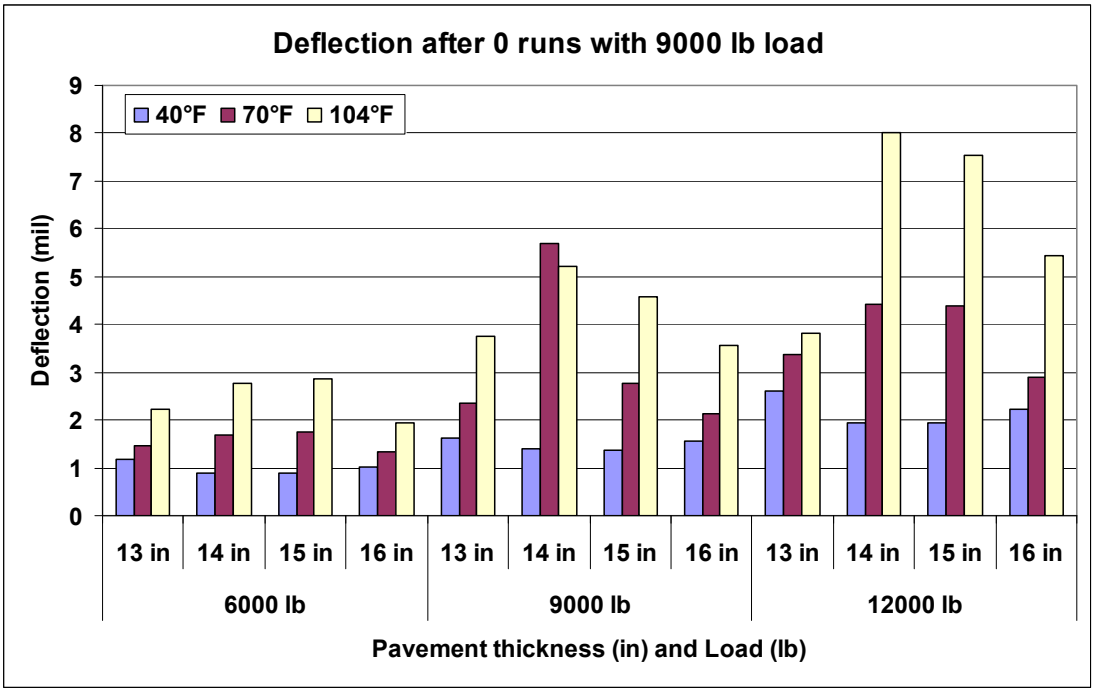

a)

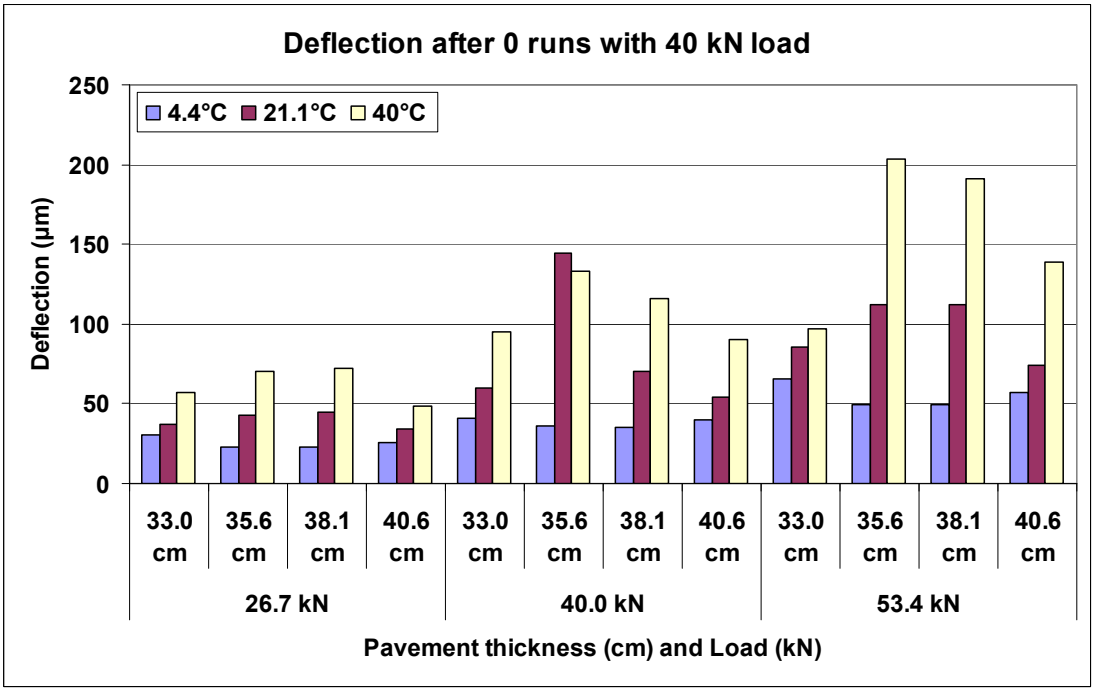

b)

Figure 30. Deflection of subgrade layer after 0 runs along the wheel path: a) English units, b) metric units.

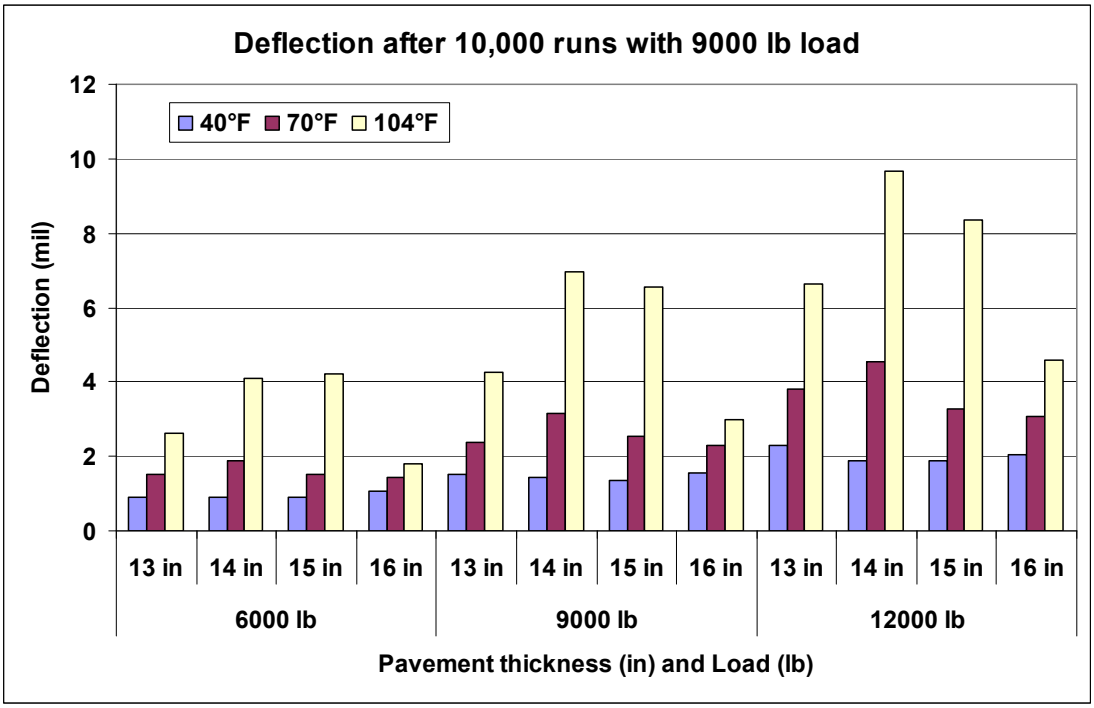

a)

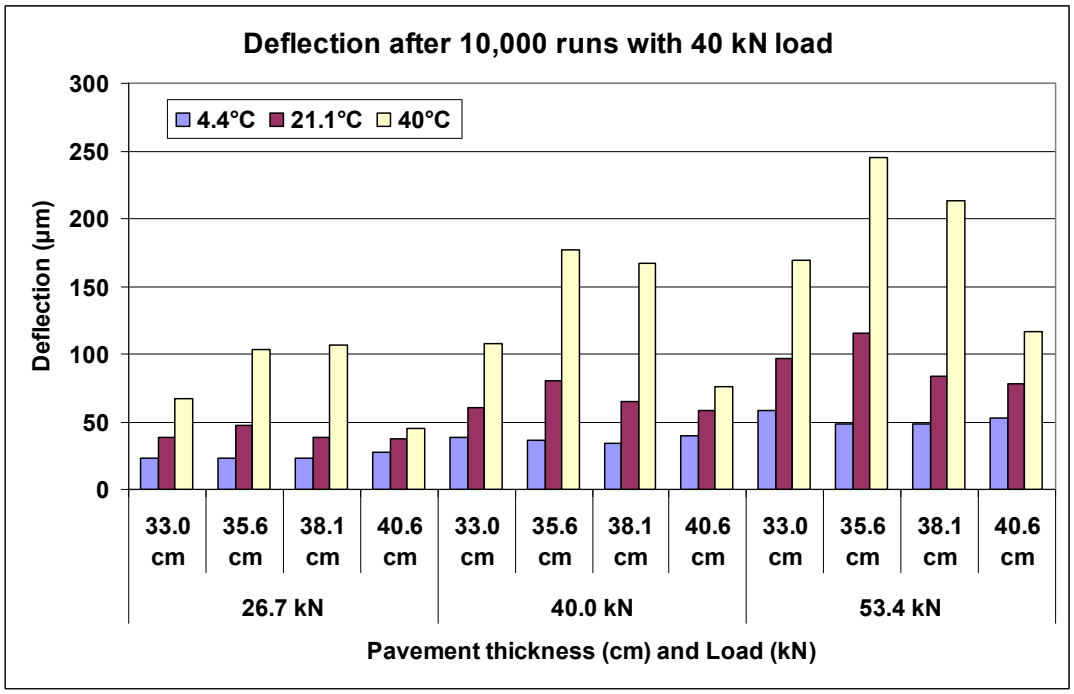

b)

Figure 31. Deflection of subgrade layer after 10,000 runs along the wheel path: a) English units, b) metric units.

7.4 Falling Weight Deflectometer Testing in APLF

7.4.1 Test Plan

The overall test plan for the APLF installation consisted of measuring dynamic responses and surface rutting in the pavement sections at 40°F (4.4°C), 70°F (21.1°C) and 104°F (40.0°C), as follows:

1. Measure dynamic deflections with a Falling Weight Deflectometer (FWD) at nominal loads of 6,000 lb (26.7 kN), 9,000 lb (40.0 kN), and 12,000 lb (53.4 kN) in all eight sections.
2. Measure dynamic deflection, strain and pressure with sensors installed in the southern sections of the test lanes during FWD loading and as 6,000 lb (26.7 kN), 9,000 lb (40.0 kN), and 12,000 lb (53.4 kN) loads were applied with rolling dual tires at 5 mph (8 km/h). The rolling tire measurements were reported in Section 7.1 through Section 7.3 above.
3. Periodically measure surface profiles in all eight sections as 10,000 rolling wheel loads were applied at 9,000 lbs. (40.0 kN).

After air temperature in the facility had been maintained at 40°F (4.4°C) sufficiently long for temperature to stabilize throughout the test pad, dynamic deflections were measured with the FWD, and dynamic responses were measured with the embedded pavement sensors as loads were applied with the FWD and rolling dual tires. Lateral surface profiles were measured across the wheel paths after 0, 100, 300, 1,000, 3,000, and 10,000 passes of the rolling dual wheels. Similar data were then collected at nominal air temperatures of 70°F (21.1°C) and 104°F (40.0°C). For each of the three series of tests, the temperature of the pavement surface was near the air temperature. At 70°F (21.1°C), temperature was nearly uniform through the pavement. At 40°F (4.4°C), and 104°F (40.0°C), there was a slight gradient of increasing and decreasing temperatures, respectively, toward the bottom of the asphalt concrete.

7.4.2 Phase 1 - FWD Responses

FWD deflections were collected along the centerline of all pavement lanes at the three temperatures after the 10,000 passes of the rolling wheel load were completed. An individual test consisted of one drop each at nominal loads of 6,000 lb (26.7 kN), 9,000 lb (40.0 kN), and 12,000 lb (53.4 kN) at each location. Three equally spaced tests were performed in the northern half of the lanes and the FWD load plate was placed over or near each of the seven response sensors in the southern half of the lanes. When the load plate was placed directly over holes housing the LVDTs, the geophone at the center of the plate would not read properly. To avoid this problem, the FWD was offset to allow all geophones to record valid data.

Table 31 is a summary of average deflections measured during the second drop and normalized to a 9,000 lb (40.0 kN) load. Deflections for Sections 1N, 2N, 3N, 4N and 4S are highlighted in the table because they have the same structural build-up and would be expected to have similar responses for a given load and temperature; the only difference being the mix used for the 1.25 in (3.2 cm) surface course). The consistent deflections shown for Df7 in Table I indicate uniform subgrade stiffness across the APLF pad.

FWD deflections increased with higher temperature and generally decreased with thicker layers of AC in the southern sections. The differences in temperature were sufficiently large to cause a consistent trend in deflection, while the one inch (2.54 cm) decreases in AC thickness were offset with corresponding increases in 304 DGAB thickness, resulting in minimal differences in overall stiffness and deflection that fell within normal variations in FWD data.

Table 31. Average normalized FWD responses by section.

Average Normalized FWD Deflection - mils / 9 kip (microns / 40 kN)											
Nominal Air Temp. °F (°C)	Section No.	Pvt. Thick. in. (cm)	Base Thick. In. (cm)	Geophone ID and Distance from Plate Center - in. (cm)							
				Df1	Df2	Df3	Df4	Df5	Df6	Df7	
				0	8 (20.3)	12 (30.5)	18 (45.7)	24(61.0)	36 (91.4)	60 (152.4)	
40 (4.4)	1N	16 (40.6)	6 (15.2)	1.84 (46.8)	1.51 (38.4)	1.43 (36.3)	1.33 (33.7)	1.20 (30.5)	1.01 (25.6)	0.65 (16.4)	
	1S	13 (33.0)	9 (22.9)	2.58 (65.7)	2.12 (53.9)	1.99 (50.6)	1.81 (45.9)	1.58 (40.2)	1.25 (31.7)	0.71 (18.1)	
	2N	16 (40.6)	6 (15.2)	1.98 (50.3)	1.58 (40.1)	1.50 (38.1)	1.40 (35.5)	1.27 (32.3)	1.07 (27.2)	0.69 (17.5)	
	2S	14 (35.6)	8 (20.3)	2.67 (67.7)	2.22 (56.4)	2.08 (52.8)	1.85 (47.1)	1.63 (41.5)	1.28 (32.4)	0.74 (18.7)	
	3N	16 (40.6)	6 (15.2)	2.01 (51.0)	1.65 (41.9)	1.57 (39.9)	1.48 (37.6)	1.33 (33.7)	1.11 (28.3)	0.72 (18.2)	
	3S	15 (38.1)	7 (17.8)	2.37 (60.2)	1.97 (50.1)	1.85 (46.9)	1.70 (43.2)	1.50 (38.0)	1.21 (30.7)	0.70 (17.9)	
	4N	16 (40.6)	6 (15.2)	2.17 (55.2)	1.77 (45.0)	1.66 (42.2)	1.53 (38.8)	1.38 (35.1)	1.11 (28.1)	0.65 (16.4)	
	4S	16 (40.6)	6 (15.2)	2.43 (61.7)	1.93 (49.0)	1.79 (45.6)	1.67 (42.4)	1.48 (37.6)	1.23 (31.2)	0.73 (18.6)	
70 (21.1)	1N	16 (40.6)	6 (15.2)	2.82 (71.6)	2.07 (52.5)	1.89 (47.9)	1.69 (42.8)	1.52 (38.7)	1.18 (30.0)	0.69 (17.5)	
	1S	13 (33.0)	9 (22.9)	3.84 (97.5)	2.78 (70.7)	2.51 (63.8)	2.19 (55.7)	1.91 (48.4)	1.37 (34.9)	0.70 (17.9)	
	2N	16 (40.6)	6 (15.2)	3.07 (78.0)	2.29 (58.2)	2.12 (53.8)	1.92 (48.7)	1.74 (44.1)	1.36 (34.7)	0.78 (19.9)	
	2S	14 (35.6)	8 (20.3)	4.02 (102.2)	2.98 (75.7)	2.69 (68.3)	2.34 (59.5)	2.02 (51.3)	1.46 (37.1)	0.75 (19.0)	
	3N	16 (40.6)	6 (15.2)	3.01 (76.5)	2.31 (58.7)	2.12 (54.0)	1.94 (49.2)	1.73 (43.9)	1.36 (34.7)	0.78 (19.9)	
	3S	15 (38.1)	7 (17.8)	3.30 (83.9)	2.64 (67.1)	2.42 (61.3)	2.13 (54.1)	1.87 (47.5)	1.38 (35.0)	0.73 (18.6)	
	4N	16 (40.6)	6 (15.2)	3.05 (77.6)	2.35 (59.6)	2.14 (54.5)	1.89 (48.1)	1.67 (42.5)	1.26 (32.0)	0.69 (17.5)	
	4S	16 (40.6)	6 (15.2)	3.09 (78.4)	2.47 (62.8)	2.28 (57.8)	2.03 (51.5)	1.79 (45.5)	1.36 (34.7)	0.74 (18.7)	
104 (40.0)	1N	16 (40.6)	6 (15.2)	4.98 (126.4)	2.67 (67.9)	2.36 (60.0)	2.03 (51.5)	1.76 (44.6)	1.28 (32.6)	0.67 (17.0)	
	1S	13 (33.0)	9 (22.9)	5.88 (149.4)	3.44 (87.3)	2.93 (74.4)	2.43 (61.8)	2.03 (51.5)	1.39 (35.4)	0.68 (17.4)	
	2N	16 (40.6)	6 (15.2)	4.49 (113.9)	3.05 (77.6)	2.74 (69.6)	2.38 (60.5)	2.06 (52.4)	1.52 (38.5)	0.79 (19.9)	
	2S	14 (35.6)	8 (20.3)	6.01 (152.6)	3.64 (92.4)	3.12 (79.2)	2.56 (65.0)	2.12 (53.9)	1.44 (36.5)	0.70 (17.9)	
	3N	16 (40.6)	6 (15.2)	4.71 (119.7)	2.97 (75.5)	2.64 (66.9)	2.27 (57.7)	1.97 (50.0)	1.44 (36.5)	0.75 (19.0)	
	3S	15 (38.1)	7 (17.8)	4.93 (125.3)	3.21 (81.5)	2.78 (70.6)	2.34 (59.5)	1.96 (49.9)	1.37 (34.9)	0.69 (17.5)	
	4N	16 (40.6)	6 (15.2)	4.64 (117.9)	2.92 (74.1)	2.57 (65.3)	2.17 (55.1)	1.83 (46.5)	1.29 (32.9)	0.65 (16.4)	
	4S	16 (40.6)	6 (15.2)	5.00 (127.1)	2.87 (72.8)	2.65 (67.3)	2.26 (57.4)	1.92 (48.9)	1.38 (35.0)	0.70 (17.9)	

7.4.3 Phase 2A - Sensor Responses under the FWD Load Plate

While the FWD load was dropped over seven sensors embedded in each of the four instrumented pavement sections, outputs from the embedded sensors were recorded with a Megadac 5108A data acquisition system at the three loads and three temperatures. Table 32 is a summary of maximum sensor responses recorded during the second drop and normalized to a 9,000 lb (40.0 kN) load. LVDT data referenced to the top of the subgrade were not included in the table. As with the FWD data, these sensor data show consistent trends of dynamic response increasing with temperature, but not with AC thickness, and generally good agreement between longitudinal and transverse strain under the FWD load plate.

Table 32. Measured sensor responses under FWD load plate, after 10,000 runs.

Measured responses from embedded sensors under FWD load normalized to 9000 lb (40 kN)				
Section	1S	2S	3S	4S
Surface Mix	Evotherm	Sasobit	Aspha-min	HMA Control
Total AC thickness	13" (33.0 cm)	14" (35.6 cm)	15" (38.1 cm)	16" (40.6 cm)
Nominal air temperature	Average longitudinal tensile strain (με)			
40°F (4.4°C)	12.5	20.2	16.1	10.1
70°F (21.1°C)	30.4	42.7	16.7	36.3
104°F (40.0°C)	55.6	70.4	52.2	51.6
	Average transverse tensile strain (με)			
40°F (4.4°C)	17.3	22.7	18.0	15.1
70°F (21.1°C)	39.6	40.0	22.3	32.3
104°F (40.0°C)	51.3	49.8	51.3	47.7
	Vertical pressure on subgrade (psi (kPa))			
40°F (4.4°C)	1.21 (8.35)	0.77 (5.32)	1.06 (7.34)	0.63 (4.36)
70°F (21.1°C)	3.06 (21.2)	2.52 (17.4)	2.27 (15.6)	1.42 (9.79)
104°F (40.0°C)	4.34 (29.9)	3.19 (22.0)	3.97 (27.4)	4.25 (29.3)
	Deep LVDT deflection (mil(μm))			
40°F (4.4°C)	1.91 (48.5)	2.03 (51.5)	1.82 (46.2)	1.48 (37.6)
70°F (21.1°C)	2.04 (51.8)	4.42 (112)	2.20 (55.9)	2.34 (59.4)
104°F (40.0°C)	6.43 (163)	4.84 (123)	4.30 (109)	3.86 (98.0)

7.5 Phase 2B - Rolling Wheel Load Responses

On the same day the FWD tests were performed, output from the pavement sensors was recorded as a matrix of three loads and four lateral offsets were run unidirectionally with the rolling dual tires at 5 mph (8 km/h). Loads were 6,000 lb (26.7 kN), 9,000 lb (40.0 kN), and 12,000 lb (53.4 kN) and lateral offsets from the centerline were 0 (midpoint between the two tires), 2 inches (5.1 cm) (inside edge of dual tire), 7 inches (17.8 cm) (center of dual tire), and 12 inches (30.5 cm) (outside edge of dual tire). Table 33 shows average maximum longitudinal strain, average maximum transverse strain, maximum vertical deflection from the deep LVDT, and maximum vertical pressure measured along the centerline of the pavement sections under the 9,000 lb. (40.0 kN) rolling dual tire load at three temperatures. Normalization was not necessary for sensor responses under the rolling tires because earlier checks with platform scales indicated that hydraulic loads applied to the rolling wheel assembly were very accurate.

Table 33. Measured sensor responses under rolling wheel load, after 10,000 runs.

Measured responses from embedded sensors under rolling wheel load of 9000 lb (40 kN)				
Section	1S	2S	3S	4S
Surface Mix	Evotherm	Sasobit	Aspha-min	HMA Control
Total AC thickness	13" (33.0 cm)	14" (35.6 cm)	15" (38.1 cm)	16" (40.6 cm)
Nominal air temperature	Average longitudinal tensile strain (με)			
40°F (4.4°C)	17.6	17.1	15.8	17.6
70°F (21.1°C)	37.2	40.4	29.6	33.3
104°F (40.0°C)	30.6	33.7	30.3	56.9
	Average transverse tensile strain (με)			
40°F (4.4°C)	22.5	21.2	19.5	18.8
70°F (21.1°C)	54.9	58.3	38.1	33.6
104°F (40.0°C)	174.8	165.7	159.1	116.2
	Vertical pressure on subgrade (psi (kPa))			
40°F (4.4°C)	1.50 (10.3)	0.74 (5.1)	1.24 (8.6)	0.86 (6.0)
70°F (21.1°C)	3.75 (25.9)	3.03 (20.9)	2.84 (19.6)	2.51 (17.3)
104°F (40.0°C)	7.59 (52.3)	6.66 (46.0)	6.64 (45.8)	6.22 (42.9)
	Deep LVDT deflection (mil(μm))			
40°F (4.4°C)	2.24 (56.7)	1.97 (50.0)	1.80 (45.7)	1.93 (49.0)
70°F (21.1°C)	4.00 (102)	4.62 (117)	2.99 (75.9)	2.97 (75.4)
104°F (40.0°C)	7.47 (190)	11.1 (282)	9.95 (253)	7.23 (184)

While trends of increasing response with increasing temperature and decreasing AC thickness generally prevailed under the FWD and rolling tires, there were two major differences between responses under the two types of loading. First, as temperature increased, transverse strain became much larger than longitudinal strain under the rolling tires and larger than transverse and longitudinal strains measured under the FWD load plate, which were both about the same as longitudinal strain under the rolling tires. Second, the magnitudes of surface deflection and vertical pressure on the subgrade also were much larger under the 5 mph (8.0 km/hr) rolling tires than under the FWD load plate at higher temperatures. Both observations confirm that rolling tire loads moving at creep speed induce certain higher responses on AC pavements than the FWD, which is designed to simulate vehicle loads traveling at normal highway speeds. Similar trends of speed dependent responses have been observed on other instrumented pavements in Ohio.

7.6 Phase 3 - Surface Rutting

Previous testing in the APLF showed that AC consolidation progresses at a near linear rate on a log-log plot of average depth vs. number of load applications, and power trendlines, of the form $y = ax^b$, fit the data quite well. For these tests, therefore, profiles were averaged at two locations in each of the eight pavement sections at 0, 100, 300, 1000, 3000 and 10000 load cycles to provide a good distribution of points along the logarithmic application axis. All loading was performed with standard dual tires loaded to 9,000 lb. (40 kN) rolling in a bidirectional

mode at 5 mph (8 kph) with no wheel wander. It required about one week to apply 10,000 bidirectional loading cycles.

Surface deformations were measured with a 10-foot (3.05 m) long rolling wheel profilometer developed by ORITE, which measures elevations to at least a 5-mil (127 micron) accuracy at 0.5 inch (1.27 cm) intervals along the profile path. To avoid any effects from loads being applied in adjacent lanes, profiles were skewed across the eight-foot wide lanes so profiler feet were located along the lane edges. Profiler lateral position and elevation were referenced by fender washers epoxied to the pad for the profiler feet to sit on during each set of measurements.

The eight pavement sections were identified by lane number and north or south end of the lane; i.e., 1S or 2N. The two profile locations within each pavement section were further identified by adding a north or south indicator to the section identifier; i.e., 1SS, 1SN, 2SS or 2NS. To minimize any vertical offsets which occasionally occurred at the ends of a profile, all profiles were aligned by: 1) moving profiles vertically so the average of the first five points matched the average of the same five points on the reference profile, and 2) rotating the profiles around the first point until the average of the last five points on each profile matched the average of the last five points on the reference profile.

Figure 32 shows a typical profile history measured in Section 1S at 104°F (40.0°C). The heavy line is the initial reference profile recorded after completion of the 40°F (4.4°C) and 70°F (21.1°C) tests. This plot shows:

1. Changes in the lateral profile of the pavement surface as repeated rolling wheel loads were applied to the pavement. These profile changes are the result of permanent deformations in the pavement structure which include zones of downward consolidation under the tires and upward shoving/heaving outside the tires. Consolidation and shoving/heaving were calculated as areas by integrating incremental differences in elevation from a reference profile. The depth of consolidation was calculated as the linear change in elevation under the tires from the initial reference profile and, if the height of shoving/heaving were also used, it would be calculated similarly outside the tires.

   Rut and rutting are general terms often used to describe the depth or extent of consolidation in pavement wheelpaths. Rut depth is a linear difference in elevation between certain high and low points on a profile. Unfortunately, however, the calculation of rut depths varies with procedures used to measure profiles and define ruts. In this study, average depth of consolidation was used to define deformation under the tires.

   Long straightedges are the most practical method of measuring ruts in the field since references are usually not available to compare profiles. While ruts measured vertically from a straightedge laid across the wheelpath to the lowest point in the wheelpath are what drivers feel on the road and what ponds water, they usually contain elements of consolidation and shoving/heaving. In a controlled setting like the APLF, however, referenced profiles make it possible to monitor consolidation and shoving/heaving separately. This information provides a more detailed picture of how pavement build up, asphalt concrete mix and temperature affect surface deformation.
2. Zones of AC consolidation are bounded by inflection points on the profiles, the lateral position of which remained stable throughout 10,000 loading cycles. The position of these points varied slightly over the 16 profiling locations on the test pad, probably due to

slight variations in the layout of the reference washers and the location of the profiler on the washers, but were very close to the edges of the rolling tires in all profiles.

3. Initial consolidation in the wheelpaths was caused by earlier testing at 40°F (4.4°C) and 70°F (21.1°C), both of which resulted in minimal surface deformation and were considered as seating runs for the 104°F (40.0°C) tests. Because of equipment malfunctions, approximately one year was required to complete all rolling wheel tests at three temperatures in the APLF, instead of the anticipated three months. As a result, it was difficult to compare as-built profiles with subsequent profiles because of changing test temperatures in the facility and loading in adjacent lanes which caused some minor surface deformations over time. In general, there was little change in profiles at 40° F (4.4° C), minimal deformation under the tires at 70°F (21.1°C), and substantial consolidation under the tires and shoving/heaving outside the tires at 104° F (40° C). The as-built profile in Figure 28 can be approximated by continuing the 0 pass line from before the left tire up to the 0 pass peak between the tires and on past the right tire to form a smooth concave surface.
4. If rut depth was measured with a straightedge in Figure 4 after 10,000 loading cycles, it would be about 0.45 inches (1.14 cm), of which 0.30 inches (0.76 cm) is the depth of consolidation and 0.15 inches (0.38 cm) is the height of shoving/heaving. A rut depth of 0.5 inches (1.27 cm) is often used as a criterion to grind or overlay AC pavements.
5. Undulations within the consolidated portion of the profiles were likely caused by the five treads in each tire, which remained in the same lateral position for all passes of the tires due to the lack of wander in the rolling wheel tests. These treads are shown in Figure 33.

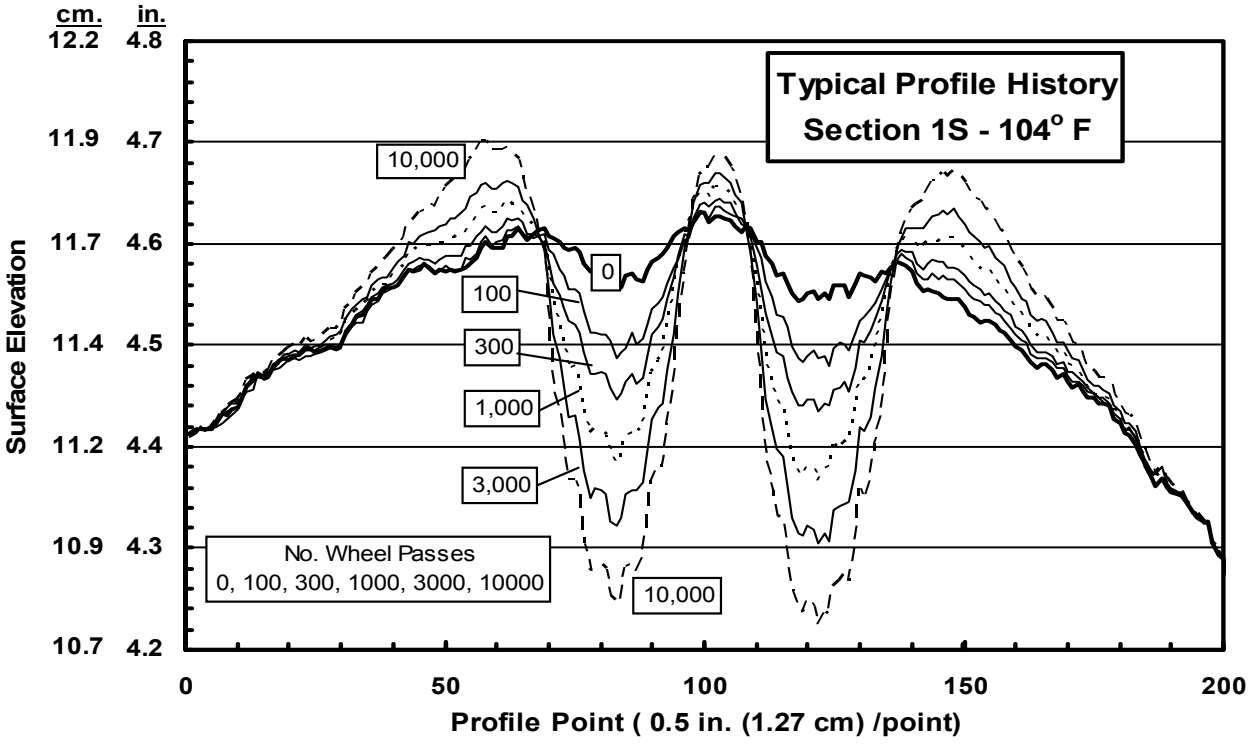

Figure 32. Profile history in Section 1S.

Figure 33. Treads on the rolling dual tires (load wheel).

Figure 34 and Figure 35 show aligned profiles measured at 0, 100, 300, 1000, 3000 10000 cycles at Location 1SS during the 40°F (4°C) and 70°F (21°C) tests, respectively, which were typical of profiles obtained at other locations. Profile changes at 40°F (4°C) were on the order of the accuracy of the profiler. Changes at 70°F (21°C) were minimal with maximum differences in elevation being less than 0.1 inches (2.5 mm) and very little deformation outside the tires. While 10,000 load cycles were applied and profiles recorded at all temperatures on all pavement sections, only the 104°F (40°C) profiles were considered sufficiently reliable to evaluate the deformation characteristics of warm AC mixes in this study.

Figure 36 and Figure 37 show the raw and aligned profiles for Location 1SS at 104°F (40°C). The most obvious difference between these two sets of profiles occurs at both ends where alignment improved agreement with the reference profile. Initial deformation was generated by the lower temperature tests run earlier, and deformation patterns under the tires were caused by the five treads in each tire, which ran in the same lateral position during the three series of tests. These treads were approximately 1.25 inches (3.2 cm) wide and separated by approximately 1 inch (2.5 cm) wide grooves. Figure 36 and Figure 37 also show how AC material consolidated under the dual tires and was shoved or heaved outside the tire boundaries as wheel passes accumulated over time.

Tire 1 was the tire closest to the profiler home position and the location of Rut 1 in all figures. Because of space limitations around the edges of the AC pad, profiles in Lane 1 and Lane 2 were measured with the computer (and profiler home position) on the east side of the lane, and profiles in Lane 3 and Lane 4 were measured with the computer (and profiler home position) on the west side of the lane. Consequently, Rut 1 was the eastern rut in Lane 1 and Lane 2, and the western rut in Lane 3 and Lane 4.

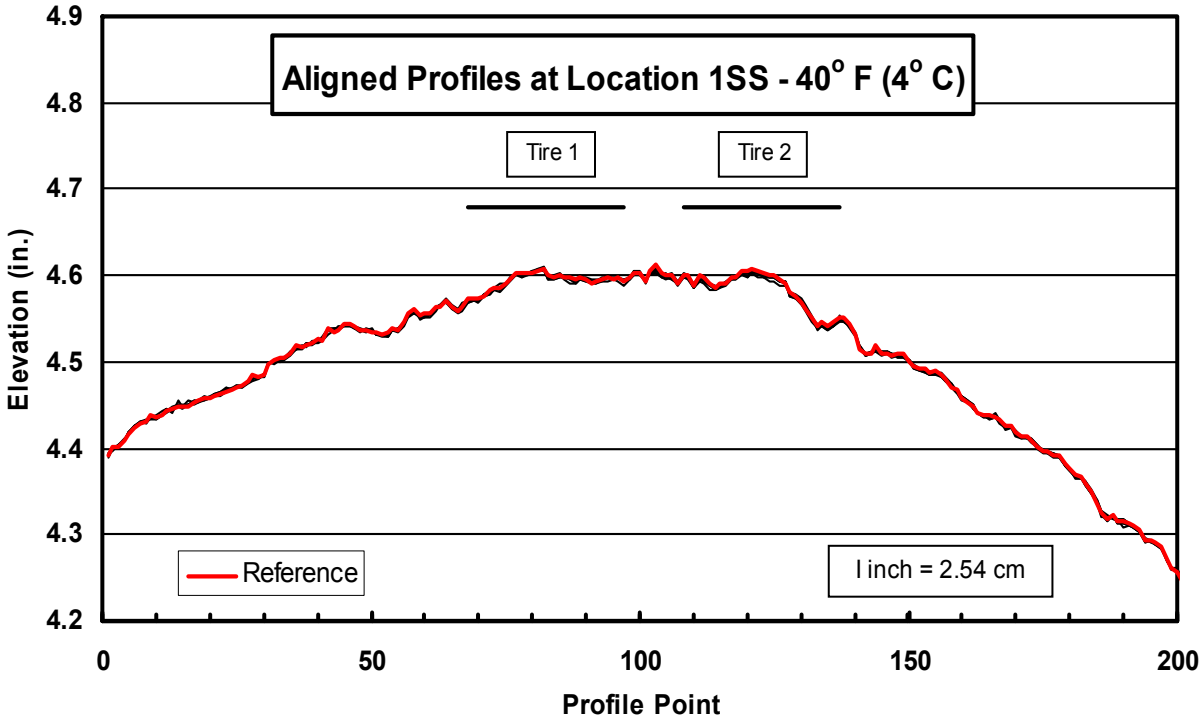

Figure 34. Aligned 40°F (4°C) profiles at Location 1SS. See Color Plate 11 in Appendix E.

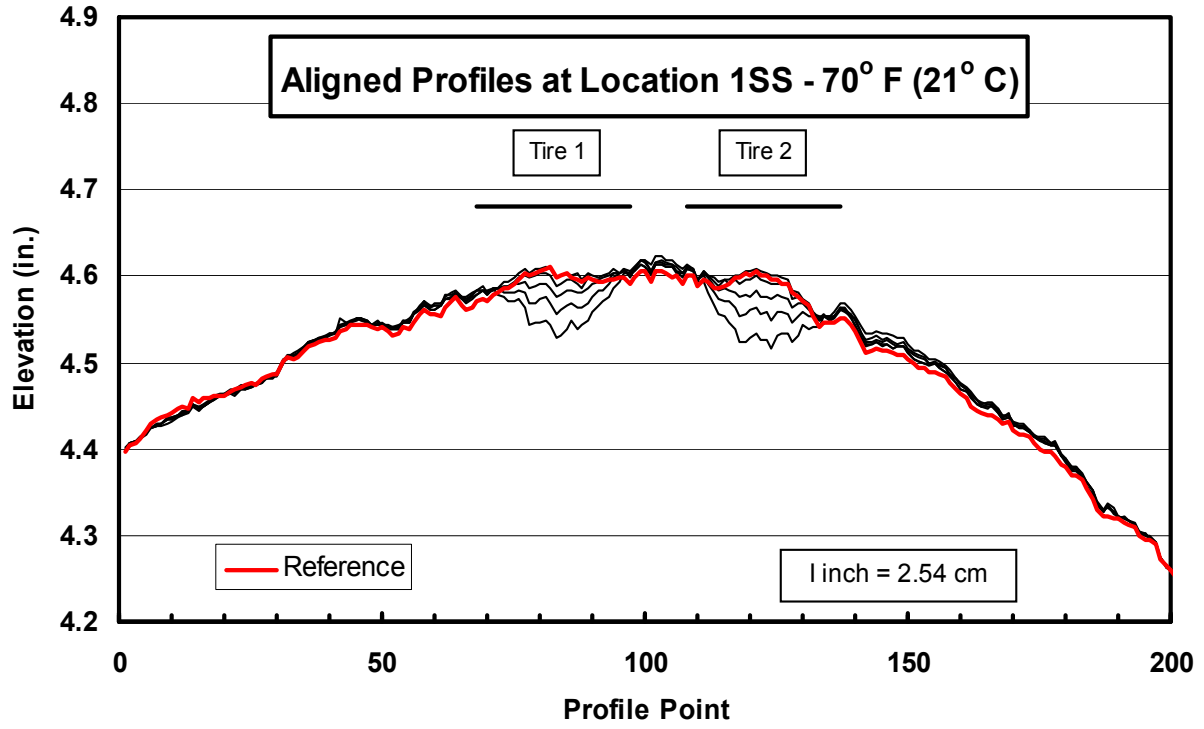

Figure 35. Aligned 70°F (21°C) profiles at Location 1SS. See Color Plate 12 in Appendix E.

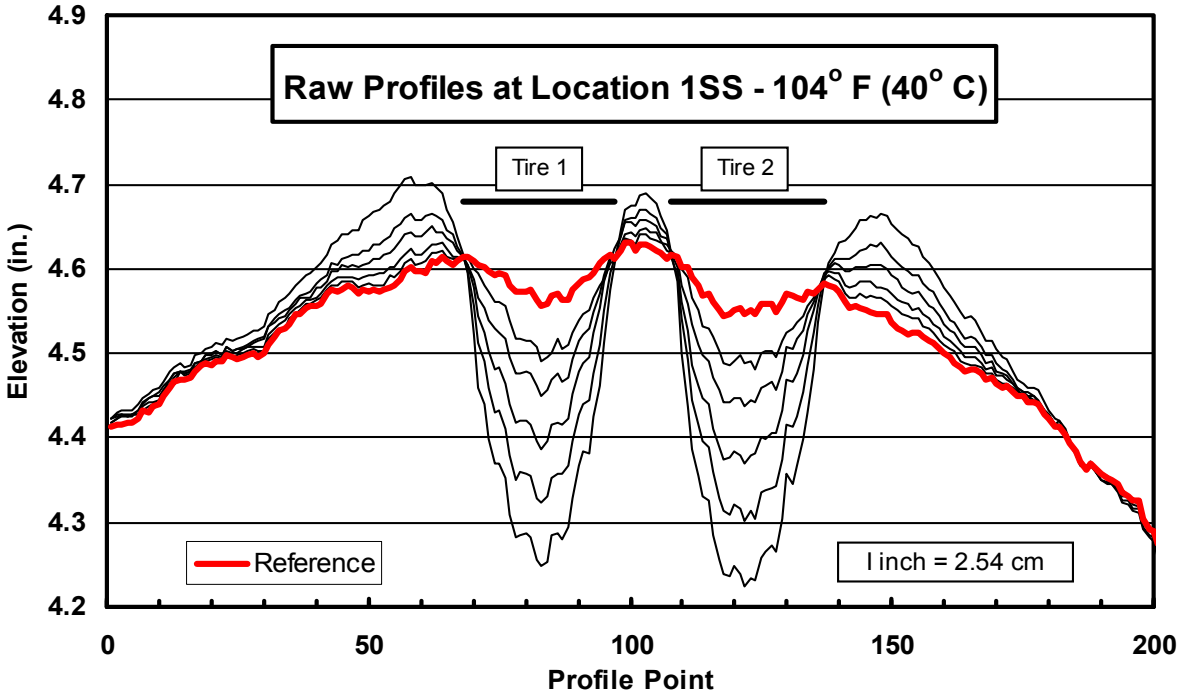

Figure 36. Raw 104°F (40°C) profiles at Location 1SS. See Color Plate 13 in Appendix E.

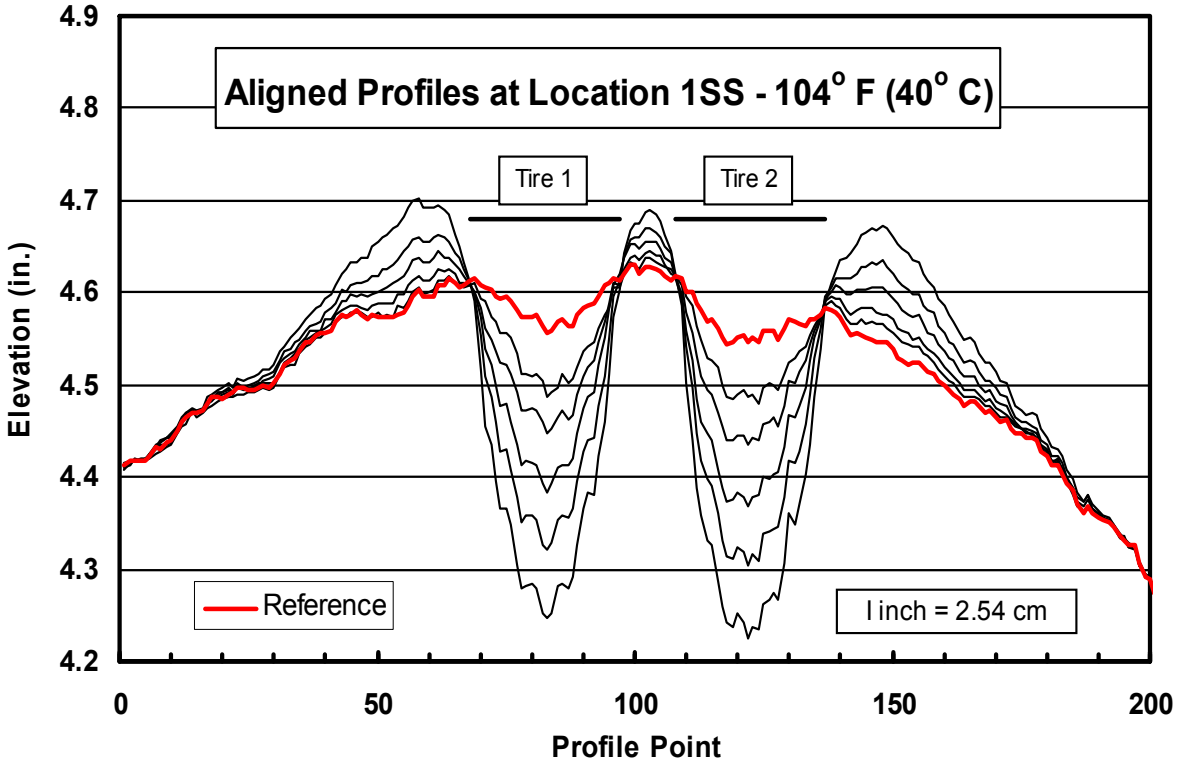

Figure 37. Aligned 104°F (40°C) profiles at Location 1SS. See Color Plate 14 in Appendix E.

Figure 38 and Figure 39 show typical details of how the AC material deformed around individual rolling tires during the 104°F (40°C) tests, and how these ruts include elements of consolidation under the tires and shoving/heaving outside the tires. On in-service pavements, lateral tire wander causes the area of consolidation to broaden out into a single depression across the wheelpath and, when ruts are measured there with a straightedge, the relative contributions of consolidation and shoving/heaving are unknown. Of particular interest in Figure 38 and Figure 39 are inflection points just inside the tires edges that the AC material appears to rotate around as it deforms during repeated loading. The lateral stability of these points facilitated the analysis of the profile measurements by not having to account for changing deformation patterns. This study was focused on the effects of AC surface mixes and AC thickness on pavement deformation.

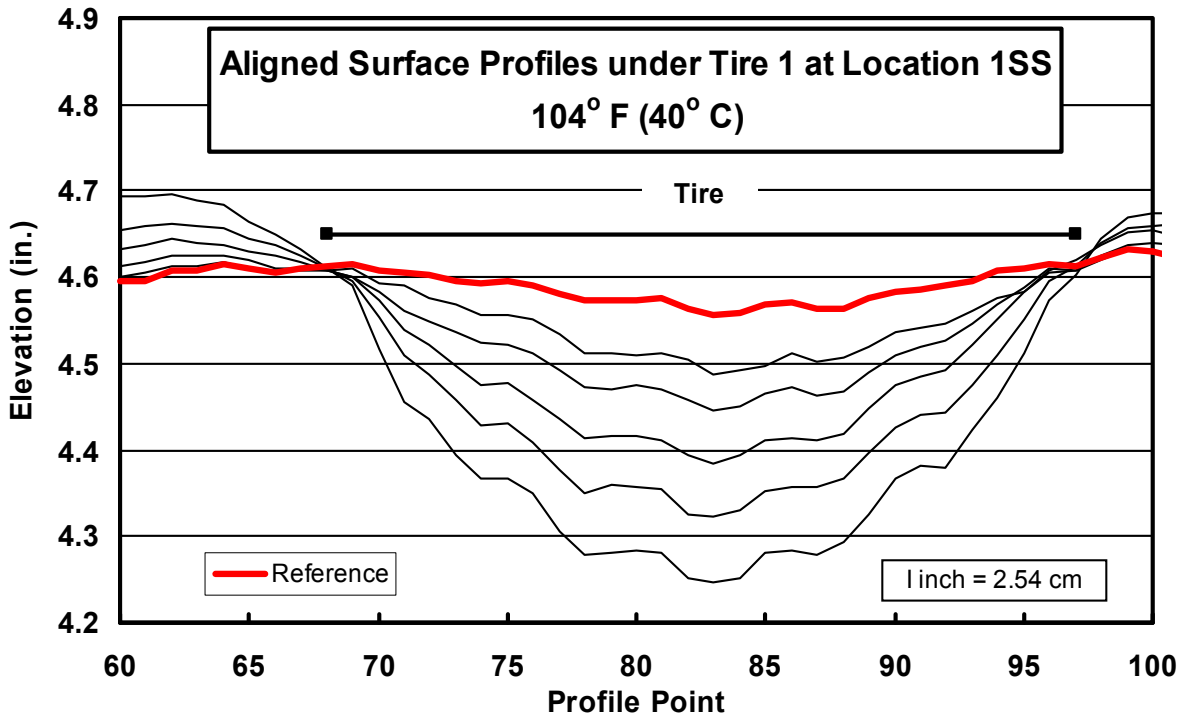

Figure 38. Aligned 104°F (40°C) profiles under Tire 1 at Location 1SS. See Color Plate 15 in Appendix E.

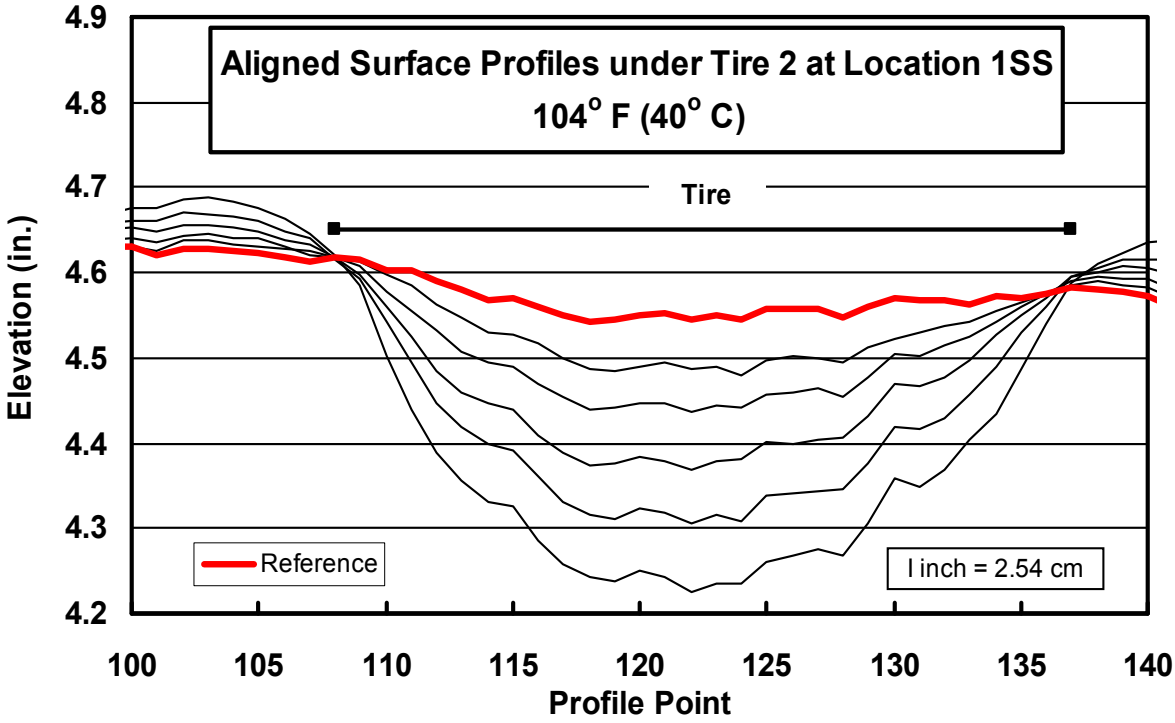

Figure 39. Aligned 104°F (40°C) profiles under Tire 2 at Location 1SS. See Color Plate 16 in Appendix E.

Figure 40, Figure 41, and Figure 42 show average depths of consolidation for the 104°F (40°C) tests at Location 1SS plotted as linear, semi-log, and log-log charts, respectively. Power and logarithmic trendlines are included in each graph to determine which type best describes the data. Statistically, both trendlines are excellent with an $R^2 = 0.99$, but there are some subtle and practical differences. In Figure 40, the logarithmic trendline follows the data to 10,000 cycles, but appears to fall below the data after 10,000 cycles, making long term predictions unreliable. The power trendline does not follow the data as closely to 10,000 cycles, and appears to be going well above the data after 10,000 cycles. In Figure 41, the logarithmic trendline again fits the data better than the power trendline. Both trendlines fit the data about the same in Figure 42, but power trendlines of the form $y = ax^b$ are easier to use on log-log plots since they are straight lines, and since constant a is the average depth of consolidation calculated at one cycle and b defines the slope of the trendline. Direct comparisons of a and b in this study should be limited to sections in a single lane where thickness is the only variable or across the northern half of lanes where surface mix is the only variable. All comparisons of depth of consolidation were made at 104°F (40°C), and loading cycles applied at 40°F (4°C) and 70°F (21°C) were considered as seating passes since the maximum depth of consolidation after these runs was less than 0.1 in. (2.5 mm).

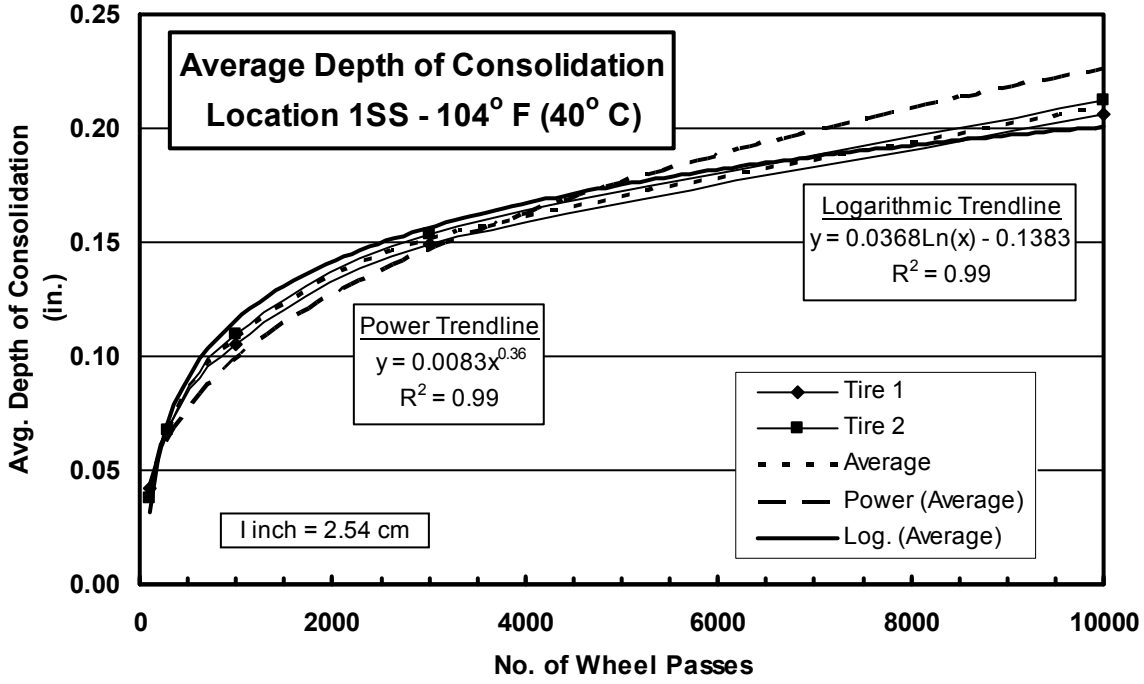

Figure 40. Linear plot of average consolidation at Location 1SS and 104°F (40°C).

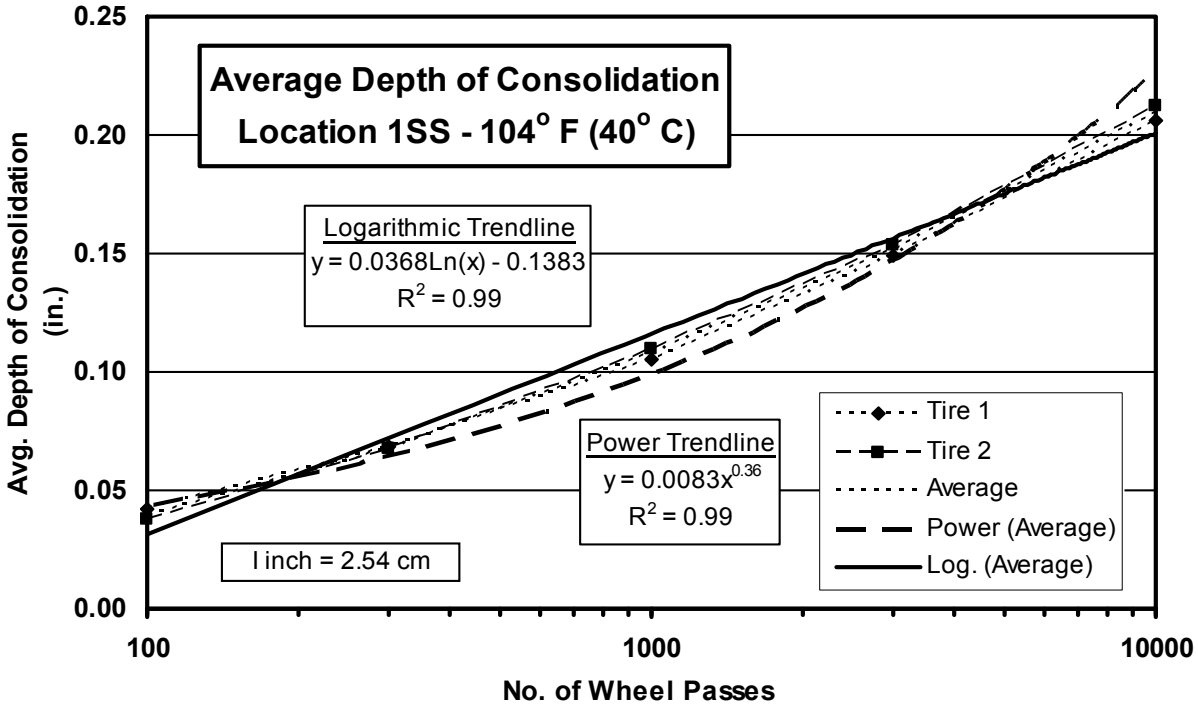

Figure 41. Semi-log plot of average rut depth at Location 1SS and 104°F (40°C).

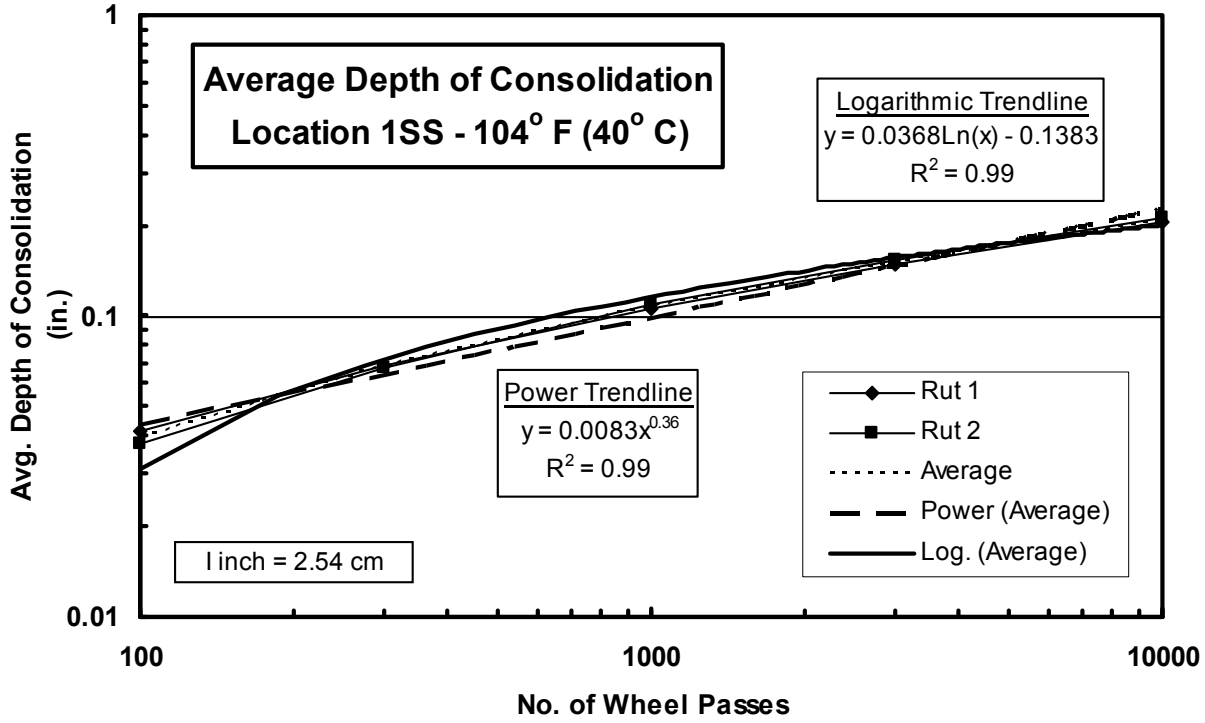

Figure 42. Log-log plot of average rut depth at Location 1SS and 104°F (40°C).

Table 34 summarizes the values of *a* and *b* calculated for depth of consolidation trendlines under individual tires and for average consolidation under the two ruts at all sixteen profile locations at 70°F (21°C) and 104°F (40°C). Both temperatures were included to show how R^2 degraded at lower temperatures, especially in Lane 3. R^2 for the 40°F (4°C) trendlines were highly erratic due to consolidation being on the same order of magnitude as the profiler accuracy. Table 35 summarizes the average trendline parameters calculated for each of the eight pavement sections at 104°F (40°C).

7.6.1 Effect of AC Surface Mix on Depth of Consolidation

The northern half of Lanes 1, 2 and 3, and the entire length of Lane 4 were 16 inches (40.6 cm) of AC over 6 inches (15.2 cm) of ODOT 304 DGAB, making Sections 1N, 2N, 3N, 4N and 4S ideal for comparing the effects of the surface mix on the depth of consolidation.

Figure 43 and Figure 44 compare the five 16-inch (40.6 cm) thick AC sections where the only variable was surface mix. Each curve represents the average of two locations in each section and parameters for the trendlines are shown in Table VIII. The linear plot in Figure 43 shows: 1) excellent agreement between redundant Sections 4N and 4S, 2) higher early consolidation in the three warm AC mixes than in the conventional mix, and 3) especially high consolidation in the Evotherm mix. The slightly reduced slope between 1,000 and 10,000 cycles for the warm AC mixes in Sections 1N, 2N and 3N, as compared to the standard AC mix Sections 4N and 4S, is confirmed in the log-log plot in Figure 44 and by exponents *b* shown for these sections in Table VIII. In summary, the three warm mix AC mixes, and especially the Evotherm mix, exhibit more

early consolidation than the standard ODOT Type I 446 mix, but this difference may be slowly mitigated as the long term rate of consolidation for the conventional mix was slightly higher than that for the warm AC mixes.

While intercept *a*, as the calculated consolidation at one load cycle is a preliminary indicator of early consolidation, it is not necessarily a reliable measure of early consolidation, as shown in Figure 43 and Figure 44, and in Table VIII. In Figure 43, the Evotherm mix in Section 1N clearly has the most early consolidation, but intercept *a* in Table VIII is larger in Section 3N than in Section 1N. This can be explained in Figure 44 where the Aspha-Min mix in Section 3N has about equal consolidation as the Evotherm mix in Section 1N at 100 and 300 cycles, but tapered off after 300 cycles to give an overall flatter slope *b* and a higher intercept *a* when extrapolated back to 1 cycle in the trendline equation.

Table 34. Depth of consolidation parameters by tire and profile location.

Trendline Parameters for Avg. Depth of Consolidation = a×(No. Load Applications)^b									
Profile Location	Tire Rut	70° F (21° C)				104° F (40° C)			
		a (in)	a (cm)	b	R^2	a (in)	a (cm)	b	R^2
1NN	Rut 1	0.00030	0.00076	0.5074	0.9845	0.00750	0.01905	0.3775	0.9845
	Rut 2	0.00020	0.00051	0.5451	0.9951	0.00840	0.02134	0.3708	0.9770
	Average	0.00020	0.00051	0.5270	0.9914	0.00800	0.02032	0.3740	0.9809
1NS	Rut 1	0.00007	0.00018	0.6604	0.9868	0.00760	0.01930	0.3687	0.9883
	Rut 2	0.00008	0.00020	0.6993	0.9512	0.00950	0.02413	0.3544	0.9786
	Average	0.00008	0.00020	0.6803	0.9711	0.00850	0.02159	0.3612	0.9836
1SN	Rut 1	0.00040	0.00102	0.4826	0.9995	0.00860	0.02184	0.3442	0.9845
	Rut 2	0.00003	0.00008	0.8253	0.9200	0.00820	0.02083	0.3636	0.9804
	Average	0.00030	0.00076	0.5055	0.9988	0.00840	0.02134	0.3543	0.9824
1SS	Rut 1	0.00002	0.00005	0.7871	0.9712	0.00910	0.02311	0.3454	0.9903
	Rut 2	0.00004	0.00010	0.7410	0.9778	0.00750	0.01905	0.3732	0.9796
	Average	0.00003	0.00008	0.7619	0.9749	0.00830	0.02108	0.3591	0.9853
2NN	Rut 1	0.00030	0.00076	0.4694	0.9899	0.00610	0.01549	0.3864	0.9926
	Rut 2	0.00020	0.00051	0.5245	0.9856	0.00530	0.01346	0.4109	0.9897
	Average	0.00020	0.00051	0.4948	0.9880	0.00570	0.01448	0.3987	0.9912
2NS	Rut 1	0.00002	0.00005	0.7681	0.9722	0.00750	0.01905	0.3554	0.9869
	Rut 2	0.00001	0.00003	0.7972	0.9629	0.00500	0.01270	0.3949	0.9844
	Average	0.00002	0.00005	0.7804	0.9683	0.00620	0.01575	0.3736	0.9859
2SN	Rut 1	0.00009	0.00023	0.5807	0.9997	0.00540	0.01372	0.3661	0.9927
	Rut 2	0.00006	0.00015	0.5987	0.9816	0.00420	0.01067	0.4067	0.9912
	Average	0.00007	0.00018	0.5886	0.9953	0.00480	0.01219	0.3866	0.9921
2SS	Rut 1	0.00002	0.00005	0.7447	0.9927	0.00500	0.01270	0.3795	0.9942
	Rut 2	0.00006	0.00015	0.6332	0.9995	0.00480	0.01219	0.4110	0.9889
	Average	0.00004	0.00010	0.6868	0.9770	0.00490	0.01245	0.3965	0.9915
3NN	Rut 1	0.00110	0.00279	0.3103	0.8488	0.01050	0.02667	0.3198	0.9895
	Rut 2	0.00090	0.00229	0.2477	0.6236	0.00780	0.01981	0.3608	0.9872
	Average	0.00100	0.00254	0.2893	0.7894	0.00910	0.02311	0.3400	0.9886
3NS	Rut 1	0.00310	0.00787	0.2225	0.8856	0.01090	0.02769	0.3038	0.9884
	Rut 2	0.00120	0.00305	0.3231	0.9297	0.01230	0.03124	0.3091	0.9855
	Average	0.00200	0.00508	0.2656	0.9150	0.01160	0.02946	0.3067	0.9870
3SN	Rut 1	0.00250	0.00635	0.2301	0.8871	0.00460	0.01168	0.3920	0.9745
	Rut 2	0.00190	0.00483	0.2874	0.9040	0.00710	0.01803	0.3781	0.9770
	Average	0.00220	0.00559	0.2599	0.8992	0.00580	0.01473	0.3839	0.9760
3SS	Rut 1	0.00090	0.00229	0.3713	0.7771	0.00420	0.01067	0.3992	0.9725
	Rut 2	0.00060	0.00152	0.2791	0.8977	0.00360	0.00914	0.4464	0.9667
	Average	0.00070	0.00178	0.3449	0.8039	0.00390	0.00991	0.4245	0.9697
4NN	Rut 1	0.00100	0.00254	0.2559	0.6833	0.00210	0.00533	0.4808	0.9991
	Rut 2	0.00090	0.00229	0.3302	0.8692	0.00370	0.00940	0.4321	0.9972
	Average	0.00090	0.00229	0.2993	0.8057	0.00280	0.00711	0.4540	0.9984
4NS	Rut 1	0.00030	0.00076	0.3714	0.9263	0.00460	0.01168	0.3863	0.9991
	Rut 2	0.00010	0.00025	0.4800	0.8455	0.00490	0.01245	0.3819	0.9991
	Average	0.00020	0.00051	0.4163	0.8970	0.00480	0.01219	0.3841	0.9991
4SN	Rut 1	0.00050	0.00127	0.3637	0.9854	0.00190	0.00483	0.4829	0.9932
	Rut 2	0.00060	0.00152	0.4131	0.9873	0.00440	0.01118	0.4193	0.9893
	Average	0.00050	0.00127	0.3959	0.9869	0.00310	0.00787	0.4445	0.9917
4SS	Rut 1	0.00009	0.00023	0.5293	0.9886	0.00220	0.00559	0.4613	0.9977
	Rut 2	0.00020	0.00051	0.5195	0.9954	0.00450	0.01143	0.4127	0.9930
	Average	0.00010	0.00025	0.5229	0.9933	0.00330	0.00838	0.4330	0.9961

Table 35. Average depth of consolidation parameters by pavement section.

Pavement Section	Trendline Parameters @ 104° F (40° C)			
	a (in.)	a (cm.)	b	R^2
1N	0.0083	0.0211	0.3677	0.98
1S	0.0083	0.0211	0.3567	0.98
2N	0.0059	0.0150	0.3868	0.99
2S	0.0048	0.0122	0.3918	0.99
3N	0.0103	0.0262	0.3232	0.99
3S	0.0048	0.0122	0.4028	0.97
4N	0.0037	0.0094	0.4179	1.00
4S	0.0032	0.0081	0.4387	0.99

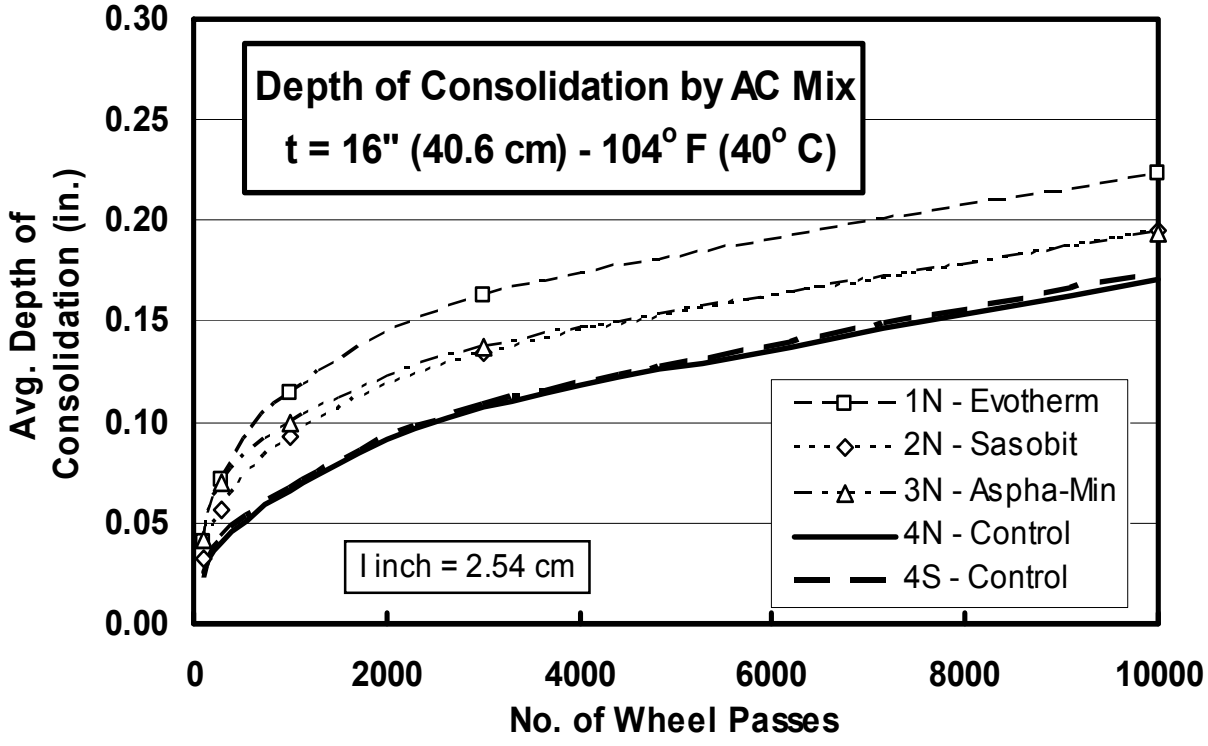

Figure 43. Linear plot of consolidation depth by AC surface mix.

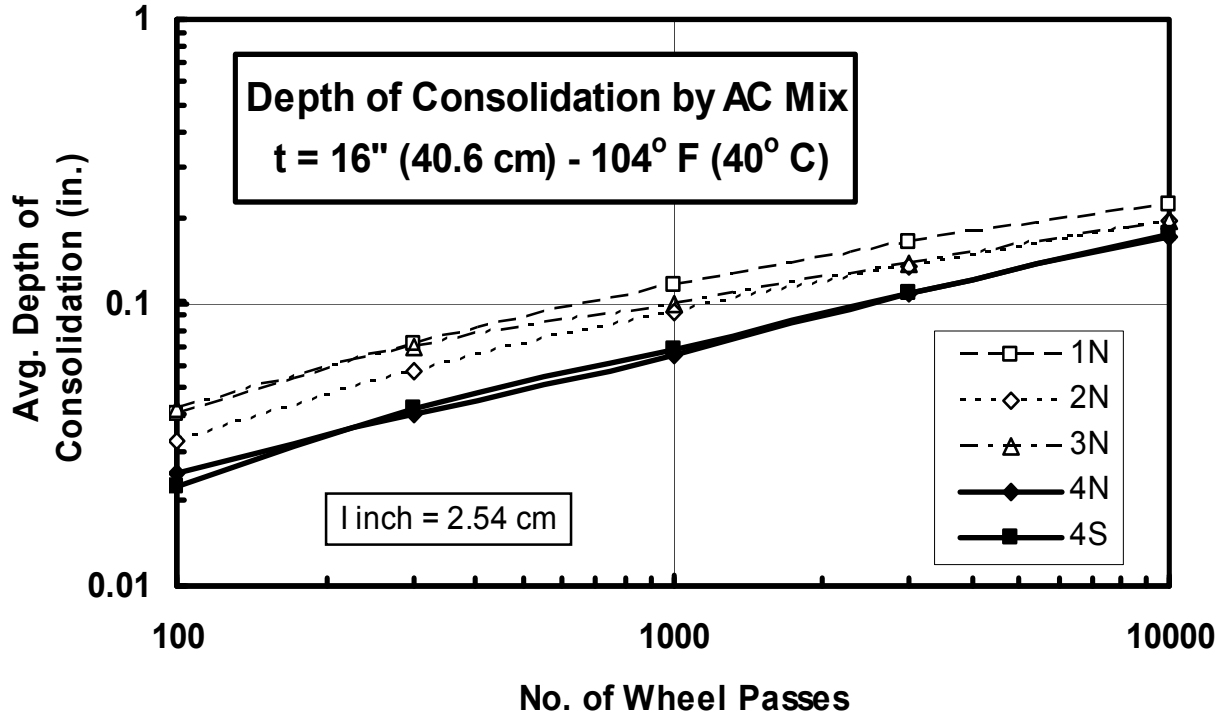

Figure 44. Log-log plot of consolidation depth by AC surface mix.

7.6.2 Effect of AC Thickness on Depth of Consolidation

The entire length of Lanes 1, 2 and 3 had warm-mix AC surface mixes with Evotherm, Sasobit and Aspha-Min, respectively, making the northern and southern halves of these lanes useful for comparing the effects of AC thickness on depth of consolidation. The northern sections in these lanes all had an AC thickness of 16 inches (40.6 cm). Figure 45 and Figure 46 show depth of consolidation plots for Lane 1 where Section 1S had an AC thickness of 13 inches (33.0 cm), Figure 47 and Figure 48 show depth of consolidation plots for Lane 2 where Section 2S had an AC thickness of 14 inches (35.6 cm), and Figure 49 and Figure 50 show depth of consolidation plots where Section 3S had an AC thickness of 15 inches (38.1 cm). In all three lanes, the 16-inch (40.6 cm) thick layers of AC had more depth of consolidation than the thinner layers of AC, but these differences in depth of consolidation were not proportional to the differences in thickness. Equation parameters and R^2 for power trendlines describing the log-log plots in Figure 46, Figure 48, and Figure 50 are shown in Table 35 above.

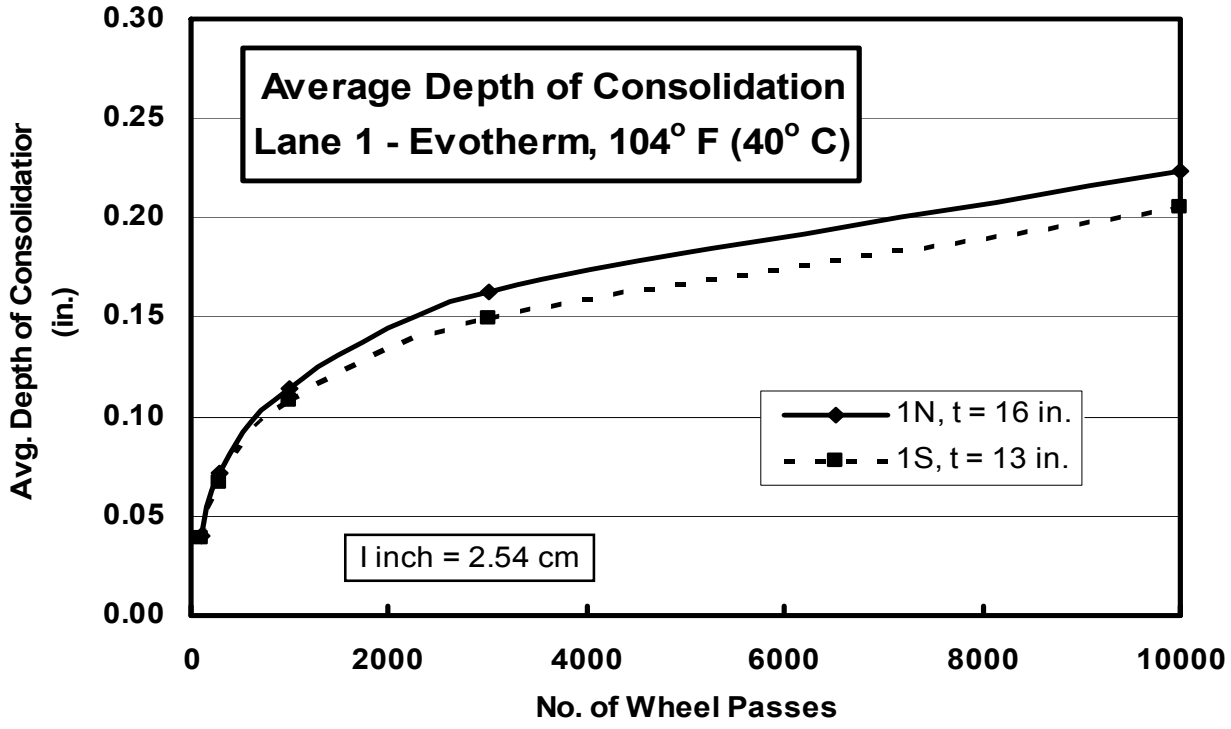

Figure 45. Effect of pavement thickness on depth of consolidation, Lane 1, linear plot.

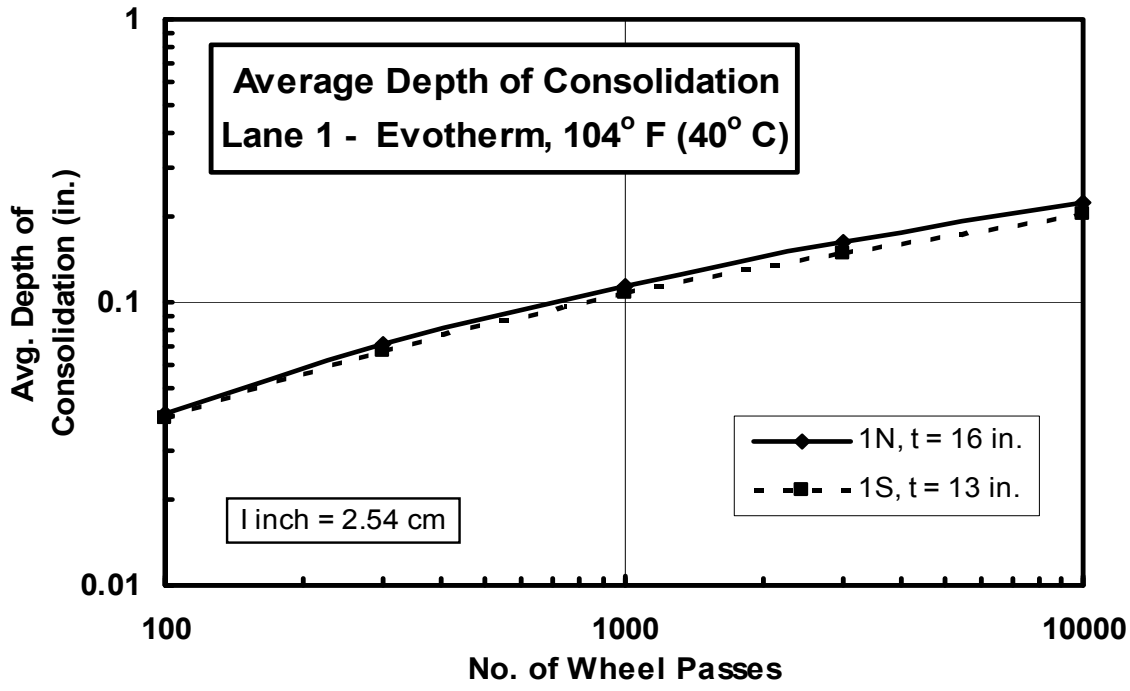

Figure 46. Effect of pavement thickness on depth of consolidation, Lane 1, log-log plot.

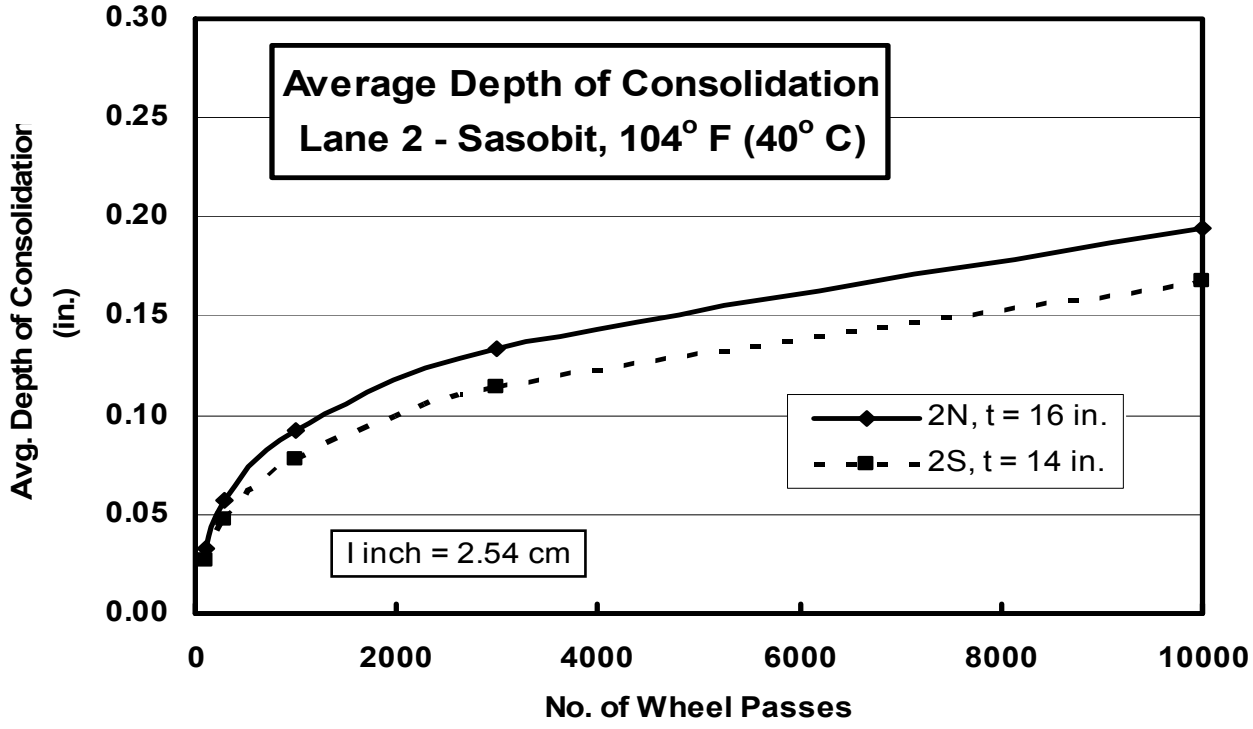

Figure 47. Effect of pavement thickness on depth of consolidation, Lane 2, linear plot.

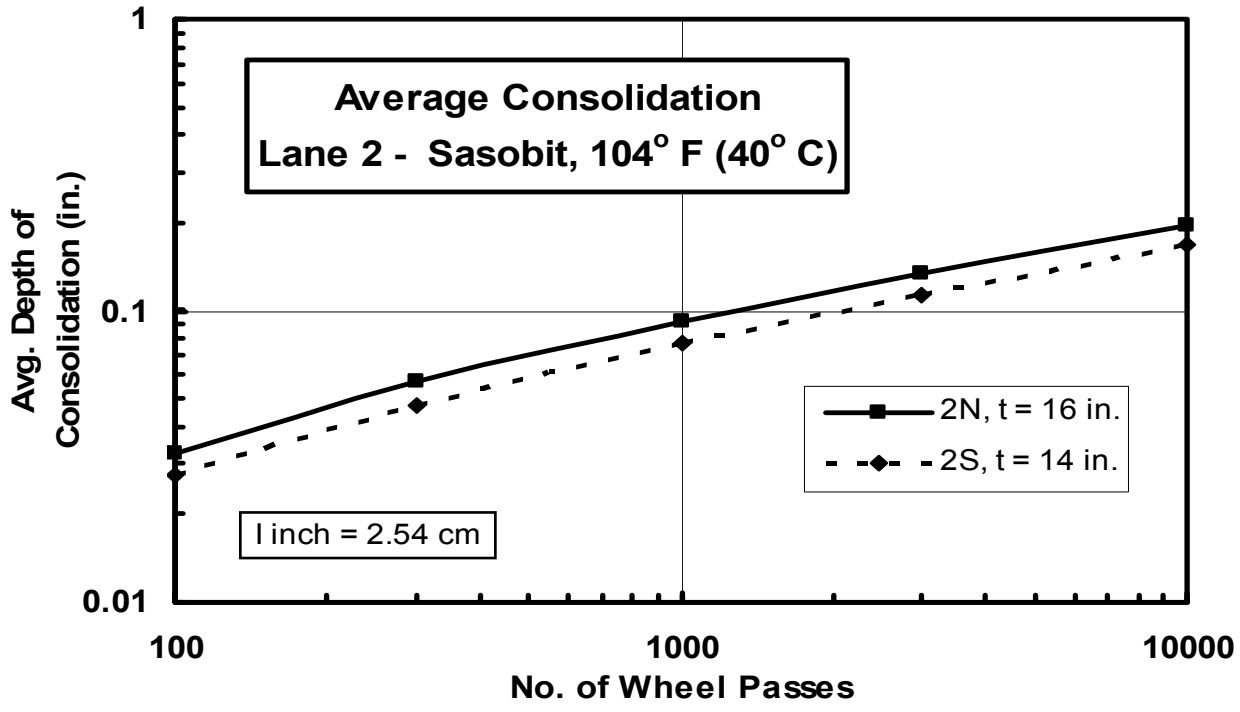

Figure 48. Effect of pavement thickness on depth of consolidation, Lane 2, log-log plot.

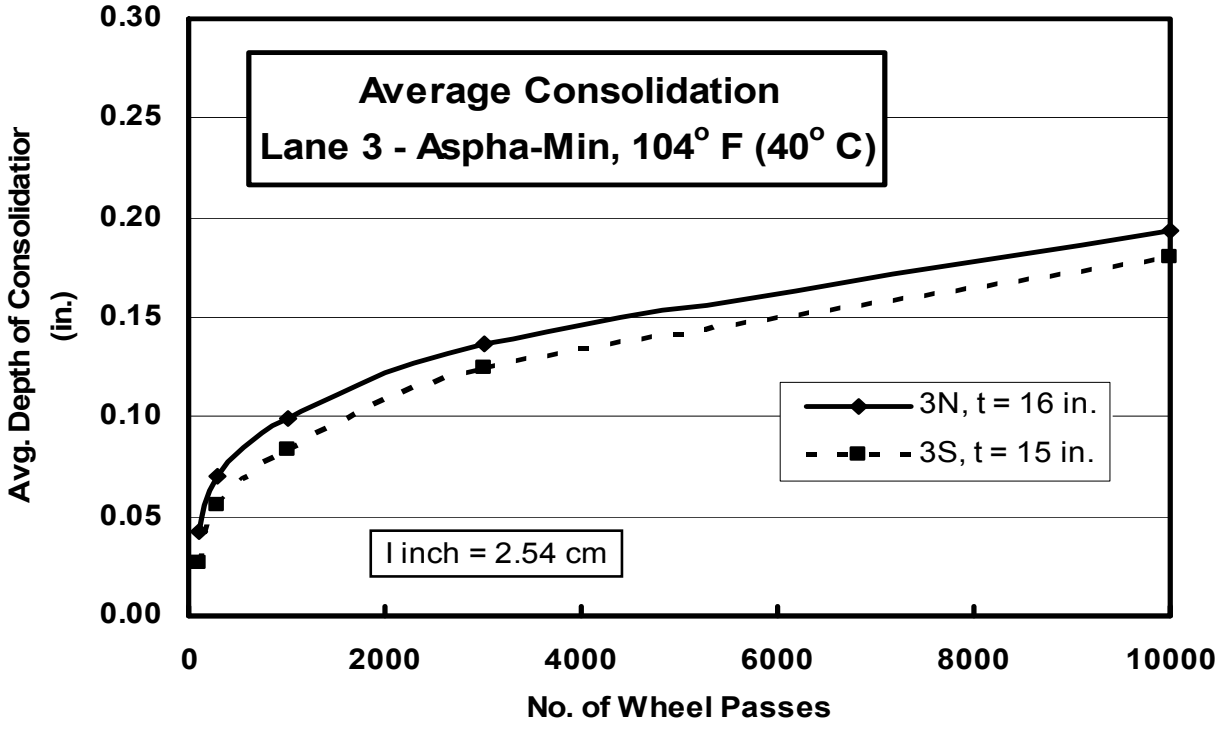

Figure 49. Effect of pavement thickness on depth of consolidation, Lane 3, linear plot.

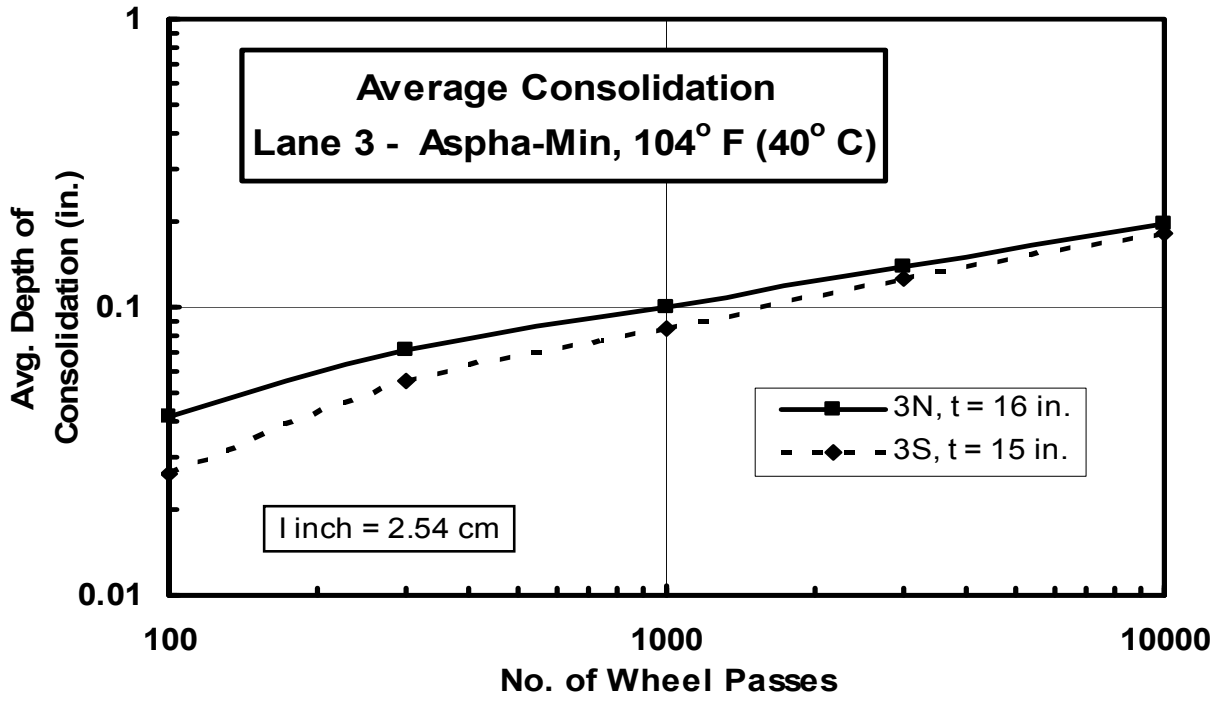

Figure 50. Effect of pavement thickness on depth of consolidation, Lane 3, log-log plot.

7.6.3 Profile Deformations

As noted earlier, surface profiles were divided into zones of consolidation and shoving/heaving as delineated by profile inflection points located just inside the edges of the rolling tires. The lateral position of these inflection points remained quite stable throughout the 10,000 loading cycles. Since detailed profiles were obtained with the profilometer, it was of interest to separate AC deformation into areas of negative consolidation under the two tires, areas of positive shoving/heaving between and outside the tires, and net deformation being the arithmetic sum of consolidation and shoving/heaving. These areas were calculated by integrating changes in elevation across profiles and plotting these values versus the number of loading cycles to determine if there were certain trends which might further characterize the effects of surface mix and AC thickness on deformation. Figure 36 and Figure 37 show how areas of consolidation and shoving/heaving expanded with an increasing number of load applications. Since all profiles were skewed across the wheelpaths, the calculated areas were adjusted to bring them perpendicular to the wheelpath. This adjustment was not necessary for average consolidation since it was calculated solely from the average of elevations measured between the inflection points, which remained the same for perpendicular and skewed profiles.

Figure 51 shows a linear plot of how areas of consolidation, shoving/heaving, and net deformation progressed in Section 1N during the 10,000 loading cycles. Consolidation is shown as negative, shoving/heaving is shown as positive, and net deformation is the sum of the two areas which, as expected, was also negative. Figure 52 shows the same data with power trendlines on a log-log plot where consolidation and net deformation were plotted as absolute values (ABS) since zero and negative numbers cannot be used in a log scale.

Plots of ABS area of consolidation in Figure 53 are identical in shape to curves in Figure 43 for average depth of consolidation. This is because areas in Figure 53 are the product of the average values in Figure 43 times the skewed profile length adjusted back perpendicular across the wheelpath. This adjusted profile length is essentially the same for all profiles and, therefore, cancels out as a variable in the area calculations. Figure 54 and Figure 55 show similar profile areas calculated for shoving/heaving and ABS net deformation in the five 16-inch (40.6 cm) thick AC sections which, as expected, is consolidation. In summary, warm AC mixes had higher initial and higher long term consolidation, higher initial shoving/heaving which quickly dissipated, and persistent higher net consolidation than the conventional AC mix.

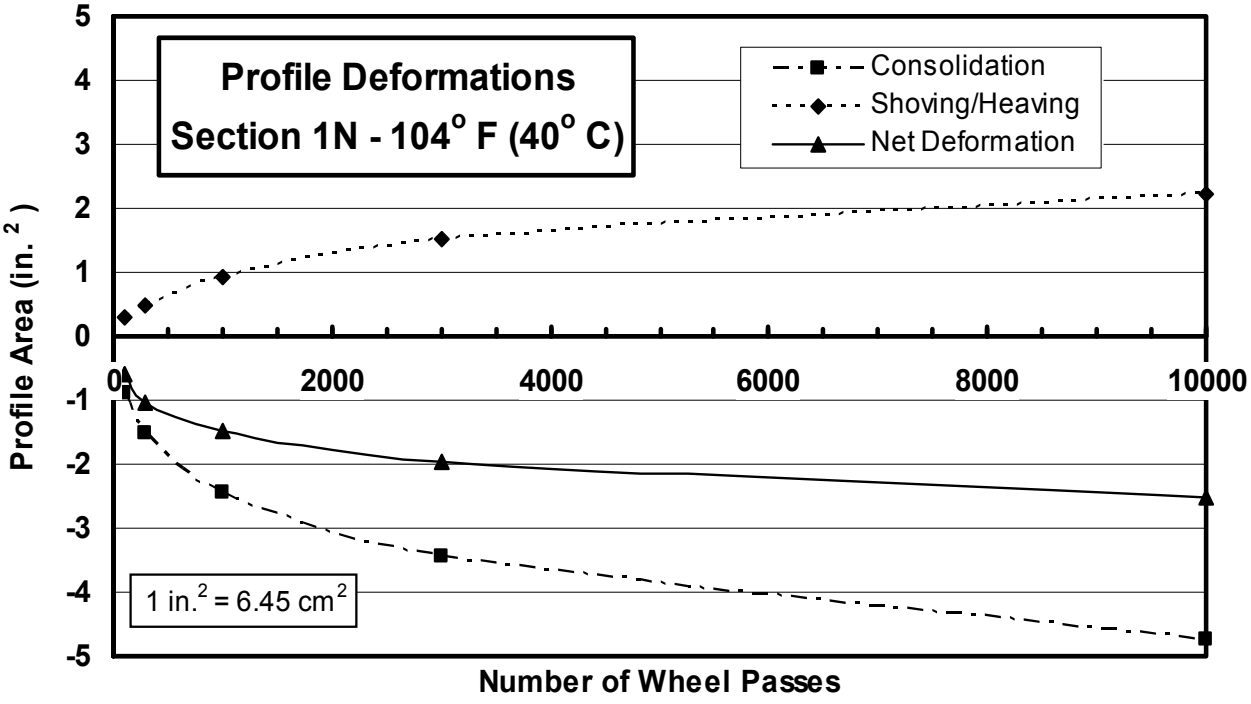

Figure 51. Linear plot of profile deformations in Section 1N.

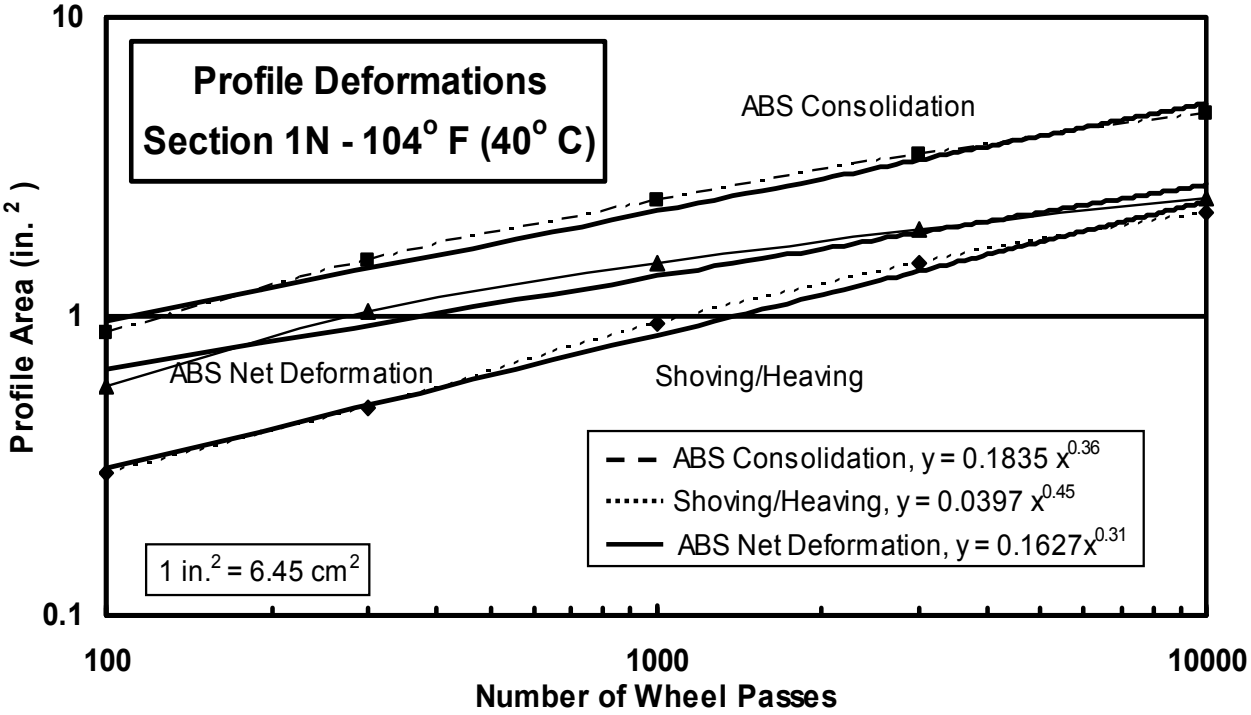

Figure 52. Log-log plot of profile deformations in Section 1N.

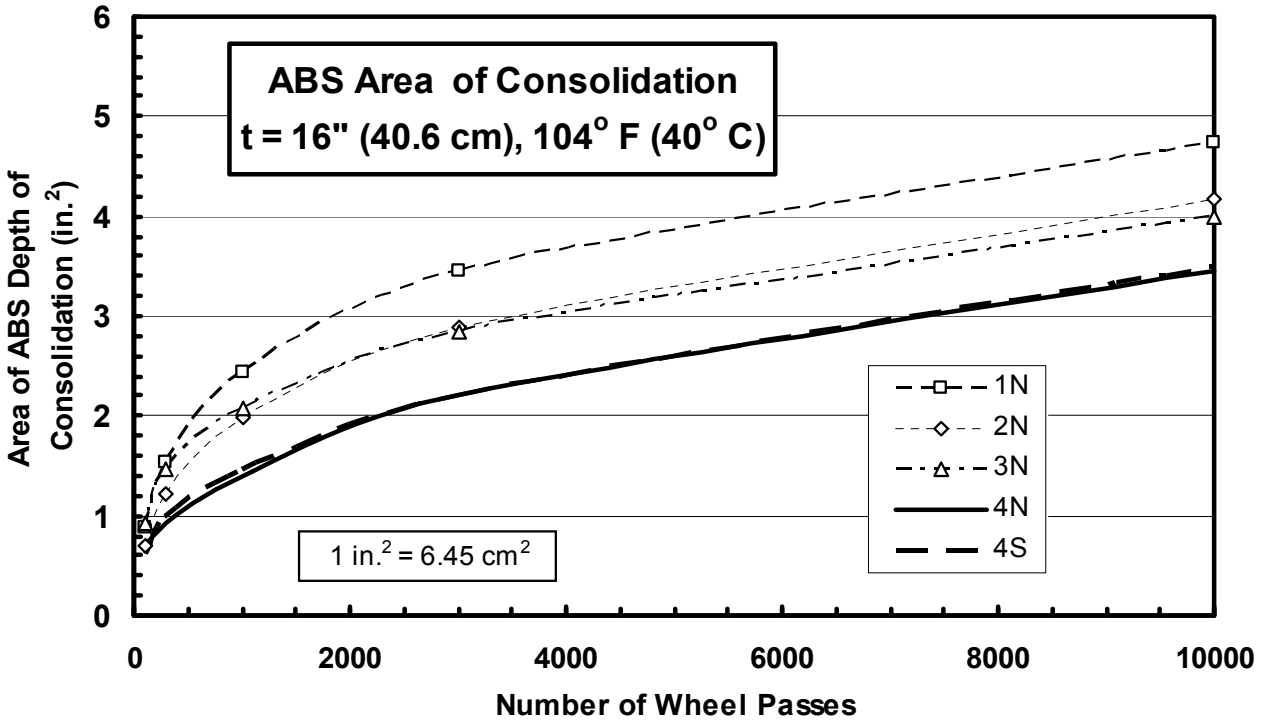

Figure 53. Effect of surface mix on consolidation.

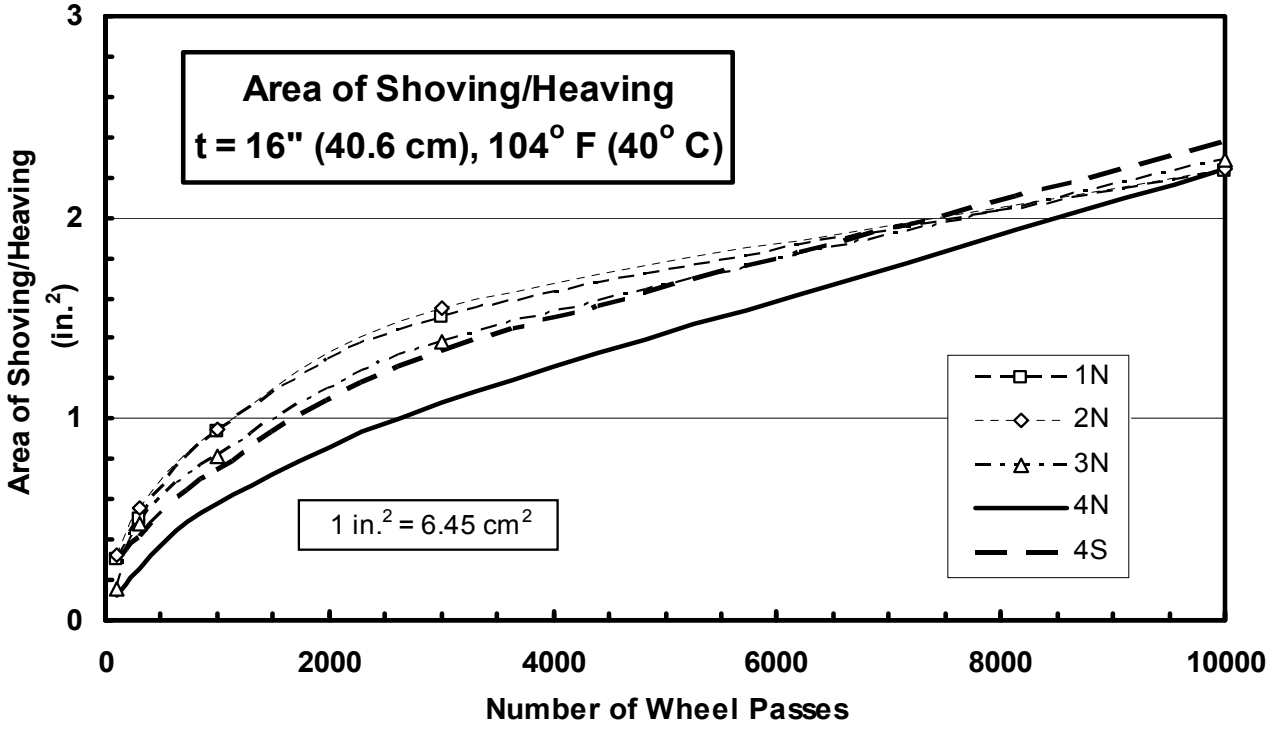

Figure 54. Effect of surface mix on shoving and heaving.

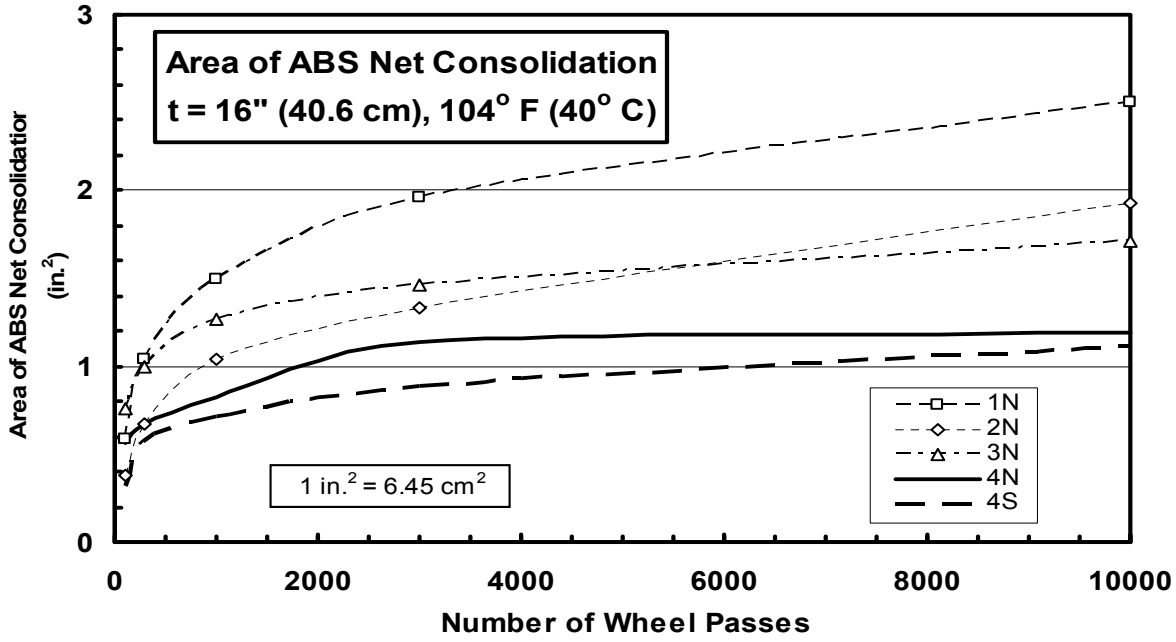

Figure 55. Effect of surface mix on net consolidation.

Table 36 shows trendline parameters and R^2 values for profile areas of consolidation, shoving/heaving and net deformation in the eight pavement sections. Since consolidation and net deformation remained negative throughout loading, absolute values were used for these parameters so they could be plotted on log-log charts.

Table 36. Parameters for profile area trendlines.

Trendline Parameters @ 104° F (40° C)				
Pavement Section	ABS Consolidation			
	a ($in.^2$)	a (cm^2)	b	R^2
1N	0.1835	1.184	0.3621	0.98
1S	0.1908	1.231	0.3485	0.99
2N	0.1302	0.840	0.3836	0.99
2S	0.1056	0.681	0.3859	0.99
3N	0.2332	1.504	0.3121	0.99
3S	0.1151	0.742	0.3822	0.98
4N	0.1253	0.808	0.3570	1.00
4S	0.1115	0.719	0.3741	1.00
Shoving/Heaving				
1N	0.0397	0.256	0.4463	0.99
1S	0.0416	0.268	0.4371	0.98
2N	0.0482	0.311	0.4252	0.99
2S	0.0321	0.207	0.4637	0.99
3N	0.0158	0.102	0.5548	0.96
3S	0.1176	0.759	0.3356	1.00
4N	0.0069	0.045	0.6311	1.00
4S	0.0313	0.202	0.4663	0.99
ABS Net Consolidation				
1N	0.1627	1.049	0.3071	0.96
1S	0.1689	1.089	0.2900	0.98
2N	0.0873	0.563	0.3424	0.98
2S	0.0874	0.564	0.3045	0.99
3N	0.3601	2.323	0.1738	0.98
3S	0.0045	0.029	0.6341	0.78
4N	0.2475	1.596	0.1773	0.96
4S	0.1132	0.730	0.2566	0.94

8 CONCLUSIONS AND RECOMMENDATIONS

This research project had two major components, the outdoor field study on SR541 in Guernsey County and the indoor study in the Accelerated Pavement Load Facility (APLF). Each study included the application of four types of asphalt used on the surface layer, including standard hot mix asphalt as a control and three warm mixes: Evotherm, Aspha-min, and Sasobit. The outdoor study began with testing of the preexisting pavement and subgrade, the results of which indicated that while the pavement and subgrade were not uniform, there were no significant problems or variations that would be expected to lead to differences in performance of the planned test sections. During construction, the outdoor study included collection of emissions samples at the plant and on the construction site as well as thermal readings from the site. Afterwards, the outdoor study included the periodic collection and laboratory analysis of core samples and visual inspections of the road.

The indoor study involved the construction of four lanes of perpetual pavement, each topped with one of the test mixes. The lanes were further divided into northern and southern halves, with the northern halves having a full 16 in (40 cm) perpetual pavement, and with the southern halves with thicknesses decreasing in one in (2.5 cm) increments by reducing the intermediate layer. The dense graded aggregate base was increased to compensate for the change in pavement thickness. The southern half of each lane was instrumented to measure temperature, subgrade pressure, deflection relative to top of subgrade and to a point 5 ft (1.5 m) down, and longitudinal and transverse strains at the base of the fatigue resistance layer (FRL). The APLF had the temperature set to 40°F (4.4°C), 70°F (21.1°C), and 104°F (40°C), in that order. At each temperature, rolling wheel loads of 6000 lb (26.7 kN), 9000 lb (40 kN), and 12,000 lb (53.4 kN) were applied at lateral shifts of 3 in (76 mm), 1 in (25 mm), -4 in (-102 mm), and -9 in (-229 mm) and the response measured. Then each plane was subjected to 10,000 passes of the rolling wheel load of 9000 lb (40 kN) at about 5 mph (8 km/h). Profiles were measured after 100, 300, 1000, 3000, and 10,000 passes with a profilometer to assess consolidation of each surface. After the 10,000 passes of the rolling wheel load were completed, a second set of measurements was made under rolling wheel loads of 6000 lb (26.7 kN), 9000 lb (40 kN), and 12,000 lb (53.4 kN) at the same lateral shifts as before. Additionally, the response of the pavement instrumentation was recorded during drops of a Falling Weight Deflectometer (FWD).

From these observations and measurements, the following conclusions can be drawn.

Warm Mix Asphalt Conclusions:

The four different sections of the outdoor GUE-541 overlay showed no obvious differences in visual inspection after 20 months of service.

The laboratory measurements of indirect tensile strength indicated no significant difference between the WMA mixes and the HMA control mix. The variations in observed strength appear to be due to differences in conditions under which cores were retrieved and normal measurement fluctuations.

The working temperatures of the warm asphalt mixes were 38.0°F (21.1C°) to 65.8°F (36.5C°) lower than the HMA.

Emissions at the paving site of total particulate matter for all three warm mixes were 67%-77% less than those for the HMA control mix. Emissions of benzene soluble matter were decreased by 72%-81% relative to the HMA.

Emissions at the plant for Aspha-min and Sasobit were reduced by at least 50% for volatile organic compounds, 60% for carbon monoxide, 20% for nitrogen oxides, and 83% for sulfur dioxide. Evotherm measurements showed significant increases in sulfur dioxide and particularly for volatile organic compounds, a slight reduction in nitrogen oxides and a 20% reduction in carbon monoxide. The NCAT report [Hurley, Prowell, and Kvasnak, 2009] on this project also noted reductions in carbon dioxide emissions from Aspha-min and Sasobit, and attributed the increases in Evotherm emissions to increased fuel use.

Although reported differently in the recent NCAT report [Hurley, Prowell, and Kvasnak, 2009] for one section, the GUE-541 pavement has not exhibited unusual raveling during the first 14 months of service. A follow-up field review in 2009 showed no unusual raveling or other distress in any section.

In the APLF, all three of the warm mix asphalt surfaces appeared to experience more consolidation than the HMA control surface during the initial stages of application of the wheel load. After the initial consolidation, further consolidation of each pavement was about equal. The difference was about twice as great for Evotherm than for the other two WMA mixes. In the long term, this constant difference in consolidation represents a relatively small portion of total consolidation experienced by the pavement. The NCAT report also noted significantly greater rutting for the Evotherm mix in their test [Hurley, Prowell, and Kvasnak, 2009].

The AC consolidation measured with a straightedge includes components under the tires and shoving/heaving between and outside the tire edges. These components progress according to a power equation of the form $y = ax^b$ as loading cycles accumulate. If no tests had been performed at 40°F (4.4°C) and 70°F (21.1°C), more initial consolidation would have been observed in all four lanes, and constants a and b would have been somewhat different, although relative deformations would likely have remained the same.

APLF Perpetual Pavement Conclusions:

The strains measured in the Fatigue Resistant Layer (FRL) did not show significant differences between the different sections in the APLF. It thus appears that the reduction of a perpetual pavement thickness from 16 in (40 cm) to 13 in (33 cm) accompanied by a corresponding increase in the thickness of the base structure will respond about equally well to loads.

At the highest APLF temperature of 104°F (40°C), the highest longitudinal strains exceeded the FRL design strain. However, the uniformly distributed high temperature in the APLF pavement structure led to the high strains and represented an extremely harsh condition. Under real world conditions, a temperature gradient would exist between the hot surface and the cooler subgrade, which would be expected to reduce the strain at the bottom.

The transverse and longitudinal strains under FWD loading were about equal, as expected. At 104°F (40°C) and under a 9,000 lb. (40 kN) load, transverse strain one inch (2.54 cm) from the bottom of the AC, surface deflection and pressure on the subgrade were much larger under tires traveling at 5 mph (8 km/h) than under the FWD load plate.

9 IMPLEMENTATION

Based on the observed response and performance measurements, WMA performs at least as well as the HMA control mix. In addition, all three WMA mixes can be placed at significantly lower temperatures and produce reduced emissions at the paving site, leading to reduced costs. Warm Mix Asphalt has shown its ability for reducing energy consumption and emissions with no loss of pavement quality and no significant negative issues have turned up in performance to date.

It is thus recommended that WMA be more broadly deployed. ODOT has already taken steps to implement this recommendation by recently modifying its Construction and Materials Specifications to allow the use of WMA created using foaming technology on light and medium traffic roads. ODOT has installed foamed WMA technology on selected paving projects starting in 2008, as per Table 37. Four of these projects, each with a different contractor, include stack tests. The performance of these sections should be monitored since they use a WMA technology different than those tested in this project.

Performance of WMA pavements under the severe conditions in the APLF suggest that WMA surfaces may also bear heavier traffic loads. WMA should also be tested on a section of road that experiences heavy truck traffic to determine how well the material performs under such conditions. If the WMA performs well under heavy load conditions as well, then the material should be used widely so that the state can reap the benefits of reduced cost and environmental impact.

Table 37. ODOT paving projects using foamed WMA technology in 2008. Table courtesy of David Powers.

Dist	PID	Section	Length	Sale	Contractor	Stack Test
4	77838	POR-224-13.42	4.9 mi	6/4/08	Shelly	Yes
4	25554	SUM-303-8.14	2.4 mi	6/4/08	Karvo	
5	22640	LIC-40-0.58	5.7 mi	change order	Shelly	
6	78156	PIC-62-0.00	7.64 mi	5/21/08	Kokosing	Yes
7	77424	DAR/MIA-49-0.00	9.75 mi	5/21/08	Valley/ Walls	Yes
8	25378	CLE-132-0.00	12.43 mi	6/4/08	Barrett	Yes
8	83808	HAM-50		change order	Valley	
12	22896	CUY-176-12.76	0.59 mi	7/23/08	Karvo	

10 REFERENCES

AASHTO. (2000). *Standard method of test for bulk dpecific gravity of compacted asphalt mixtures using saturated surface-dry specimens*. American Association of State Highway and Transportation Officials. Washington, D.C. AASHTO Designation: T 166-00.

APAO. (2003). *Warm mix asphalt shows promise for cost reduction, environmental benefit.* Salem, OR: The Asphalt Pavement Association of Oregon.

Barthel, W., Marchand, J.P., and Von Devivere, M. (2004). *Warm Asphalt Mixes by Adding a Synthetic Zeolite.* 3rd Eurasphalt and Eurobitume Congress, Vienna, 2004.

Buttlar, W, and Roque, R. (1994). *Development and evaluation of theSHRP measurement and analysis system for Indirect Tensile Testing at low temperatures.* Transportation Research Board meeting. 1994.

Button, J.W., Estakhri, C., Wimsatt, A. (2007). *A Synreport of warm-mix asphalt*. (Report No. SWUTC/07/0-5597-1). College Station, TX: Texas Tranportation Institute, The Texas AandM University System.

Chevron, (1977). *Butumuls Mix Manual*. Chevron USA, Asphalt Division, California.

EES Group (2006), *Asphalt Emission Study: Shelly and Sands Conventional Mix and Warm Mix Asphalt Paving State Route 541 Coshocton and Guernsey Counties, Ohio August to September 2006*, Report for Project #: 2006-103-R, EES Group, Dublin OH, October 9, 2006.

Gudimettla, J.M., Allen Cooley, L, and Ray Brown, E. (2003). *Workability of hot mix asphalt.* (Report No. NCAT Report 03-03). Auburn, AL: National Center for Asphalt Technology.

Harrison, T., and Christodulaki, L. (2000). *Innovative Processes in Asphalt Production and Application—Strengthening Asphalt's Position in Helping to Build a Better World.* Proceedings, First International Conference, World of Asphalt Pavements, Australian Asphalt Pavement Association, Kew, Victoria, Australia, 2000.

http://chem.tufts.edu/faculty/robbat/research/curren1.jpg.

http://maps.google.com/

2003, http://www.aidpe.com/serv03.htm.

http://www.aspha-min.de/en/html/overview.html.

http://www.meadwestvaco.com/Products/MWV002106.

http://www.sasolwax.com/Sasobit_Technology.html.

http://www.warmmixasphalt.com/WmaTechnologies.aspx.

Hurley, G.C., and Prowell, B.D. (2005a). *Evaluation of Aspha-min Zeolite for use in warm-mix asphalt.* (Report No. NCAT Report 05-04). Auburn, AL: National Center for Asphalt Technology.

Hurley, G.C., and Prowell, B.D. (2005b). *Evaluation of Sasobit for use in warm-mix asphalt.* (Report No. NCAT Report 05-06). Auburn, AL: National Center for Asphalt Technology.

Hurley, G.C., and Prowell, B.D. (2006). *Evaluation of Evotherm for use in warm-mix asphalt.* (Report No. NCAT Report 06-02). Auburn, AL: National Center for Asphalt Technology.

Hurley, G.C., Prowell, B.D., and Kvasnak, A., (2008). *Ohio Field Trial of Warm Mix Asphalt Technologies: Construction Summary*. Draft Report. Auburn, AL: National Center for Asphalt Technology, October 2008.

Hurley, G.C., Prowell, B.D., and Kvasnak, A., (2009). *Ohio Field Trial of Warm Mix Asphalt Technologies: Construction Summary*. Final Report 09-04. Auburn, AL: National Center for Asphalt Technology, September 2009.

Jenkins, K.J., de Groot, J.L.A., van de Ven, M.F.C., and Molenaar, A.A.A. (1999). *Half-Warm Foamed Bitumen Treatment, a New Process,.* 7th Conference on Asphalt Pavements for Southern Africa (CAPSA), Victoria Falls, South Africa, 1999.

Koenders, B.G., Stoker, D.A., Bowen, C., de Groot, P., Larsen, O., Hardy, D., and Wilms, K.P. (2000). *Innovative Processes in Asphalt Production and Application to Obtain Lower Operating Temperatures*. 2nd Eurasphalt and Eurobitume Congress, Barcelona, Spain, 2000.

Koenders, B.G., Stoker, D.A., Robertus, C., Larsen, O., and Johansen, J. (2002). *WAM-Foam, Asphalt Production at Lower Operating Temperatures.* Proceedings, 9th Conference of International Society for Asphalt Pavements, Copenhagen, Denmark, 2002.

Kristjansdottir, O. (2006). *Warm mix asphalt for cold weather paving.* (Report No. WA-RD 650.1). Seattle, WA: University of Washington, Olympia, WA: Washington State Department of Transportation.

Kristjanssdottir, O., Muench, S.T., Michael, L., and Burke, G. (2007). *Assessing potential for warm-mix asphalt technology adoption*. *Transportation Research Record, 2040,* 91-99.

Maccarrone, S., Holleran, G., and Ky, A. (1994). *Cold Asphalt Systems as an Alternative to Hot Mix.* Proceedings, 9th International AAPA Conference, Surfers Paradise, Queensland, Australia, 1994, from http://asphalt.csir.co.za/FArefs/

Muthen, K.M. (1998). *Foamed asphalt mixes-mix design procedure.* (Report No. CR-98/077). Sabita 1td and Transportek, south Africa, December, 1998, from http://asphalt.csir.co.za/foamasph/foamasph.pdf

Ohio Department of Transportation (ODOT) Office of Pavement Engineering, 1998 (revised), *Pavement Condition Rating Manual*, State Job Number 14638(0), Available online at http://www.dot.state.oh.us/Divisions/TransSysDev/Innovation/InfrastructureManagement/PCRManual/Pages/default.aspx, accessed July 2, 2009, Appendix A: Description of Distresses in Flexible Pavements.

Rutgers, (2005). *Indirect tensile tester (IDT)*. 2005, from http://www.cait.rutgers.edu/prp/equipment/idtt.php.

Sargand, S. M., (2002), *Determination of Pavement Layer Stiffness on the Ohio SHRP Test Road Using Non-Destructive Testing Techniques*, Federal Highway Administration Report No. FHWA/OH-2002/031, Ohio Research Institute for Transportation and the Environment, Athens, OH.

Sargand, S.M (2005). *Instrumentation of the WAY-30 test pavements project proposal*. Athens, OH: Ohio University, Athens, OH: Ohio Research Institute for Transportation and the Environment.

Sargand, S.M. (2007). *Integrating warm asphalt and perpetual pavement – part 2*. Ohio Asphalt Magazine, spring 2007, p. 24-26.

Sargand, S.M., Figueroa, J.L., and Romanello, M., (2008), *Instrumentation of the Way-30 Test Pavements*, Technical Report No. FHWA/OH-2008/7 for the Ohio Department of Transportation, State Job No. 14815, June 2008.

Transport and Road Research Laboratory (UK), from http://www.trl.co.uk/.

Webster, S.L., Grau, R.H., and Williams, T.P. (1992). *Description and application of dual mass dynamic cone penetrometer*. (Report No. GL-92-3). Washington D.C: Department of the Army.

Witczak, M.W., Kaloush, D., Pellinen, T., El-basyouny, M., and Von Quintus, H. (2002). *Simple performance test for superpave mix design.* (Report No. NCHRP Report 465). Tempe, AZ: Arizona State University, Austin, TX: Fugro-BRE, Inc.

Wu, S-S., and Sargand, S.M., (2007), *Use of Dynamic Cone Penetrometer in Subgrade and Base Acceptance*, Report No. FHWA/OH-2007/01 for the Ohio Department of Transportation, April 2007.

Appendix A: Material specifications of surface layer mixes and bottom layer on GUE-541

Bottom layer of GUE-541 overlay hot mix design:

MARSHALL MIX DESIGN

Producer	Mar-Zane # 3		
Project		452-05 TUS	
Spec	441	Year	2002

Sieve	% Pass	ODOT SPEC. BAND Low	High
2" (50.8)	100	100	100
1-1/2" (38.1)	100	100	100
1" (25.4)	100	100	100
3/4" (19)	100	100	100
1/2" (12.7)	100	100	100
3/8" (9.5)	100	90	100
#4 (4.75)	54	45	57
#8 (2.36)	36	30	45
#16 (1.18)	29	17	35
#30 (0.6)	20	12	25
#50 (0.3)	9	5	18
#100 (0.15)	5	2	10
#200 (0.075)	3.3		

Mix Type	Type I
Usage; ("1" for Surface)	Surface
Traffic Designation: ("1" if Heavy; "2" if Light)	Medium
Line Item Reference Number(s)	
% Binder Content @ Max. Stability	6.2
% Binder Content @ Max. Unit Weight	7.2
% Binder Content @ Opt. Air Voids	6.3
Max. Theoretical @ Optimum	2.390
PG Grade by Proposal	64-22
% Virgin Binder	6.3
Virgin Binder Grade	64-22
Binder Supplier	S & S Terminal
Polymer Type (SBR -or- SBS)	N/A
Mixing Temperature	310 F
Compaction Temperature	285 F
F/A Ratio	0.5 OK
50 - 30 Ratio	+2 OK
TSR Ratio	76.6
Loaded Wheel Test Results	N/A

NOTES: USE OF PG 64-22 APPROVED BY D-11
E-MAIL ATTACHED

Coarse aggregate

%	Size	Type	Producer/Location	Code	ODOT Gsb
55	# 8	Gravel	Stocker S & G - Gnadenhutten, OH	9552	2.548

Fine aggregate

%	Size	Type	Producer/Location	Code	ODOT Gsb
30	Sand	Natural	Stocker S & G - Gnadenhutten, OH	9552	2.608
15	Sand	Manufactured	Stocker S & G - Port Washington, OH	5038A	2.621

***RAP**

%	% AC	Type	Source	Composition	Gse
					#DIV/0!

*If RAP taken from State route, enter State route and project.
If other recycled material, or RAP taken from non-State route, enter size, type and source/location of fine and coarse aggregate, and source of information.

Blend Gsb = 2.577

For Official Use Only

AT OPTIMUM AC CONTENT:

Original Rc'd:	Resubmit Rc'd:	Air Voids	VMA	UnitWt (e)	UnitWt (m)
		3.5	16.1	1.959	2.324

Maximum Theo.	Stability	Flow	Opt. At Median Air Voids?	2 Points Above and Below Opt.?
2.390	1480	8.7	—	✓

Date Approved	JMF	Calibration #
5-25-06	B446284	6284

GB2004

MARSHALL MIX DESIGN
AGGREGATE BLEND SHEET

DATE : 4/17/2006 Project : 452-05 Mix Type: Type I JMF# : 0

Sieve	Stocker S & G - Gnadenhutte Gravel # 8 % USED 55.0 % PASSING	0 0 % USED % PASSING	0 0 % USED % PASSING	Stocker S & G - Gnadenhutte Natural Sand % USED 30.0 % PASSING	Stocker S & G - Port Washington, Manufactured Sand % USED 15.0 % PASSING	0 0 % USED % PASSING	0 0 % USED % PASSING	ACCUM. % PASS.	TARGET % PASS.	Surface Medium - Traffic DESIGN LIMITS
2" (50.8)	100.0			100.0	100.0		100.0	100.0	100	100 - 100
1-1/2" (38.1)	100.0			100.0	100.0		100.0	100.0	100	100 - 100
1" (25.4)	100.0			100.0	100.0		100.0	100.0	100	100 - 100
3/4" (19)	100.0			100.0	100.0		100.0	100.0	100	100 - 100
1/2" (12.7)	100.0			100.0	100.0		100.0	100.0	100	100 - 100
3/8" (9.5)	99.0			100.0	100.0		100.0	99.5	100	90 - 100
#4 (4.75)	20.0			100.0	88.0		100.0	54.2	54	45 - 57
#8 (2.36)	2.0			88.0	55.0		100.0	35.8	36	30 - 45
#16 (1.18)	2.0			71.0	44.0		100.0	29.0	29	17 - 35
#30 (0.6)	2.0			45.0	37.0		100.0	20.2	20	12 - 25
#50 (0.3)	2.0			12.0	29.0		100.0	9.1	9	5 - 18
#100 (0.15)	2.0			2.0	19.0		100.0	4.6	5	2 - 10
#200 (0.075)	1.0			1.5	15.1		100.0	3.3	3.3	-

GB2004

Control hot mix design

177441(M

SBS
1017022
1.032

MARSHALL MIX DESIGN

Producer	Mar-Zane Materials # 13		
Project	301-06		
Spec	441	Year	2005

Mix Type	Type I
Usage; ("1" for Surface)	Surface
Traffic Designation: ("1" if Heavy ; "2" if Light)	Medium
Line Item Reference Number(s)	~~103~~ 13
% Binder Content @ Max. Stability	6.2
% Binder Content @ Max. Unit Weight	7.2
% Binder Content @ Opt. Air Voids	6.1
Max. Theoretical @ Optimum	2.429
PG Grade by Proposal	PG 70-22
% Virgin Binder	5.3
Virgin Binder Grade	PG 70-22
Binder Supplier	Seneca Petroleum (2) TOLEDO
Polymer Type (SBR -or- SBS)	SBS
Mixing Temperature	300 - 320 F
Compaction Temperature	300 F
F/A Ratio	0.5 OK
50 - 30 Ratio	1 OK
TSR Ratio	81.0 OK
Loaded Wheel Test Results	N/A

5.3 VIR
, & RA

6.1

ODOT SPEC. BAND

Sieve	% Pass	Low	High
2" (50.8)	100	100	100
1-1/2" (38.1)	100	100	100
1" (25.4)	100	100	100
3/4" (19)	100	100	100
1/2" (12.7)	100	100	100
3/8" (9.5)	92	90	100
#4 (4.75)	51	45	57
#8 (2.36)	38	30	45
#16 (1.18)	28	17	35
#30 (0.6)	18	12	25
#50 (0.3)	7	5	18
#100 (0.15)	4	2	10
#200 (0.075)	2.8		

6.1/51

NOTES: "CONTROL DESIGN" for all Warm Mix Asphalt Designs

Coarse aggregate

%	Size	Type	Producer/Location	Code	ODOT Gsb
53	No. 8	Limestone	Shelly Materials - E. Fultonham, OH	4413	2.606

Fine aggregate

%	Size	Type	Producer/Location	Code	ODOT Gsb
32	Sand	Natural	Shelly Materials - Coshocton, OH	4403	2.585

***RAP**

%	% AC	Type	Source	Composition	Gse
15	5.01	Crushed	Projects 547-97 & 766-98	Limestone / Natural	2.691

*If RAP taken from State route, enter State route and project. 5.0/63
If other recycled material, or RAP taken from non-State route, enter size, type and source/location of fine and coarse aggregate, and source of information.

Blend Gsb = 2.612

For Official Use Only

AT OPTIMUM AC CONTENT:

Original Rc'd:	Resubmit Rc'd:	Air Voids	VMA	UnitWt (e)	UnitWt (m)
8/9/06		3.5	15.7	1.974	2.342

Maximum Theo.	Stability	Flow	Opt. At Median Air Voids?	2 Points Above and Below Opt.?
2.429	2980	12.8		

Date Approved	JMF	Calibration #
8/17	[redacted] B446518	[redacted] 6518

GB2004

MARSHALL MIX DESIGN
AGGREGATE BLEND SHEET

DATE : 8/2/2006 Project : 301-06 Mix Type: Type I JMF# : 0

Sieve	Shelly Materials - E. Limestone No. 8 % USED 53.0 % PASSING	0 0 0 % USED % PASSING	0 0 0 % USED % PASSING	Shelly Materials - Coshocton, Natural Sand % USED 32.0 % PASSING	0 0 0 % USED % PASSING	0 0 0 % USED % PASSING	Projects 547-97 & 766-98 Crushed % USED 15.0 % PASSING	ACCUM. % PASS.	TARGET % PASS.	Surface Medium - Traffic DESIGN LIMITS
2" (50.8)	100.0			100.0			100.0	100.0	100	100 - 100
1-1/2" (38.1)	100.0			100.0			100.0	100.0	100	100 - 100
1" (25.4)	100.0			100.0			100.0	100.0	100	100 - 100
3/4" (19)	100.0			100.0			100.0	100.0	100	100 - 100
1/2" (12.7)	100.0			100.0			98.0	99.7	100	100 - 100
3/8" (9.5)	87.0			100.0			90.3	91.6	92	90 - 100
#4 (4.75)	18.0			99.0			63.3	50.7	51	45 - 57
#8 (2.36)	6.0			86.0			46.5	37.7	38	30 - 45
#16 (1.18)	4.0			64.0			35.3	27.9	28	17 - 35
#30 (0.6)	3.0			38.0			25.3	17.5	18	12 - 25
#50 (0.3)	3.0			11.0			12.3	6.9	7	5 - 18
#100 (0.15)	3.0			4.0			6.3	3.8	4	2 - 10
#200 (0.075)	2.0			3.1			5.1	2.8	2.8	-

GB2004

Evotherm warm mix design

1774411M

SBS
1017022M
1.032

MARSHALL MIX DESIGN

Producer	Mar-Zane Materials # 13		
Project	301-06		
Spec	441	Year	2005

Mix Type		Type I
Usage; ("1" for Surface)		Surface
Traffic Designation: ("1" if Heavy ; "2" if Light)		Medium
Line Item Reference Number(s)		100
% Binder Content @ Max. Stability		6.2
% Binder Content @ Max. Unit Weight		7.2
% Binder Content @ Opt. Air Voids		6.1
Max. Theoretical @ Optimum		2.429
PG Grade by Proposal		PG 70-22 Warm
% Virgin Binder		5.3
Virgin Binder Grade		PG 70-22 Warm
Binder Supplier		Asphalt Materials @ Gilbert, Oregon
Polymer Type (SBR -or- SBS)		SBS
Mixing Temperature		300 - 320 F
Compaction Temperature		300 F ✓
F/A Ratio	0.5 ✓	OK
50 - 30 Ratio	+1 ✓	OK
TSR Ratio	81.0 ✓	OK
Loaded Wheel Test Results	N/A	

5.3 VIRGIN
1.8 RAP

ODOT SPEC. BAND

Sieve	% Pass	Low	High
2" (50.8)	100	100	100
1-1/2" (38.1)	100	100	100
1" (25.4)	100	100	100
3/4" (19)	100	100	100
1/2" (12.7)	100	100	100
3/8" (9.5)	92	90	100
#4 (4.75)	51	45	57
#8 (2.36)	38	30	45
#16 (1.18)	28 10	17	35
#30 (0.6)	18 11	12	25
#50 (0.3)	7	5	18
#100 (0.15)	4	2	10
#200 (0.075)	2.8		

6.1/51

NOTES: "EVOTHERM" - Warm Mix Emulsion - AMI PG 70-22 Base Liquid - Delivered to the plant as an emulsion and pumped through the asphalt plant pump.

Coarse aggregate

%	Size	Type	Producer/Location	Code	ODOT Gsb
53	No. 8	Limestone	Shelly Materials - E. Fultonham, OH	4413	2.606

Fine aggregate

%	Size	Type	Producer/Location	Code	ODOT Gsb
32	Sand	Natural	Shelly Materials - Coshocton, OH	4403	2.585

***RAP**

%	% AC	Type	Source	Composition	Gse
15	5.01	Crushed	Projects 547-97 & 766-98	Limestone / Natural	2.691

*If RAP taken from State route, enter State route and project. 5,0163
If other recycled material, or RAP taken from non-State route, enter size, type and source/location of fine and coarse aggregate, and source of information.

Blend Gsb = 2.612

For Official Use Only

AT OPTIMUM AC CONTENT:

Original Rc'd:	Resubmit Rc'd:	Air Voids	VMA	UnitWt (e)	UnitWt (m)
8/9/06		3.5	15.7	1.974	2.342

Maximum Theo.	Stability	Flow	Opt. At Median Air Voids?	2 Points Above and Below Opt.?
2.429	2980	12.8		

Date Approved	JMF	Calibration #
8/17/06	B446519	6519

GB2004

MARSHALL MIX DESIGN
AGGREGATE BLEND SHEET

DATE : 8/7/2006 Project : 301-06 Mix Type: Type I JMF# : 0

Sieve	Shelly Materials - E. Limestone No. 8 % USED 53.0 % PASSING	0 0 0 % USED % PASSING	0 0 0 % USED % PASSING	Shelly Materials - Coshocton, Natural Sand % USED 32.0 % PASSING	0 0 0 % USED % PASSING	0 0 0 % USED % PASSING	Projects 547-97 & 766-98 Crushed % USED 15.0 % PASSING	ACCUM. % PASS.	TARGET % PASS.	Surface Medium - Traffic DESIGN - LIMITS
2" (50.8)	100.0			100.0			100.0	100.0	100	100 - 100
1-1/2" (38.1)	100.0			100.0			100.0	100.0	100	100 - 100
1" (25.4)	100.0			100.0			100.0	100.0	100	100 - 100
3/4" (19)	100.0			100.0			100.0	100.0	100	100 - 100
1/2" (12.7)	100.0			100.0			98.0	99.7	100	100 - 100
3/8" (9.5)	87.0			100.0			90.3	91.8	92	90 - 100
#4 (4.75)	18.0			99.0			63.3	50.7	51	45 - 57
#8 (2.36)	6.0			86.0			46.5	37.7	38	30 - 45
#16 (1.18)	4.0			64.0			35.3	27.9	28	17 - 35
#30 (0.6)	3.0			38.0			25.3	17.5	18	12 - 25
#50 (0.3)	3.0			11.0			12.3	6.9	7	5 - 18
#100 (0.15)	3.0			4.0			6.3	3.8	4	2 - 10
#200 (0.075)	2.0			3.1			5.1	2.8	2.8	-

GB2004

Sasobit warm mix design

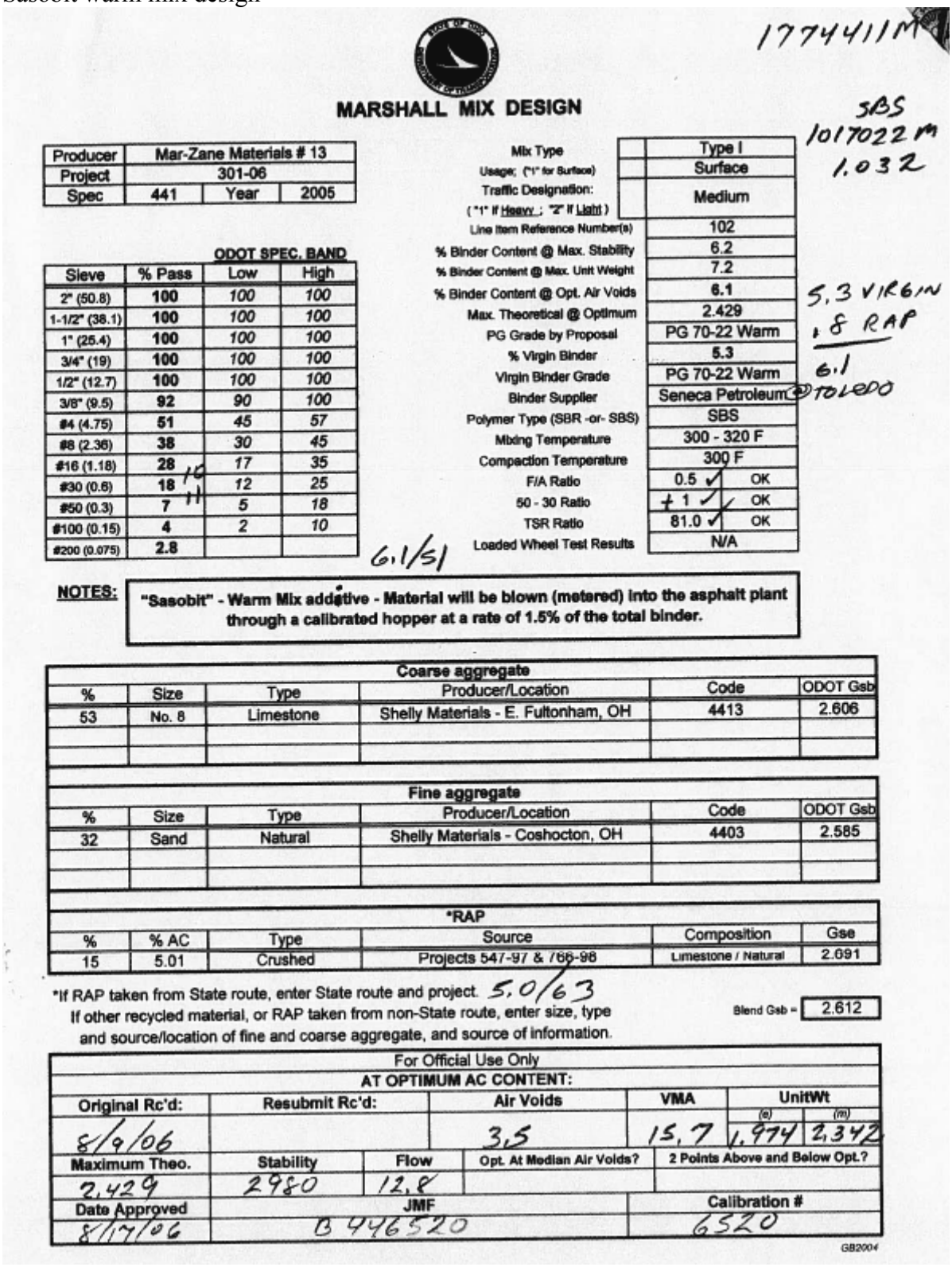

1774411M

SBS
1017022M
1.032

MARSHALL MIX DESIGN

Producer	Mar-Zane Materials # 13		
Project	301-06		
Spec	441	Year	2005

Mix Type	Type I
Usage; ("1" for Surface)	Surface
Traffic Designation: ("1" If Heavy ; "2" If Light)	Medium
Line Item Reference Number(s)	102
% Binder Content @ Max. Stability	6.2
% Binder Content @ Max. Unit Weight	7.2
% Binder Content @ Opt. Air Voids	6.1
Max. Theoretical @ Optimum	2.429
PG Grade by Proposal	PG 70-22 Warm
% Virgin Binder	5.3
Virgin Binder Grade	PG 70-22 Warm
Binder Supplier	Seneca Petroleum @ TOLEDO
Polymer Type (SBR -or- SBS)	SBS
Mixing Temperature	300 - 320 F
Compaction Temperature	300 F
F/A Ratio	0.5 ✓ OK
50 - 30 Ratio	1 ✓ OK
TSR Ratio	81.0 ✓ OK
Loaded Wheel Test Results	N/A

5.3 VIRGIN
+ .8 RAP
6.1

Sieve	% Pass	ODOT SPEC. BAND Low	High
2" (50.8)	100	100	100
1-1/2" (38.1)	100	100	100
1" (25.4)	100	100	100
3/4" (19)	100	100	100
1/2" (12.7)	100	100	100
3/8" (9.5)	92	90	100
#4 (4.75)	51	45	57
#8 (2.36)	38	30	45
#16 (1.18)	28	17	35
#30 (0.6)	18	12	25
#50 (0.3)	7	5	18
#100 (0.15)	4	2	10
#200 (0.075)	2.8		

6.1/51

NOTES: "Sasobit" - Warm Mix additive - Material will be blown (metered) into the asphalt plant through a calibrated hopper at a rate of 1.5% of the total binder.

Coarse aggregate					
%	Size	Type	Producer/Location	Code	ODOT Gsb
53	No. 8	Limestone	Shelly Materials - E. Fultonham, OH	4413	2.606

Fine aggregate					
%	Size	Type	Producer/Location	Code	ODOT Gsb
32	Sand	Natural	Shelly Materials - Coshocton, OH	4403	2.585

*RAP					
%	% AC	Type	Source	Composition	Gse
15	5.01	Crushed	Projects 547-97 & 766-98	Limestone / Natural	2.691

*If RAP taken from State route, enter State route and project. 5,0/63
If other recycled material, or RAP taken from non-State route, enter size, type and source/location of fine and coarse aggregate, and source of information.

Blend Gsb = 2.612

For Official Use Only					
AT OPTIMUM AC CONTENT:					
Original Rc'd:	Resubmit Rc'd:	Air Voids	VMA	UnitWt (a)	UnitWt (m)
8/9/06		3.5	15.7	1.974	2.342
Maximum Theo.	Stability	Flow	Opt. At Median Air Voids?	2 Points Above and Below Opt.?	
2.429	2980	12.8			
Date Approved	JMF		Calibration #		
8/17/06	B 446520		6520		

GB2004

MARSHALL MIX DESIGN
AGGREGATE BLEND SHEET

DATE : 8/7/2006 Project : 301-06 Mix Type: Type I JMF# : 0

Sieve	Shelly Materials - E. Limestone No. 8 % USED 53.0 % PASSING	0 0 0 % USED % PASSING	0 0 0 % USED % PASSING	Shelly Materials - Coshocton, Natural Sand % USED 32.0 % PASSING	0 0 0 % USED % PASSING	0 0 0 % USED % PASSING	Projects 547-97 & 766-98 Crushed % USED 15.0 % PASSING	ACCUM. % PASS.	TARGET % PASS.	Surface Medium - Traffic DESIGN LIMITS
2" (50.8)	100.0			100.0			100.0	100.0	100	100 - 100
1-1/2" (38.1)	100.0			100.0			100.0	100.0	100	100 - 100
1" (25.4)	100.0			100.0			100.0	100.0	100	100 - 100
3/4" (19)	100.0			100.0			100.0	100.0	100	100 - 100
1/2" (12.7)	100.0			100.0			98.0	99.7	100	100 - 100
3/8" (9.5)	87.0			100.0			90.3	91.6	92	90 - 100
#4 (4.75)	18.0			99.0			63.3	50.7	51	45 - 57
#8 (2.36)	6.0			86.0			46.5	37.7	38	30 - 45
#16 (1.18)	4.0			64.0			35.3	27.9	28	17 - 35
#30 (0.6)	3.0			38.0			25.3	17.5	18	12 - 25
#50 (0.3)	3.0			11.0			12.3	6.9	7	5 - 18
#100 (0.15)	3.0			4.0			6.3	3.8	4	2 - 10
#200 (0.075)	2.0			3.1			5.1	2.8	2.8	-

GB2004

Aspha-min warm mix design:

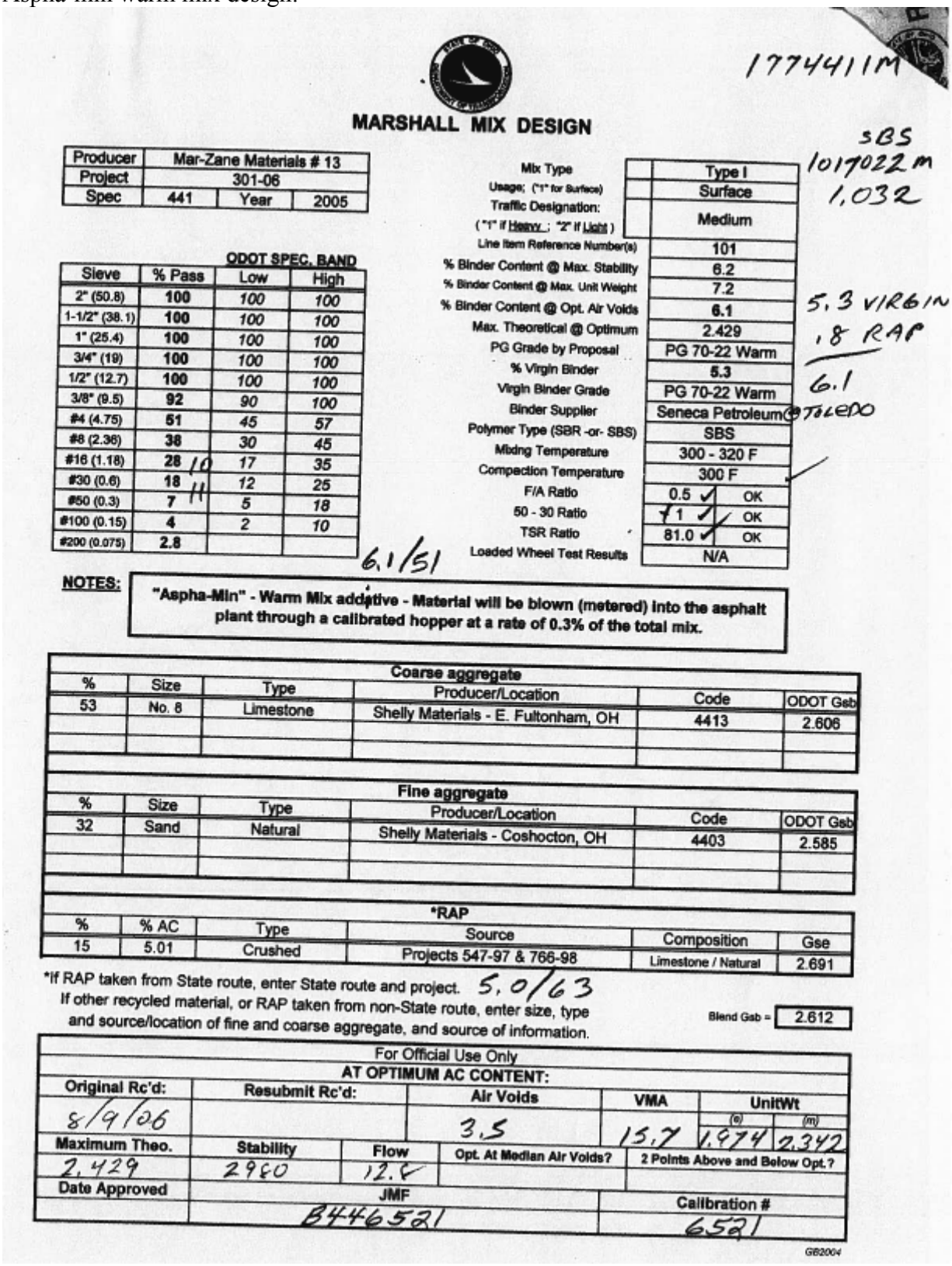

1774411M

MARSHALL MIX DESIGN

SBS
1017022M
1,032

Producer	Mar-Zane Materials # 13		
Project	301-06		
Spec	441	Year	2005

Sieve	% Pass	ODOT SPEC. BAND Low	High
2" (50.8)	100	100	100
1-1/2" (38.1)	100	100	100
1" (25.4)	100	100	100
3/4" (19)	100	100	100
1/2" (12.7)	100	100	100
3/8" (9.5)	92	90	100
#4 (4.75)	51	45	57
#8 (2.36)	38	30	45
#16 (1.18)	28 10	17	35
#30 (0.6)	18 11	12	25
#50 (0.3)	7	5	18
#100 (0.15)	4	2	10
#200 (0.075)	2.8		

6.1/51

Mix Type	Type I	
Usage; ("1" for Surface)	Surface	
Traffic Designation: ("1" if Heavy ; "2" if Light)	Medium	
Line Item Reference Number(s)	101	
% Binder Content @ Max. Stability	6.2	
% Binder Content @ Max. Unit Weight	7.2	
% Binder Content @ Opt. Air Voids	6.1	
Max. Theoretical @ Optimum	2.429	
PG Grade by Proposal	PG 70-22 Warm	
% Virgin Binder	5.3	
Virgin Binder Grade	PG 70-22 Warm	
Binder Supplier	Seneca Petroleum @ Toledo	
Polymer Type (SBR -or- SBS)	SBS	
Mixing Temperature	300 - 320 F	
Compaction Temperature	300 F	
F/A Ratio	0.5 ✓	OK
50 - 30 Ratio	1 ✓	OK
TSR Ratio	81.0 ✓	OK
Loaded Wheel Test Results	N/A	

5.3 VIRGIN
1.8 RAP
6.1

NOTES: "Aspha-Min" - Warm Mix additive - Material will be blown (metered) into the asphalt plant through a calibrated hopper at a rate of 0.3% of the total mix.

Coarse aggregate

%	Size	Type	Producer/Location	Code	ODOT Gsb
53	No. 8	Limestone	Shelly Materials - E. Fultonham, OH	4413	2.606

Fine aggregate

%	Size	Type	Producer/Location	Code	ODOT Gsb
32	Sand	Natural	Shelly Materials - Coshocton, OH	4403	2.585

***RAP**

%	% AC	Type	Source	Composition	Gse
15	5.01	Crushed	Projects 547-97 & 766-98	Limestone / Natural	2.691

*If RAP taken from State route, enter State route and project. 5,0/63
If other recycled material, or RAP taken from non-State route, enter size, type and source/location of fine and coarse aggregate, and source of information.

Blend Gsb = 2.612

For Official Use Only

AT OPTIMUM AC CONTENT:

Original Rc'd:	Resubmit Rc'd:	Air Voids	VMA	UnitWt (e)	UnitWt (m)
8/9/06		3.5	15.7	1.974	2.342

Maximum Theo.	Stability	Flow	Opt. At Median Air Voids?	2 Points Above and Below Opt.?
2.429	2980	12.4		

Date Approved	JMF	Calibration #
	B446521	6521

GB2004

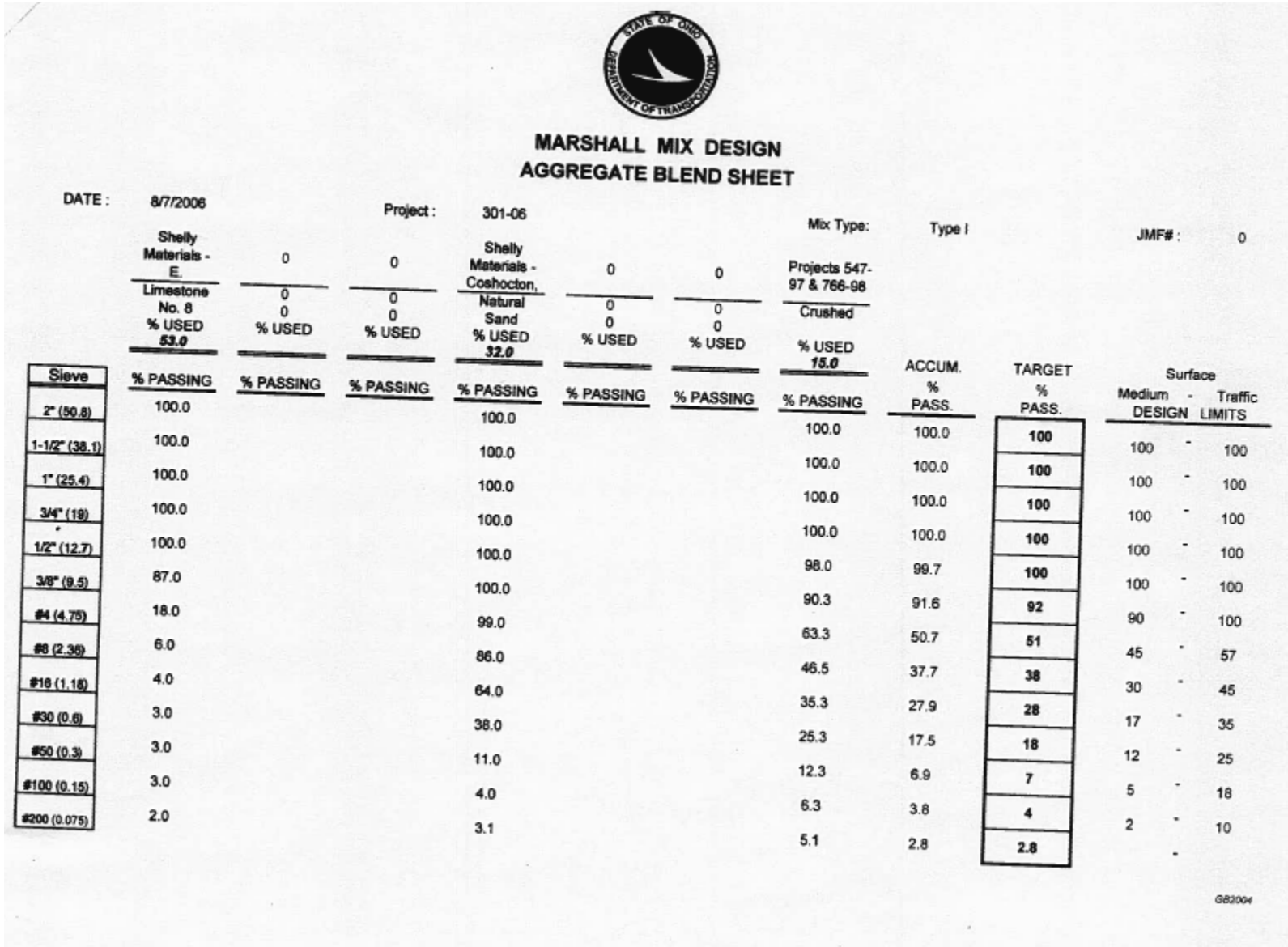

MARSHALL MIX DESIGN
AGGREGATE BLEND SHEET

DATE : 8/7/2006 Project : 301-06 Mix Type: Type I JMF# : 0

Sieve	Shelly Materials - E. Limestone No. 8 % USED 53.0 % PASSING	0 0 0 % USED % PASSING	0 0 0 % USED % PASSING	Shelly Materials - Coshocton, Natural Sand % USED 32.0 % PASSING	0 0 0 % USED % PASSING	0 0 0 % USED % PASSING	Projects 547-97 & 766-98 Crushed % USED 15.0 % PASSING	ACCUM. % PASS.	TARGET % PASS.	Surface Medium - Traffic DESIGN - LIMITS
2" (50.8)	100.0			100.0			100.0	100.0	100	100 - 100
1-1/2" (38.1)	100.0			100.0			100.0	100.0	100	100 - 100
1" (25.4)	100.0			100.0			100.0	100.0	100	100 - 100
3/4" (19)	100.0			100.0			100.0	100.0	100	100 - 100
1/2" (12.7)	100.0			100.0			98.0	99.7	100	100 - 100
3/8" (9.5)	87.0			100.0			90.3	91.6	92	90 - 100
#4 (4.75)	18.0			99.0			63.3	50.7	51	45 - 57
#8 (2.36)	6.0			86.0			46.5	37.7	38	30 - 45
#16 (1.18)	4.0			64.0			35.3	27.9	28	17 - 35
#30 (0.6)	3.0			38.0			25.3	17.5	18	12 - 25
#50 (0.3)	3.0			11.0			12.3	6.9	7	5 - 18
#100 (0.15)	3.0			4.0			6.3	3.8	4	2 - 10
#200 (0.075)	2.0			3.1			5.1	2.8	2.8	-

GB200d

Appendix B: Stack Emissions Test Report Summary

CHIEF ENVIRONMENTAL GROUP, LTD.
3570 South River Road
P.O. Box 1585
Zanesville, Ohio 43702-1585
(740) 453 - 0721

Emission Test Results
for:

Warm Mix Asphalt Trial Project
Mar-Zane Materials, Inc. Asphalt Plant #13
Byesville, Ohio
OhioEPA # 06-60-00-0081

Mar-Zane Materials, Inc. Asphalt Plant #13

Byesville, Ohio

OhioEPA # 06-60-00-0081

WMA Emissions Report

Performed Velocity, Temperature, Moisture, O2, CO2, NOx, SO_2, CO, and VOC Determinations for:

Control Mix
Evotherm
Aspha-Min
Sasobit

Sampling at the Baghouse Exhaust
P901

Anthony Ruggiero III
Chief Enviromental Group Ltd.

TABLE OF CONTENTS

Mar-Zane Materials, Inc. Asphalt Plant #13

Byesville, Ohio

OhioEPA # 06-60-00-0081

TOTAL RESULTS SUMMARY

	Control	Evotherm	Aspha-min	Sasobit	
Date	8/30/2006	9/7/2006	9/11/2006	9/16/2006	
Production Rate	165	167	168	167	TPH
Fuel	Natural Gas	Natural Gas	Natural Gas	Natural Gas	
Standard Meter Volume	37.972	34.762	32.353	31.840	dscf
Average Stack Gas Velocity	55.10	55.45	46.91	47.02	ft/sec.
Dry Standard Stack Flow Rate	27,718	24,009	23,266	23,141	ft/hr.
Actual Stack Flow Rate	46,559	46,855	39,636	39,732	ft/hr.
Calculated Moisture %	22.3	29.5	24.4	24.8	%
Isokinicty %	99.0	104.6	100.5	99.5	%
Carbon Dioxide %	3.5	4.2	2.8	2.0	%
Oxygen %	15.7	15.0	15.8	15.7	%
Nitrogen %	80.8	80.8	81.3	82.3	%
Sulfur Dioxide	0.24 0.0014	0.37 0.0022	0.04 0.0022	0.04 0.0002	lbs/hr lb/ton
Nitric Oxide	5.2 0.0313	5.1 0.0307	3.6 0.0216	4.1 0.0243	lbs/hr lb/ton
Carbon Monoxide	63.1 0.3822	50.3 0.3012	24.0 0.1431	23.2 0.1386	lbs/hr lb/ton
V.O.C. USEPA Method 25	45.2 0.2741	61.4 0.3677	37.5 0.2234	27.2 0.1627	lbs/hr lb/ton
V.O.C. USEPA Method 25A	7.8 0.0473	20.2 0.1212	2.9 0.0173	3.8 0.0229	lbs/hr lb/ton
Percent of RAP	15	15	15	15	%

NOTES:

WMA PROJECT SUMMARY

Introduction:

On June 21, 2006 the Ohio Department of Transportation let project 060301, a Warm Mix Asphalt Trial Project. This project was a two lane resurfacing project that would utilize three warm mix technologies along with a control section of hot mix asphalt. As part of this project , testing of the plant emission gases was included in the proposal. These plant emission tests were conducted along with emissions surrounding laydown operations testing of the warm mix asphalt to give ODOT a complete overview of the environmental impact of Warm Mix Asphalt. This report is only the results of the plant emissions. Emission results for the laydown operations were conducted by EES Group, Inc., Dublin, Ohio. This report may be accessed online at www.eesinc.com.

The plant emission testing was conducted at Mar-Zane Materials, Inc. Asphalt Plant #13 in Byesville, Ohio. This facility operated at a rate of 270 tons per hour and used natural gas to fire the drying burner for this project. The plant is a counter flow, double drum system with a bucket elevator that feeds tow silos.

Emission Testing:

The emission testing was conducted by Chief Environmental Group, Inc. for Mar-Zane Materials, Inc. Chief Environmental used USEPA Methods 1,2,3,4,5,6, 6C, 7E,10, 25A. And 25 to conduct results on velocity, temperature, moisture, SO_2, NO_X, O_2, CO, CO_2, VOC. USEPA Method 25 was conducted because the OhioEPA requires this test method for volatile organic compounds. Chief Environmental used a method 5/6 combination train as a back up for 6C. Due to the low sulfur dioxide reading, method 6C was not used due to reliability issues. Chief Environmental submitted to Resolution Antalyticals of Sanford, N.C. the backup aliquots for Method 6 SO_2 titrations. These results are reported for sulfur dioxide emissions.

Emission testing was conducted for the Control Mix, Evotherm, Aspha-min, and Sasobit. The test dates were 8/30/2006, 9/7/2006, 9/11/2006, and 9/16/2006 respectfully.

Each of the warm mix technologies was added at the mixing drum stage of the process. The Evotherm technology was introduced as a emulsion. The Aspha-Min and Sasobit was added as a fine granular material.

Emission Results for Each Product:

Control Mix:

The control mix had emission rate of 0.24 ponds per hour for sulfur dioxide, 5.2 pounds per hour for nitric oxide, 63.1 pounds per hour for carbon monoxide, and 7.8 pounds per hour for VOC's using USEPA Method 25A. The emissions are shown in graph form in Figures 1-4.

Evotherm:

Evotherm was the first WMA made on this project. The SO_2 emissions was 0.37

pounds per hour. For the NO_x and VOC emissions, the results were 5.1 and 20.2 pounds per hour respectfully. Evotherm had emissions for SO_2 and VOC higher than the control mix. CO emissions were 50.3 pounds per hour. This was a reduction of 20.2 % over the control mix.

Aspha-Min:

Aspha-Min had very good reductions in emissions compared to the control mix. The SO_2 emissions was 0.04 pounds per hour. This was a 83.1% decrease from the control mix. For the NO_x and VOC emissions, the results were 3.6 and 2.9 pounds per hour respectfully. The emissions reduction for NO_x was 29.7% compared to the control mix, and 62.8% for the VOC's. CO emissions were 24.0 pounds per hour. This was a reduction of 61.9 % over the control mix.

Sasobit:

Sasobit also had very good reductions in emissions compared to the control mix. The SO_2 emissions was 0.04 pounds per hour. This was a 83.1% decrease from the control mix. For the NO_x and VOC emissions, the results were 4.1 and 3.8 pounds per hour respectfully. The emissions reduction for NO_x was 21.3% compared to the control mix, and 50.9% for the VOC's. CO emissions were 23.2 pounds per hour. This was a reduction of 63.2 % over the control mix.

Chief Environmental Group uses IsoCalc, the integrated Isokinetic Stationary Source Sampling Computer Workbook. Isocalc provides the worksheets necessary to complete the USEPA Methods 1-5. Isocalc takes worksheet data filled in by the user and applies the calculations for Methods 1-5 data results. Data cells must be filled out to produce data results on the Method 5 Results page.

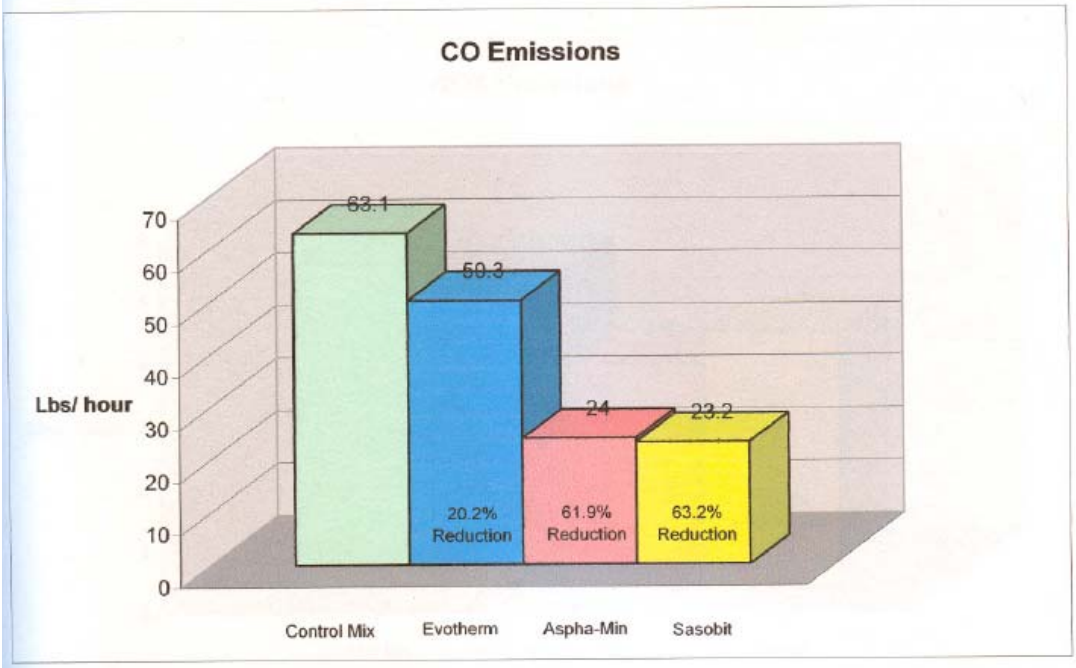

Figure 1

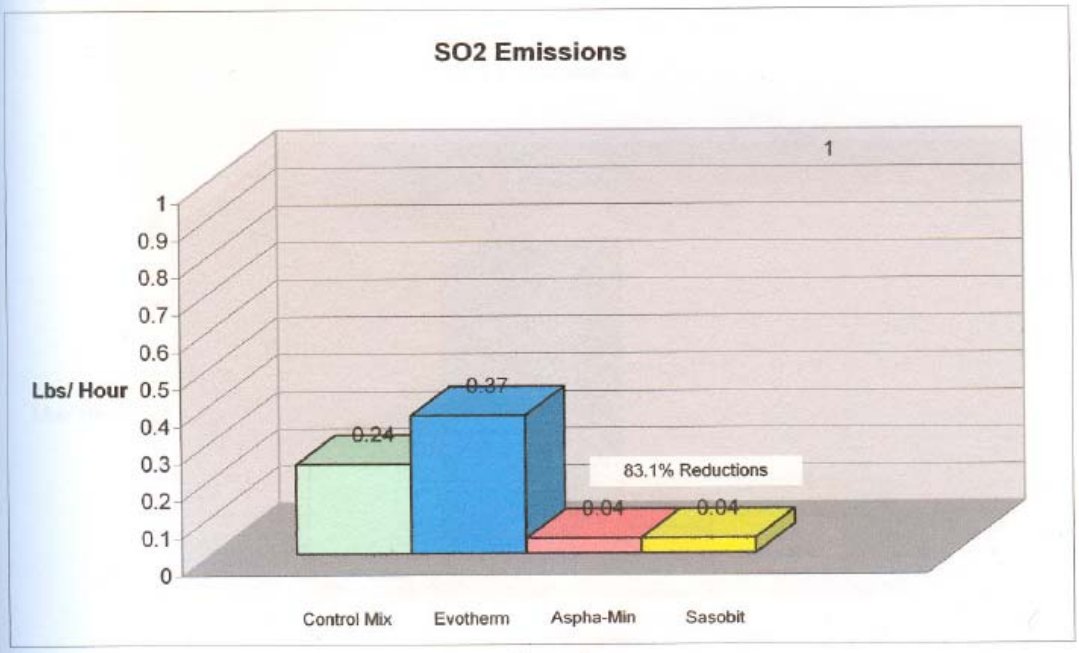

Figure 2

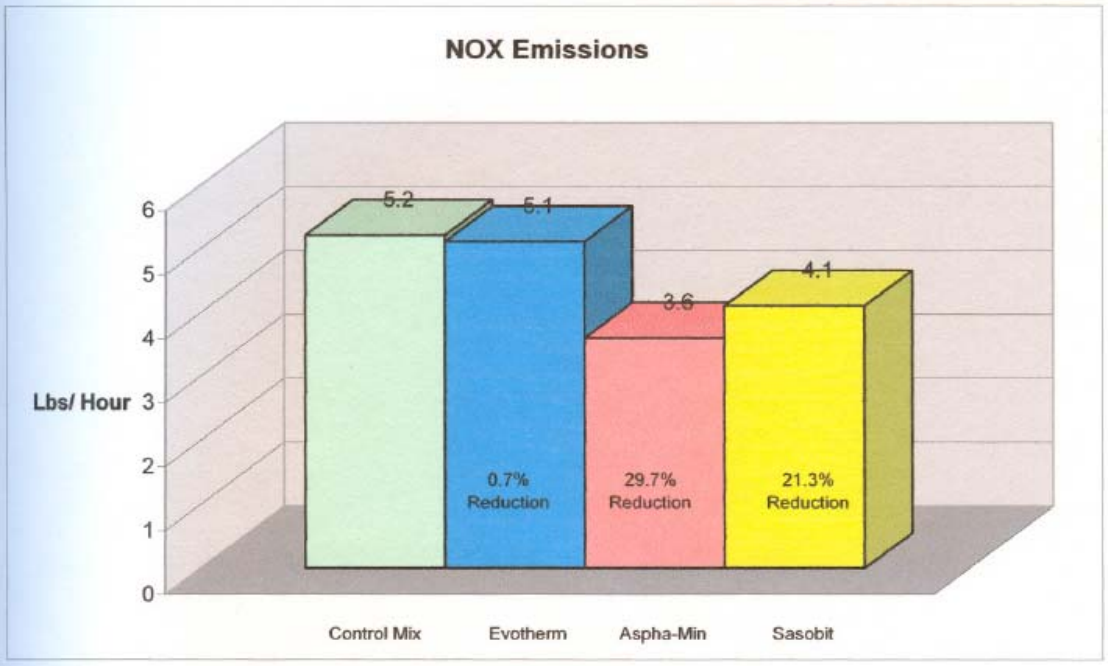

Figure 3

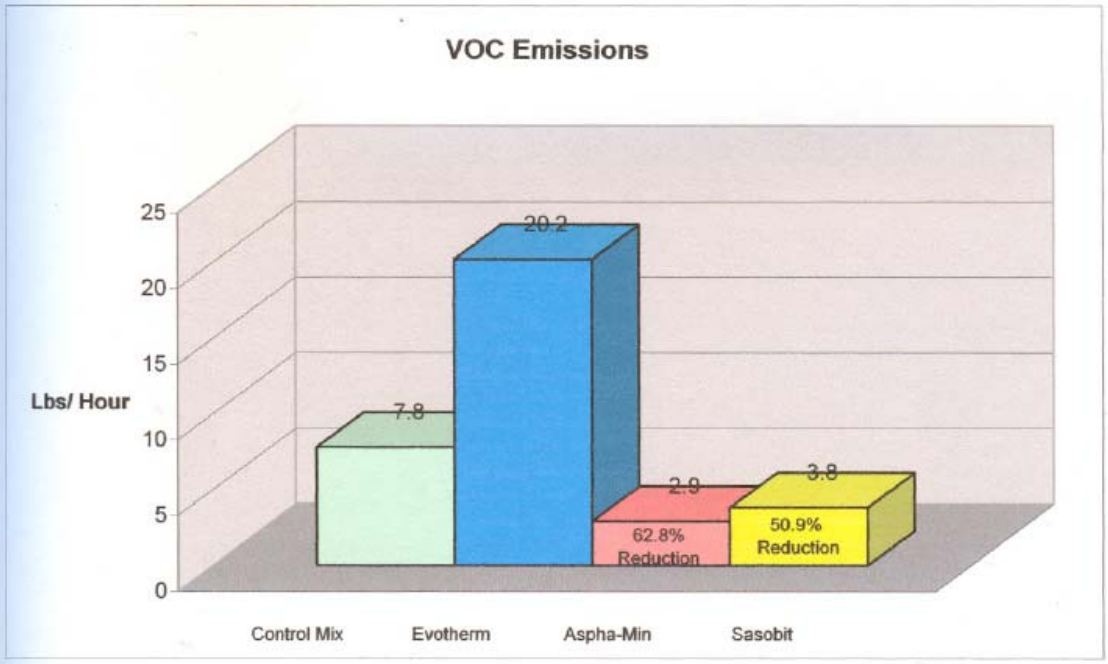

Figure 4

Appendix C: Description of Raveling from Appendix A of ODOT Pavement Condition Rating Manual [ODOT, 1998]

FLEXIBLE PAVEMENT

Distress Type:	**Raveling**	
Description:	Disintegration of the pavement from the surface downward due to the loss of aggregate particles. Raveling may occur as a result of asphalt binder aging, poor mixture quality, segregation, or insufficient compaction.	
Severity Level:	**L**ow--	Very little coarse aggregate has worn away. Loss of fine aggregate. Coarse aggregate exposed.
	Medium--	Surface has an open texture and is moderately rough with considerable loss of fine aggregate and some coarse aggregate removed.
	High--	Most of the surface aggregate has worn away or become dislodged. Surface is severely rough and pitted and may be completely removed in places.
Extent Level:	**O**ccasional--	Less than 20 percent of the surface area is raveling.
	Frequent--	Between 20 and 50 percent of the surface area is raveling.
	Extensive--	More than 50 percent of the surface area is raveling.

Photo A-1. Raveling in Flexible Pavement, Medium Severity

Photo A-2. Raveling in Flexible Pavement, High Severity

Appendix D: Implementation Plan

OHIO DEPARTMENT OF TRANSPORTATION
OFFICE OF PAVEMENT ENGINEERING
RESEARCH IMPLEMENTATION PLAN

Title: Performance Assessment of Warm Mix Asphalt (WMA) Pavements
State Job Number: 134312
PID Number:
Research Agency: Ohio University
Researcher(s): Shad Sargand and J. Ludwig Figueroa
Technical Liaison(s): Roger Green
Research Manager: Monique Evans
Sponsor(s): ODOT
Study Start Date: August 28, 2006
Study Completion Date: February 28, 2009
Study Duration: 30 Months
Study Cost: $250,223.39
Study Funding Type:

STATEMENT OF NEED: .

Warm Mix Asphalt (WMA) is a new technology which was introduced in 1995 in Europe. WMA is gaining attention in all over the world because it offers several advantages over conventional asphalt concrete mixes. The benefits include (1) Reduced energy consumption in asphalt mixture production process; (2) Reduced emissions, fumes, and undesirable odors; (3) More uniform coating of aggregate with binder, which should reduce surface aging; and (4) Extended construction season in temperate climates.

WMA requires the use of additives to reduce the temperature of production and compaction of asphalt mixtures. It offers an alternative to hot mix asphalt (HMA), which is produced at a temperature between 280°F (138°C) and 320°F (160°C). Warm mix asphalt is compacted at a temperature range of 250°F (121°C) to 275°F (135°C). Three techniques have been used to improve the workability of asphalt mixes at a lower temperature. These include:

- Aspha-min, the addition of sodium aluminum silicate or zeolite to the asphalt mix.
- Sasobit, the addition of a paraffin-wax compound extracted from coal gasification.
- Evotherm, the addition of an emulsion to improve the coating and workability of WMA mixes.

A fourth technique, WAM Foam, was excluded from the study after consultation with ODOT and Flexible Pavements of Ohio. WMA techniques were used to reduce the viscosity of asphalt binder at certain temperatures and to dry and fully coat the aggregates at a lower production temperature than conventional hot mix asphalt. The reduction in mixing and compaction temperatures of asphalt mixtures leads to a 30 percent reduction in both fuel energy consumption and emissions.

RESEARCH OBJECTIVES:

- To conduct a detailed laboratory study to evaluate the engineering and physical properties of WMA mixtures prepared according to the three techniques mentioned above and a conventional HMA mixture.
- To build and test pavement sections containing each of the selected mixtures (3 WMA types and one conventional) as a wearing (sacrificial) course compacted on conventional HMA layers designed following perpetual pavement guidelines. All sections will be subjected to repeated loads in the (APLF) at Ohio University under high, medium and low temperatures. It is planned to support each of the 4 types of wearing course on two different thicknesses of the planned perpetual pavements, for a total of 8 test sections. It will be necessary to develop a comprehensive instrumentation plan to monitor environmental conditions and response of the pavement structures when subjected to dynamic loading with properly installed instrumentation.
- To examine the influence of pavement thickness on the tensile strain developed at the bottom of the perpetual pavement layer.
- To monitor and test pavement sections containing the three techniques mentioned above to be built on

GUE-541. This section was selected by engineers from the Ohio Department of Transportation, as a demonstration and evaluation project.

- To compare the performance of WMA mixtures and pavements with that of conventional HMA in the controlled setting of the APLF and in the field section.
- To document the performance of perpetual pavements containing 3 types of WMA and one conventional wearing course and to monitor pavement response in the form of deflections, strains and pressures in and under perpetual pavements. These data will be of extreme importance in future validations of perpetual pavements' analysis and design procedures
- To assess the advantages of WMA over conventional HMA in regards to reduced energy utilization and fume emanation during processing and placement.

RESEARCH TASKS:

This research project had two major components, the outdoor field study on SR541 in Guernsey County and the indoor study in the Accelerated Pavement Load Facility (APLF). Each study included the application of four types of asphalt surface layer, including a standard hot mix asphalt as a control and three warm mixes: Evotherm, Aspha-min, and Sasobit. The outdoor study began with testing of the preexisting pavement and subgrade, the results of which indicated that while the pavement and subgrade were not uniform, there were no significant problems or variations that would be expected to lead to differences in performance of the planned test sections. During construction, the outdoor study included collection of emissions samples at the plant and on the construction site as well as thermal readings from the site. Afterwards, the outdoor study included the periodic collection and laboratory analysis of core samples and visual inspections of the road.

The indoor study involved the construction of four lanes of perpetual pavement, each topped with one of the test mixes. The lanes were further divided into northern and southern halves, with the northern halves having a full 16 in (40 cm) perpetual pavement, and with the southern halves with thicknesses decreasing in one in (2.5 cm) increments by reducing the intermediate layer. The dense graded aggregate base was increased to compensate for the change in pavement thickness. The southern half of each lane was instrumented to measure temperature, subgrade pressure, deflection relative to top of subgrade and to a point 5 ft (1.5 m) down, and longitudinal and transverse strains at the base of the fatigue resistance layer (FRL). The APLF had the temperature set to 40°F (4.4°C), 70°F (21.1°C), and 104°F (40°C), in that order. At each temperature, rolling wheel loads of 6000 lb (26.7 kN), 9000 lb (40 kN), and 12,000 lb (53.4 kN) were applied at lateral shifts of 3 in (76 mm), 1 in (25 mm), -4 in (-102 mm), and -9 in (-229 mm) and the response measured. Then each plane was subjected to 10,000 passes of the rolling wheel load of 9000 lb (40 kN) at about 5 mph (8 km/h). Profiles were measured after 100, 300, 1000, 3000, and 10,000 passes with a profilometer to assess consolidation of each surface. After the 10,000 passes of the rolling wheel load were completed, a second set of measurements was made under rolling wheel loads of 6000 lb (26.7 kN), 9000 lb (40 kN), and 12,000 lb (53.4 kN) at the same lateral shifts as before. Additionally, the response of the pavement instrumentation was recorded during drops of a Falling Weight Deflectometer (FWD).

RESEARCH DELIVERABLES:

Final Report, Executive Summary

RESEARCH RECOMMENDATIONS:

Warm Mix Asphalt Conclusions:

The four different sections of the outdoor GUE-541 overlay showed no obvious differences in visual inspection after 20 months of service.

The laboratory measurements of indirect tensile strength indicated no significant difference between the WMA mixes and the HMA control mix. The variations in observed strength appear to be due to differences in conditions under which cores were retrieved and normal measurement fluctuations.

The working temperatures of the warm asphalt mixes were 38.0°F (21.1C°) to 65.8°F (36.5C°) lower than the HMA.

Emissions at the paving site of total particulate matter for all three warm mixes were 67%-77% less than those for the HMA control mix. Emissions of benzene soluble matter were decreased by 72%-81% relative to the HMA.

Emissions at the plant for Aspha-min and Sasobit were reduced by at least 50% for volatile organic compounds, 60% for carbon monoxide, 20% for nitrogen oxides, and 83% for sulfur dioxide. Evotherm measurements showed significant increases in sulfur dioxide and particularly for volatile organic compounds, a slight reduction in nitrogen oxides and a 20% reduction in carbon monoxide. The NCAT report on this project also noted reductions in carbon

dioxide emissions from Aspha-min and Sasobit, and attributed the increases in Evotherm emissions to increased fuel use.

Although reported differently in the recent NCAT report for one section, the GUE-541 pavement has not exhibited unusual raveling during the first 14 months of service. A follow-up field review in 2009 showed no unusual raveling or other distress in any section.

In the APLF, all three of the warm mix asphalt surfaces appeared to experience more consolidation than the HMA control surface during the initial stages of application of the wheel load. After the initial consolidation, further consolidation of each pavement was about equal. The difference was about twice as great for Evotherm than for the other two WMA mixes. In the long term, this constant difference in consolidation represents a relatively small portion of total consolidation experienced by the pavement. The NCAT report also noted significantly greater rutting for the Evotherm mix in their test.

The AC consolidation measured with a straightedge includes components under the tires and shoving/heaving between and outside the tire edges. These components progress according to a power equation of the form $y = ax^b$ as loading cycles accumulate. If no tests had been performed at 40°F (4.4°C) and 70°F (21.1°C), more initial consolidation would have been observed in all four lanes, and constants a and b would have been somewhat different, although relative deformations would likely have remained the same.

APLF Perpetual Pavement Conclusions:

The strains measured in the Fatigue Resistant Layer (FRL) did not show significant differences between the different sections in the APLF. It thus appears that the reduction of a perpetual pavement thickness from 16 in (40 cm) to 13 in (33 cm) accompanied by a corresponding increase in the thickness of the base structure will respond about equally well to loads.

At the highest APLF temperature of 104°F (40°C), the highest longitudinal strains exceeded the FRL design strain. However, the uniformly distributed high temperature in the APLF pavement structure led to the high strains and represented an extremely harsh condition. Under real world conditions, a temperature gradient would exist between the hot surface and the cooler subgrade, which would be expected to reduce the strain at the bottom.

The transverse and longitudinal strains under FWD loading were about equal, as expected. At 104°F (40°C) and under a 9,000 lb. (40 kN) load, transverse strain one inch (2.54 cm) from the bottom of the AC, surface deflection and pressure on the subgrade were much larger under tires traveling at 5 mph (8 km/h) than under the FWD load plate.

PROJECT PANEL COMMENTS:

IMPLEMENTATION STEPS and TIME FRAME:

Based on the observed response and performance measurements, WMA performs at least as well as the HMA control mix. In addition, all three WMA mixes can be placed at significantly lower temperatures and produce reduced emissions at the paving site, leading to reduced costs. Warm Mix Asphalt has shown its ability for reducing energy consumption and emissions with no loss of pavement quality and no significant negative issues have turned up in performance to date.

It is thus recommended that WMA be more broadly deployed. ODOT has already taken steps to implement this recommendation by recently modifying its Construction and Materials Specifications to allow the use of WMA created using foaming technology on light and medium traffic roads. ODOT has installed foamed WMA technology on selected paving projects starting in 2008. Four of these projects, each with a different contractor, include stack tests. The performance of these sections should be monitored since they use a WMA technology different than those tested in this project.

Performance of WMA pavements under the severe conditions in the APLF suggest that WMA surfaces may also bear heavier traffic loads. WMA should also be tested on a section of road that experiences heavy truck traffic to determine how well the material performs under such conditions. If the WMA performs well under heavy load conditions as well, then the material should be used widely so that the state can reap the benefits of reduced cost and environmental impact.

EXPECTED BENEFITS:

EXPECTED RISKS, OBSTACLES, and STRATEGIES TO OVERCOME THEM:

OTHER ODOT OFFICES AFFECTED BY THE CHANGE:

PROGRESS REPORTING and TIME FRAME:

TECHNOLOGY TRANSFER METHODS TO BE USED:

IMPLEMENTATION COST and SOURCE OF FUNDING:

Approved By: (attached additional sheets if necessary)

Office Administrator(s):

Signature: _____ Office: _____ Date: _____

Signature: _____ Office: _____ Date: _____

Division Deputy Director(s):

Signature: _____ Division: _____ Date: _____

Signature: _____ Division: _____ Date: _____

Appendix E: Color Plates

Color versions of figures from the text.

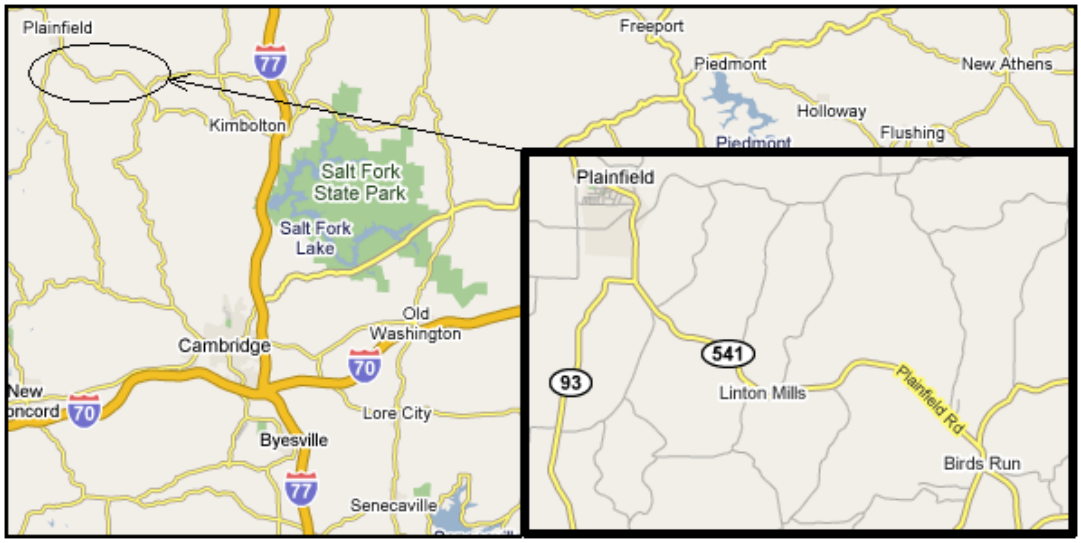

Color Plate 1. Map Location SR 541 [Google Map]. See Figure 1.

Color Plate 2. DCP test device: at left is the DCP rod and driving weight assembly, and on the right is the DCP in use. [Wu and Sargand, 2007]. See Figure 5.

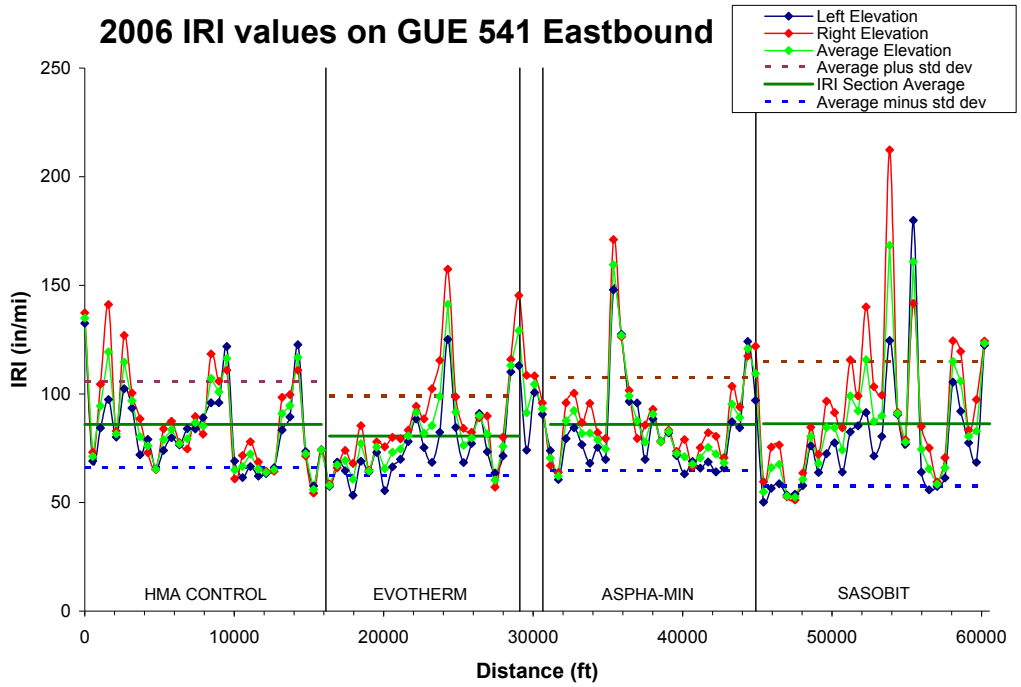

Color Plate 3. IRI values measured in December 2006 on GUE-541 Eastbound, with averages and single standard deviation ranges marked in each section. (1 in/mi = 15.78 mm/km = 0.00001578 in dimensionless units). See Figure 16.

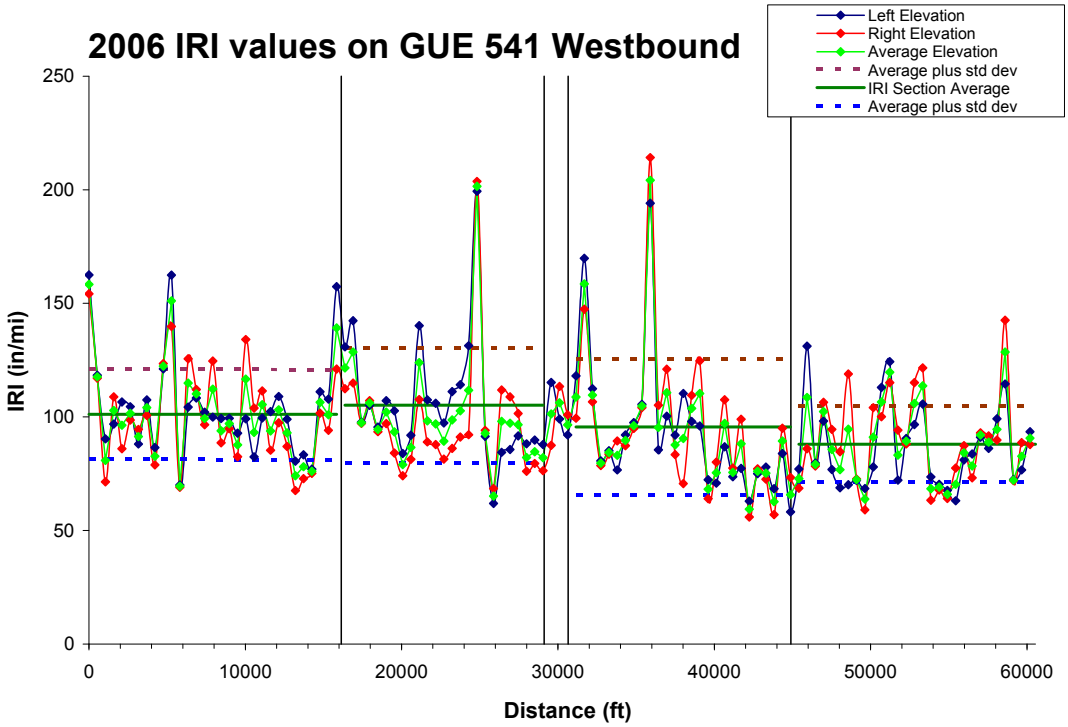

Color Plate 4. IRI values measured in December 2006 on GUE-541 Westbound, with averages and single standard deviation ranges marked in each section. (1 in/mi = 15.78 mm/km = 0.00001578 in dimensionless units). See Figure 17.

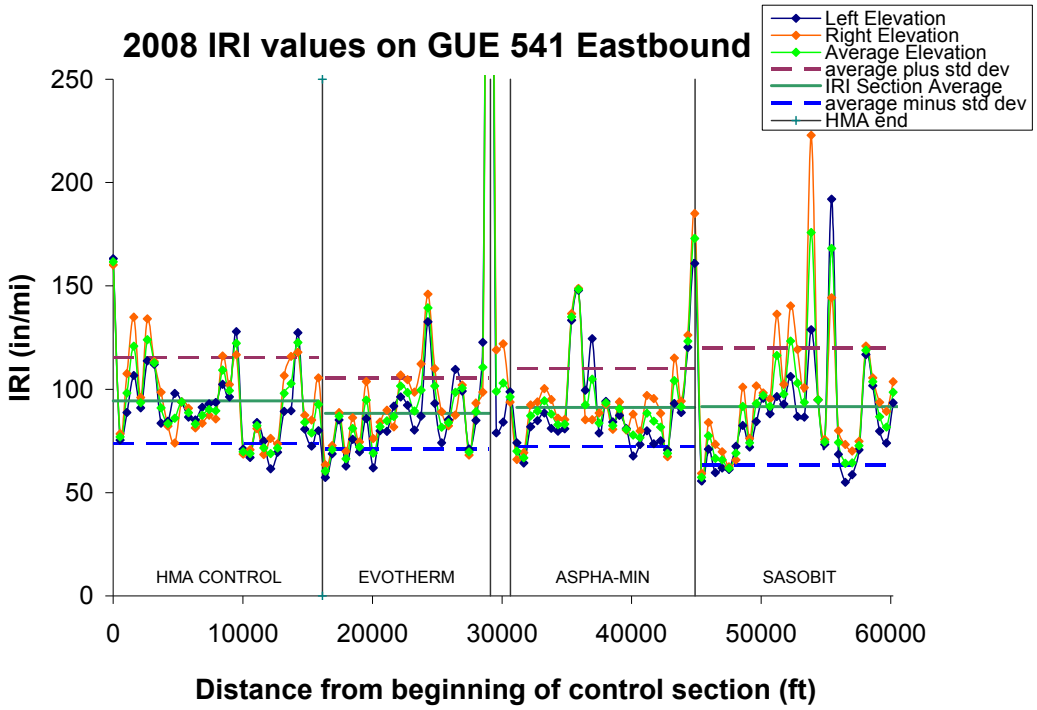

Color Plate 5. IRI values measured in December 2008 on GUE-541 Eastbound, with averages and single standard deviation ranges marked in each section. (1 in/mi = 15.78 mm/km = 0.00001578 in dimensionless units). See Figure 18.

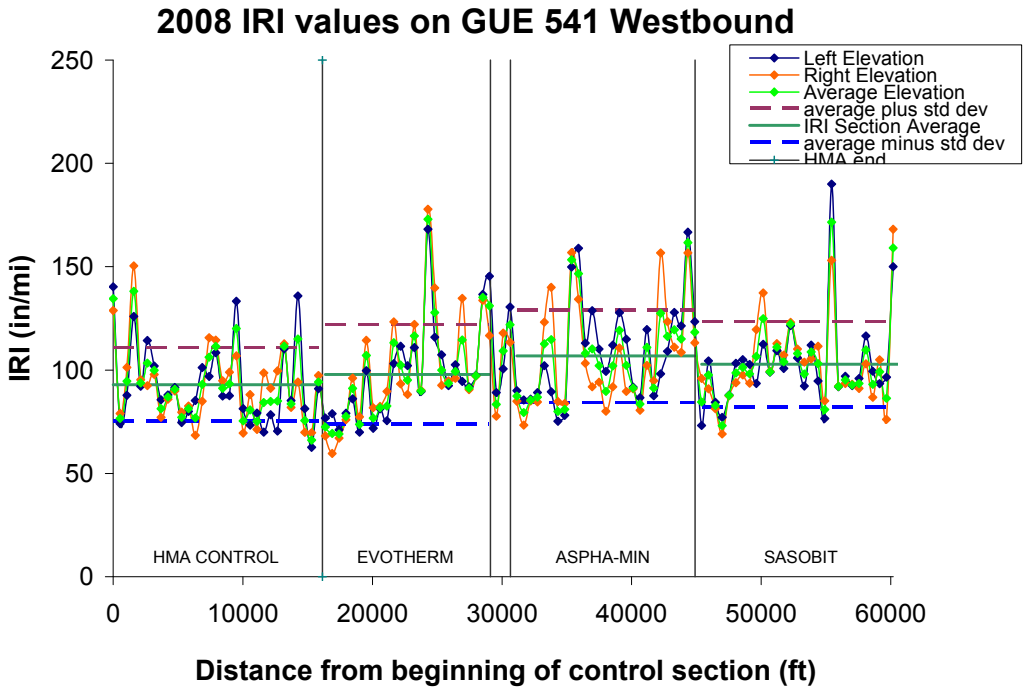

Color Plate 6. IRI values measured in December 2008 on GUE-541 Westbound, with averages and single standard deviation ranges marked in each section. (1 in/mi = 15.78 mm/km = 0.00001578 in dimensionless units). See Figure 19.

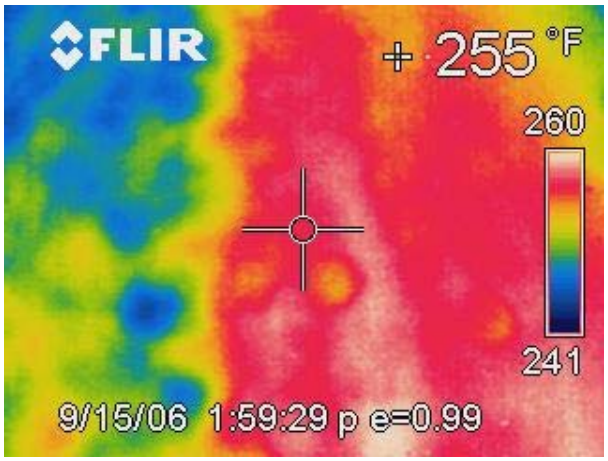

a) Aspha-min on SR541

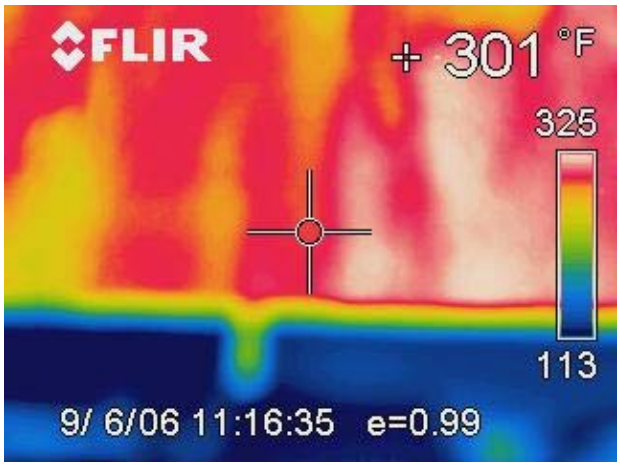

b) HMA Control mix in APLF

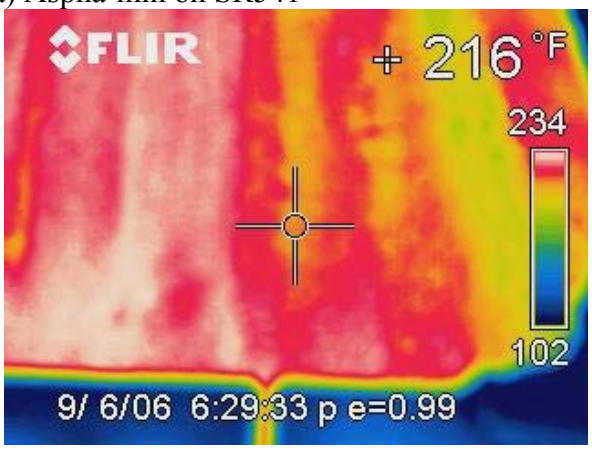

c) Evotherm mix in APLF

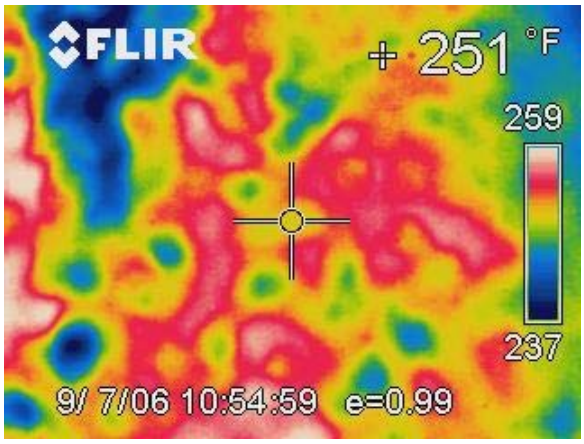

d) Evotherm mix on SR541

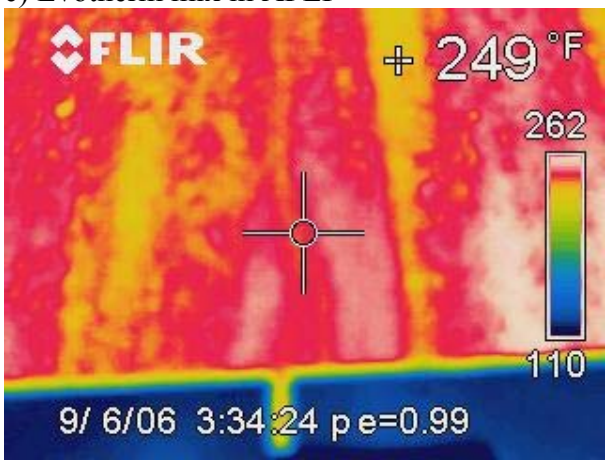

e) Sasobit mix in APLF

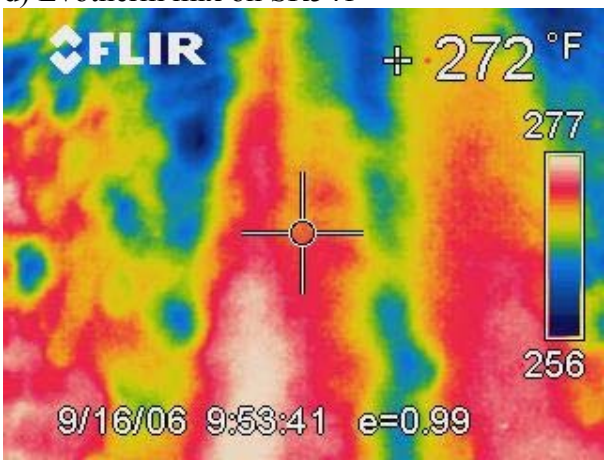

f) Sasobit mix on SR541

Color Plate 7. Infrared camera pictures of HMA and WMA mixes at time of construction. The number in the upper right corner is the temperature registered at the location of the large cross-hairs in the image, and the scale at the right edge shows the colors associated with temperatures over the entire image. All temperatures are in Fahrenheit. The lowest temperatures in the APLF images are off the pavement area. See Figure 20.

Color Plate 8. Photograph of the paving operation on SR541 showing monitoring equipment attached to paver, indicated with arrows. See Figure 21.

Color Plate 9. Photograph of paving operation on SR541, showing ambient air sampling equipment on tripods in foreground. The ambient air samplers are upwind of the paving. See Figure 22.

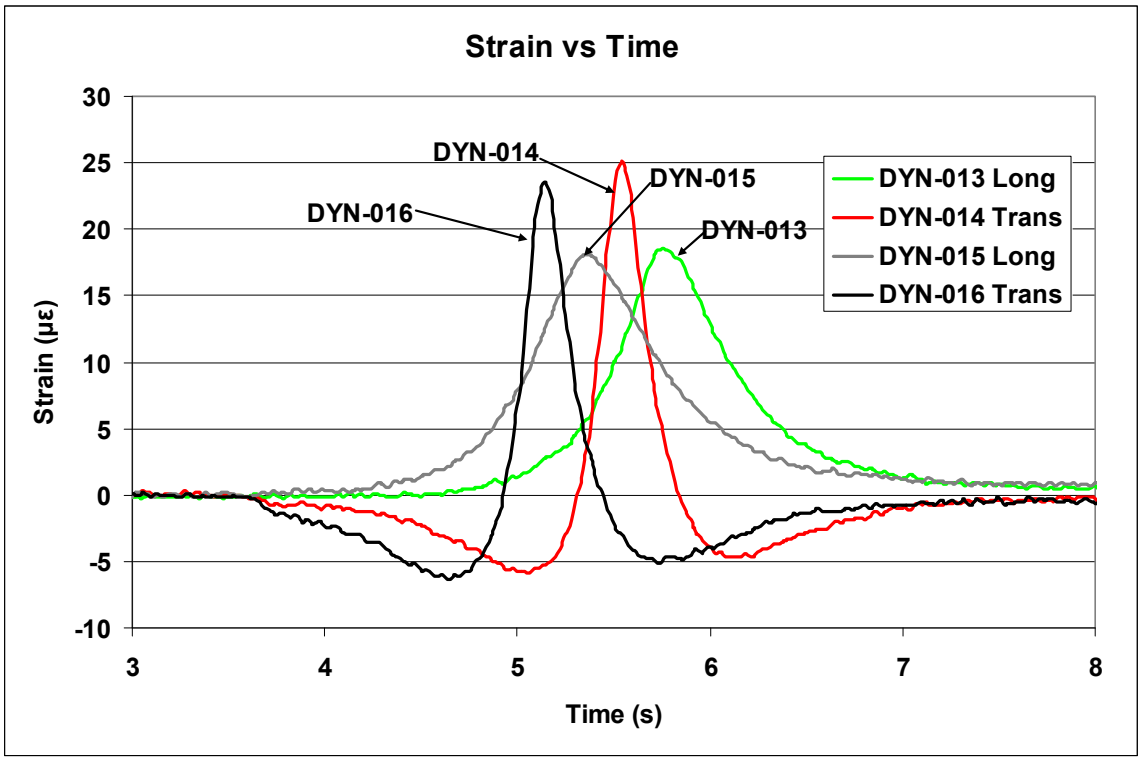

Color Plate 10. Example data for Longitudinal and Transverse Strain as function of time during loaded rolling wheel pass in Fatigue Resistance Layer (FRL) in APLF. See Figure 25.

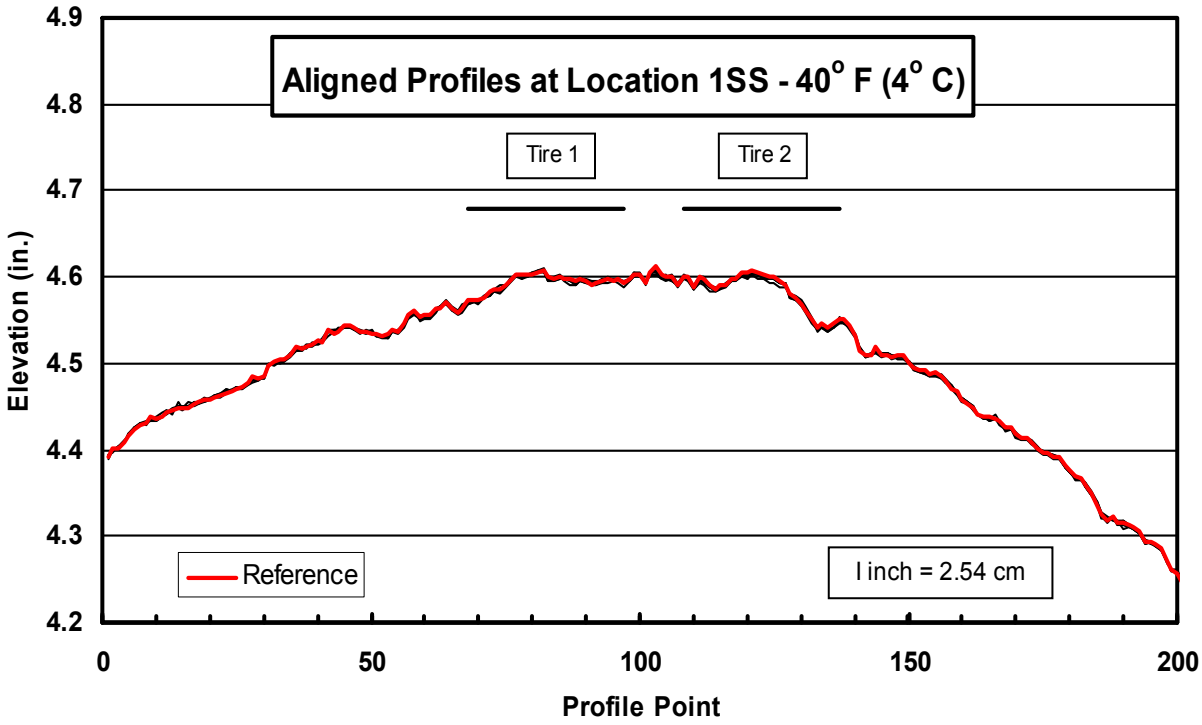

Color Plate 11. Aligned 40°F (4°C) profiles at Location 1SS. See Figure 34.

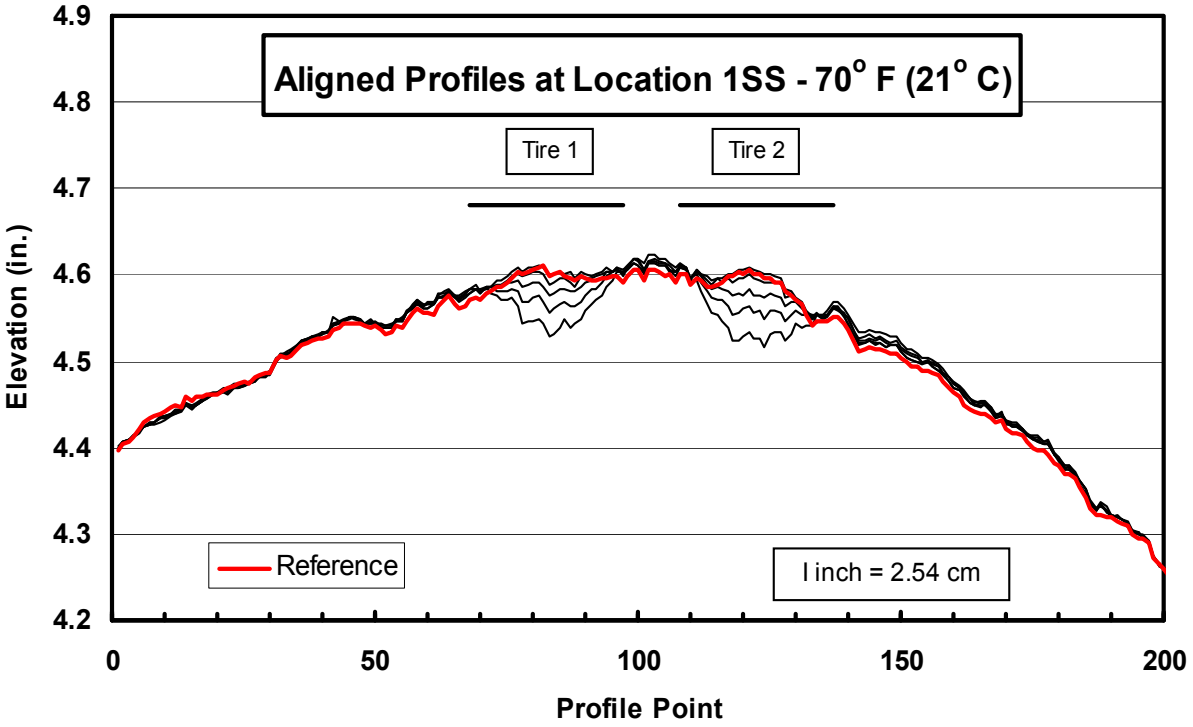

Color Plate 12. Aligned 70°F (21°C) profiles at Location 1SS. See Figure 35.

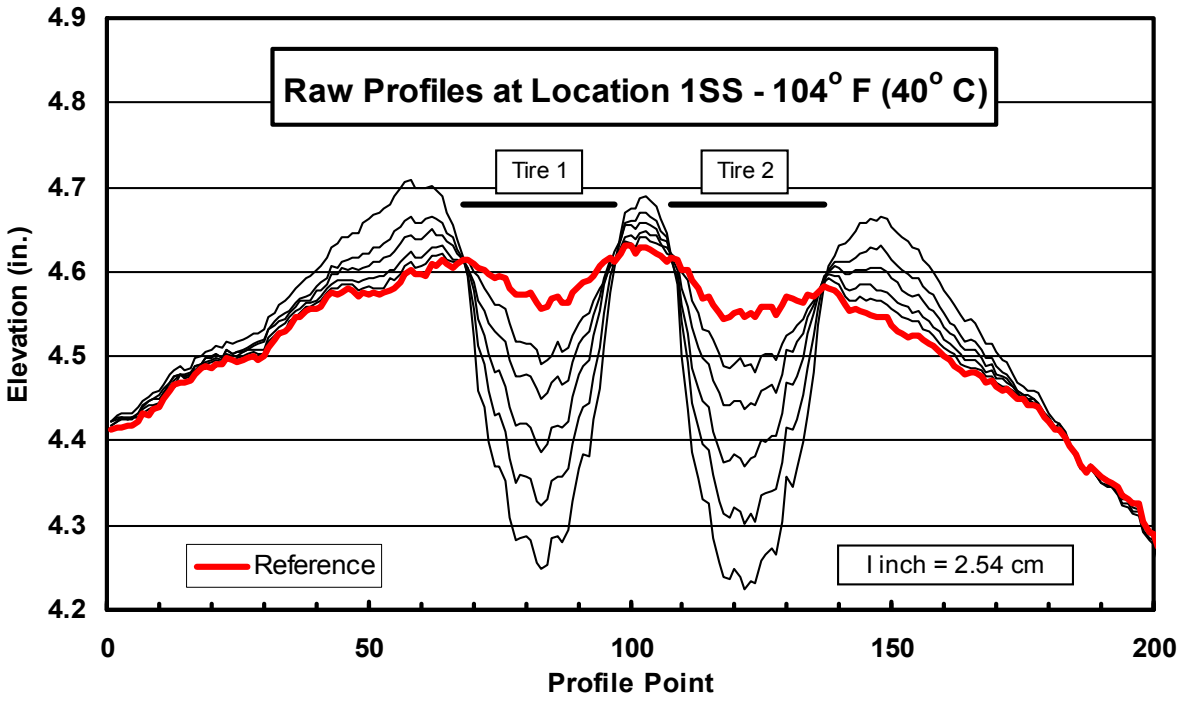

Color Plate 13. Raw 104°F (40°C) profiles at Location 1SS. See Figure 36.

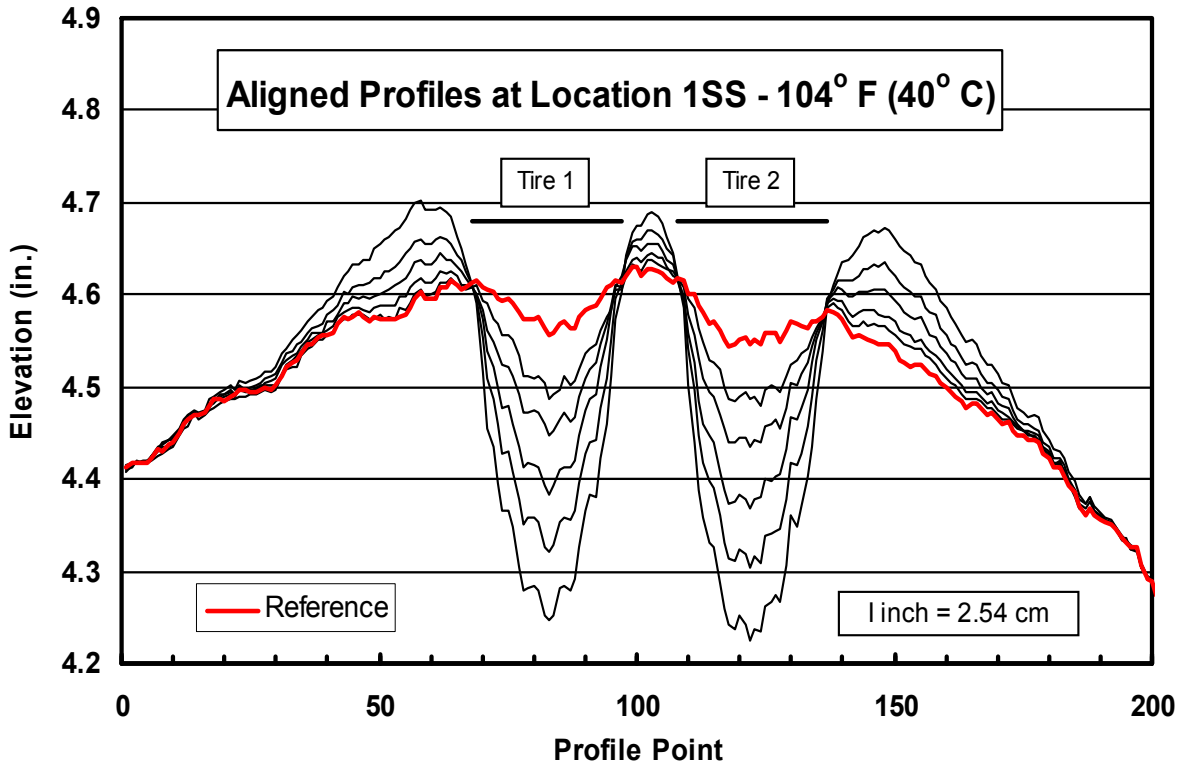

Color Plate 14. Aligned 104°F (40°C) profiles at Location 1SS. See Figure 37.

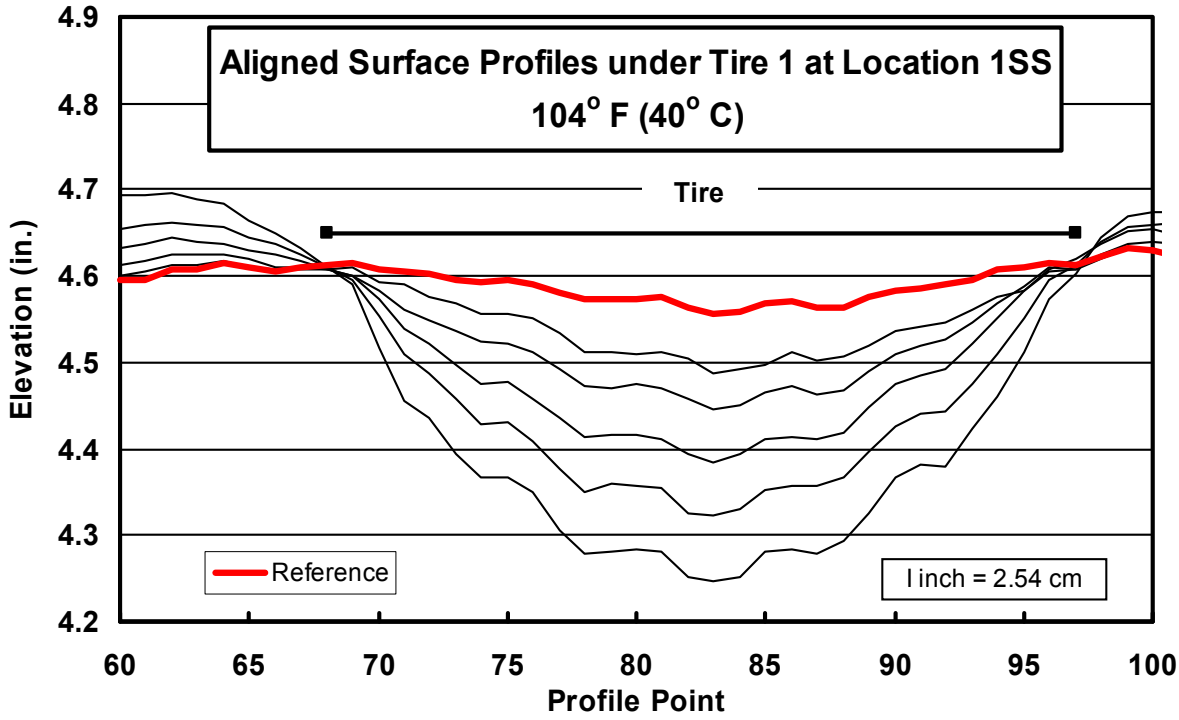

Color Plate 15. Aligned 104°F (40°C) profiles under Tire 1 at Location 1SS. See Figure 38.

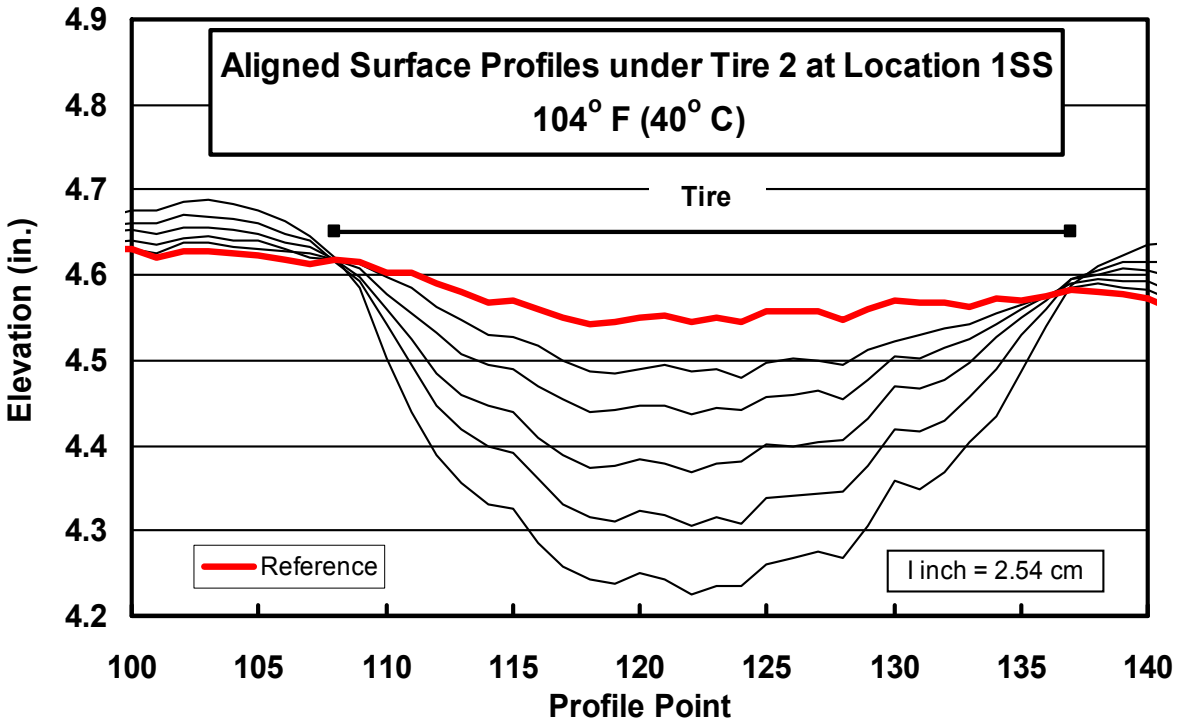

Color Plate 16. Aligned 104°F (40°C) profiles under Tire 2 at Location 1SS. See Figure 39.

ORITE • 141 Stocker Center • Athens, Ohio 45701-2979 • 740-593-2476
Fax: 740-593-0625 orite@bobcat.ent.ohiou.edu http://webce.ent.ohiou.edu//orite/